SEISMIC STRATIGRAPHY AND LATE QUATERNARY SEDIMENTARY HISTORY OF BONAVISTA BAY, NORTHEASTERN NEWFOUNDLAND

EWAN HUGH CUMMING, B.Sc.

NOTICE

The quality of this microform is heavily dependent upon the quality of the original thesis submitted for microfilming. Every effort has been made to ensure the highest quality of reproduction possible.

If pages are missing, contact the university which granted the degree.

Some pages may have indistinct print especially if the original pages were typed with a poor typewriter ribbon or if the university sent us an inferior photocopy.

Reproduction in full or in part of this microform is governed by the Canadian Copyright Act, R.S.C. 1970, c. C-30, and subsequent amendments

AVIS

La qualité de cette microforme dépend grandement de la qualité de la thèse soumise au microfilmage. Nous avons tout fait pour assurer une qualité supérieure de reproduction.

S'il manque des pages, veuillez communiquer avec l'université qui a conféré le grade

La qualité d'impression de certaines pages peut laisser à désirer, surtout si les pages originales ont été dactylographiées à l'aide d'un ruban usé ou si l'université nous a fait parvenir une photocopie de qualité inférieure.

La reproduction, même partielle, de cette microforme est soumise à la Loi canadienne sur le droit d'auteur, SRC 1970, c. C-30, et ses amendements subséquents

SEISMIC STRATIGRAPHY AND LATE QUATERNARY SEDIMENTARY HISTORY OF BONAVISTA BAY, NORTHEASTERN NEWFOUNDLAND.

© Ewan Hugh Cumming, B.Sc.

A thesis submitted to the School of Graduate Studies in partial fulfilment of the requirements for the degree of Master of Science

Department of Earth Sciences
Memorial University of Newfoundland
December, 1990

St. John's Newfoundland

ISBN 0-315-68231-0

Canada

Abstract

The Late Quaternary glacial and sedimentary history of Bonavista Bay, on the NE coast of Newfoundland, is interpreted from 545 line km of high-resolution seismic reflection data and three piston cores. Seismic data from the open, outer region of Bonavista Bay display three seismic units (1-3) overlying acoustic basement within two broad, shallow basins. The surveyed inner region of Bonavista Bay contains narrow, deep basins which commonly host four seismic units (A-D) above acoustic basement.

Glacial sediments are represented by seismic units 1 and A, both of which are acoustically incoherent. Unit 1 is generally <15 ms thick and has a variable morphology. It is correlated with a stiff, sandy, gravelly mud (diamicton). Unit A is up to 110 ms thick and ponded. Units 2, B and C are proglacial sequences. Unit 2 is acoustically stratified, <20 ms thick and has a draping basin-fill morphology. It is correlated with an interlaminated sequence of distal turbidites and hemipelagic/ice-rafted sediment. Unit B is acoustically transparent, ponded and up to 30 ms thick. It corresponds with a proglacial homogeneous silty mud, rapidly deposited under open water conditions until 12,790 y BP (in Chandler Reach). Unit C, overlying B, is acoustically stratified, up to 90 ms thick and has a draping basin-fill morphology. It is correlated with a sandy, pebbly and shelly mud, deposited by hemipelagic, terrestrial and ice-rafted sedimentation from 12,790 y BP to 10,170 y BP. Seismic units 3 and D are acoustically transparent post-glacial sequences with an average thickness of 20 ms. They display a draping basin-fill morphology which has been altered by erosion and are correlated with a sandy, pebbly and shelly hemipelagic mud; initially deposited in the outer bay by 13,500 y BP and in the inner bay by 10,170 y BP (Chandler Reach).

Bonavista Bay was host to a grounded Late Wisconsinan

ice sheet. Deglaciation of the bay was rapid and occurred at a time of rising sea level. Initially a thin basal till was deposited beneath grounded ice. With lift-off, an ice shelf formed over the basins of the outer bay. Retreat of the grounding line paused briefly on the basin margins, where discontinuous moraines were deposited. The ice sheet also became buoyant within the northeasternmost basin of the inner bay during this period. Diamictons (seismic units 1 and A) were subaqueously deposited within basins beneath the floating ice. Following ablation of the ice shelf, ice margins persisted near the SW and western regions of the outer bay, providing sediment for proglacial turbidity currents within the basins (unit 2). Geostrophic currents largely limited deposition of hemipelagic sediments to within the basins of the outer bay.

The basins of the inner bay were gradually deglaciated while unit 2 was deposited. Fine-grained outwash sediment (unit B), transported by interflows, was rapidly deposited as the ice margin retreated to a terrestrial position by at least 12,790 y BP. The region of the inner bay remained under the influence of one or more ice margins until 10,170 y BP, with ice at the position of an inland end moraine and probably on the Bonavista and Gander Peninsulas. Normal marine conditions were present in the outer bay by 13,500 y BP and throughout the entire region by 10,170 y BP. The Labrador Current has eroded Holocene and perhaps Wisconsinan sediments.

The deglacial sequence of events within Bonavista Bay and the sediments present, suggest that ice was channelized in the bay during the Late Wisconsinan, either at glacial maximum or during a deglacial surge which was driven by a collapsing ice cap from the SW.

Acknowledgements

Sincere thanks are extended to Dr. A.E. Aksu for supervision of this thesis. Funding was through National Science and Engineering Research Council (NSERC) grants to Dr. Aksu and a Special Scholarship for Studies in the Sciences Related to Resource Development from the Provincial Government of Newfoundland and Labrador. Ship time was provided by the Department of Fisheries and Oceans through the Bedford Institute of Oceanography, with equipment supplied by the Department of Energy, Mines and Resources.

Many thanks are owed to the following people for providing invaluable assistance: the officers and crew of C.S.S. Dawson and C.S.S. Hudson; Chief Scientists Dr. A.E. Hay and Dr. G. Vilks, for ship time on cruises 87-030 and 87-033, respectively; Dr. D.J.W. Piper for the funding of a radiocarbon date and Ms. M.G. Parsons for acritarch identification. Scientific and technical advice was freely given by B. Sears, P. Benham, S. Awadallah, H. Gillespie and by Drs. D. Grant, R. Hiscott and R. Mason. This thesis was reviewed by Dr. D. Proudfoot and G. Fader.

Numerous people provided friendship and moral support. A partial list includes S. Awadallah, P. Benham, M. Duman, S. Edwards, M. Gipp, R. Grenier, K. Hudson, R. Husain, K. Roy, B.Sears, D. van Everdingen, J. van Gool and J. Waterfield. Special thanks to my parents and to my wife, Heather, for their understanding and patience.

Table of Contents

List of Tables

List of Figures

CHAPTER 1

INTRODUCTION

1.1 Study Area

Bonavista Bay is located on the northeast coast of the island of Newfoundland (Fig. 1.1). It is bounded to the west by the Gander Peninsula and to the east by the Bonavista Peninsula. The bay has an open outer region, host to a broad depression of up to 350 metres (m) depth and numerous small fjords within inner regions. Narrow, deep (~300 m) basins within the fjords are often separated from the rest of the bay by one or more sills. A deep (450 m) basin separates the surveyed fjords of Newman Sound and Chandler Reach/Clode Sound from the bay's outer region.

1.2 Bedrock Geological Setting

The region surrounding Bonavista Bay has been studied by many geologists, dating back to Jukes (1843). More recent workers have included Christie, (1950), Jenness (1957, 1958a,b, 1963), Younce (1970), Blackwood (1976), Dal Bello (1977), Hussey (1979) and O'Brien (1987). Jenness' (1963) study was of greatest extent, examining almost all of the coastal and inland region of Bonavista Bay. All other studies have been limited by comparison. Present in the region are Precambrian to early Palaeozoic volcanic and sedimentary rocks which have commonly experienced low grade

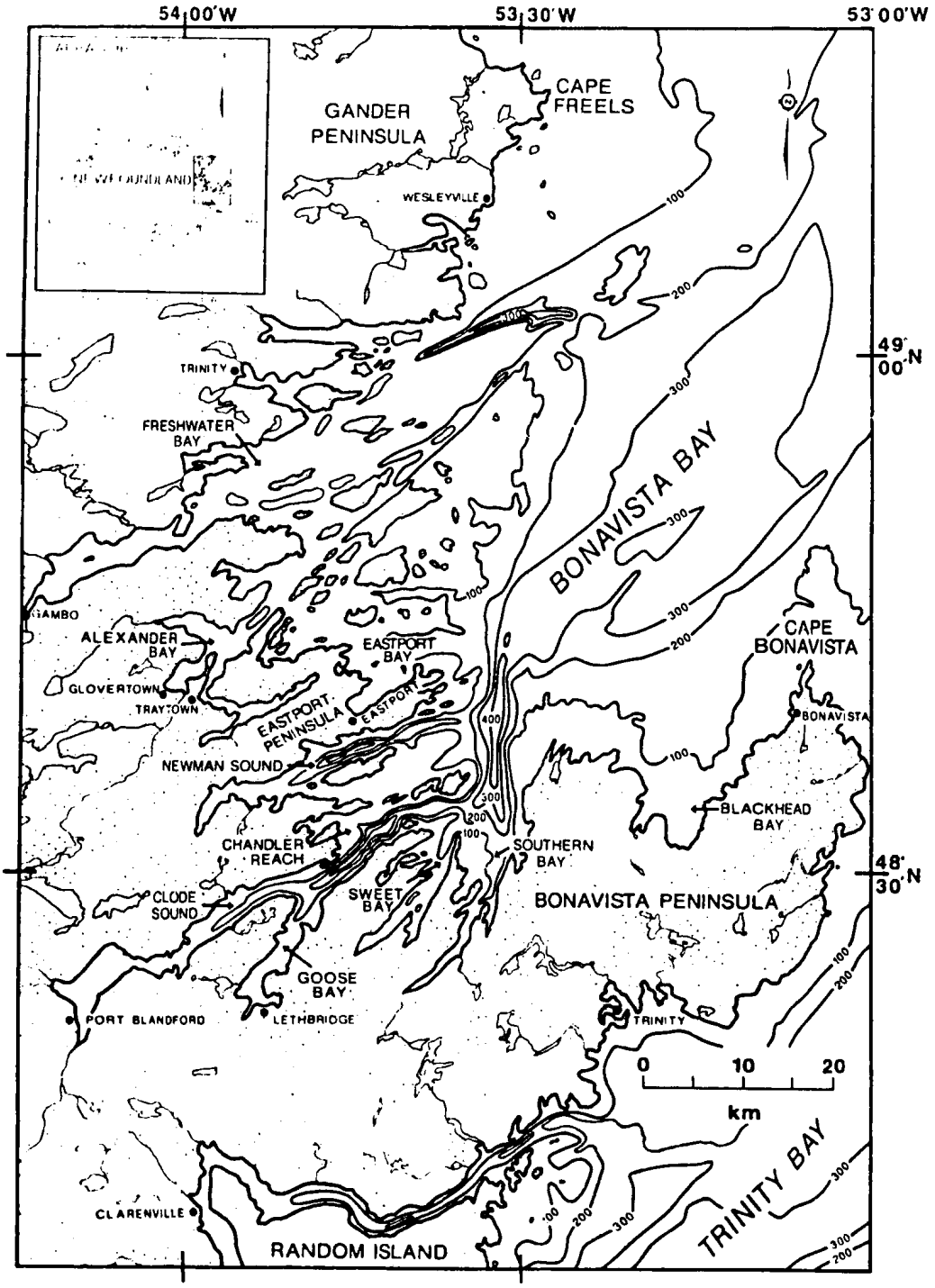

Figure 1.1. Map of Bonavista Bay and surrounding region.

metamorphic alteration. Granitic intrusions are abundant. The general trend of contacts (primarily faults) between lithological units is NNE-SSW (Jenness, 1963; O'Brien, 1987) (Fig. 1.2).

Three of the tectonostratigraphic zones defined by Williams et al. (1972) for the Appalachian Orogen are present within the region of Bonavista Bay. Rocks of the Avalon Zone, east of the Dover Fault (Blackwood and Kennedy, 1975), comprise most of the shoreline of the bay. The Gander Peninsula is largely comprised of rocks of the Gander Zone. The Gander River Ultrabasic Belt (Jenness, 1958b) and the Davidsville Group (Kennedy and McGonigal, 1972) form the NE boundary of the Dunnage Zone (Fig. 1.2). These three zones represent terranes of unknown palaeogeography which accreted to a miogeoclinal sequence on the west coast of Newfoundland (Williams and Hatcher, 1982). The miogeocline is of late Precambrian to early Palaeozoic age and formed the western margin of the Iapetus Ocean. The Dunnage, Gander and Avalon Zones were accreted and deformed during the closure of Iapetus, between the early Ordovician and the end of the Palaeozoic. The Dunnage Zone consists largely of Precambrian to Ordovician island arc rocks, developed upon the crust of Iapetus (Haworth et al., 1985). The Gander Zone consists of Cambrian to Ordovician clastic (meta)sediments which may have developed upon the margin of the Avalon Zone to the east (Kennedy, 1976). Both zones

Figure 1.2. Terrestrial bedrock geology of the study area (compiled from Colman-Sadd et al., 1990; Dallmeyer et al., 1981; O'Brien, 1987 and Hussey, 1979). Offshore bedrock geology from Haworth et al. (1985).

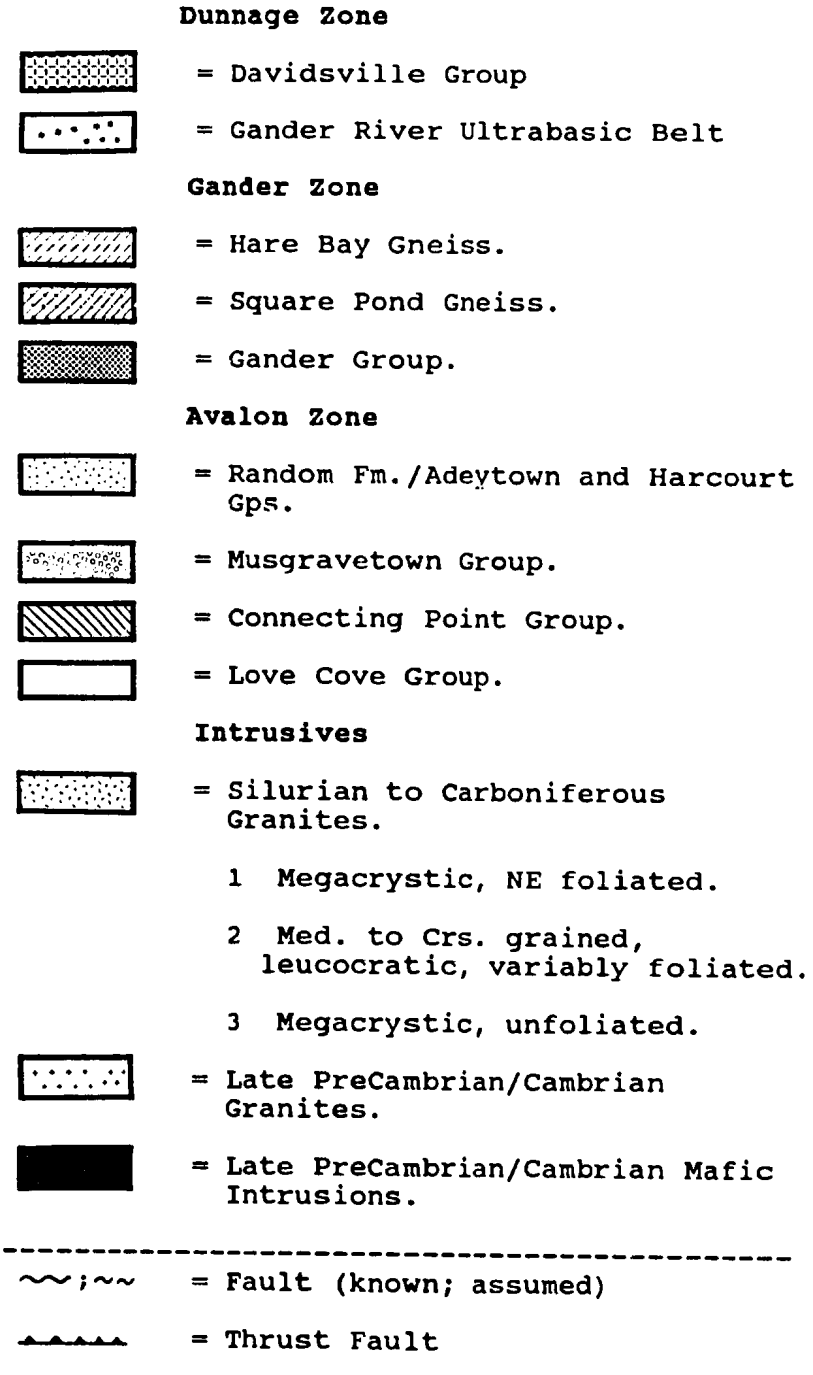

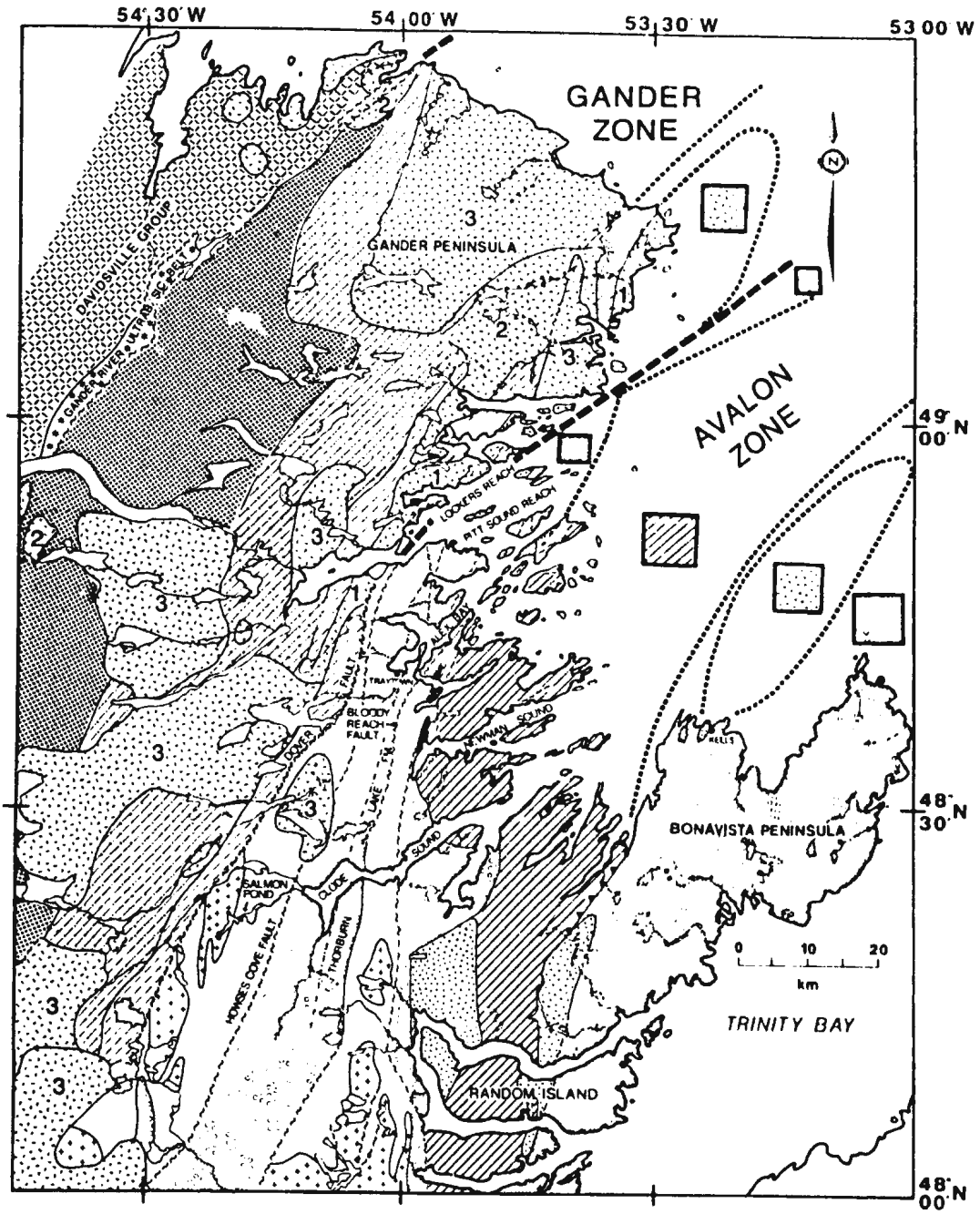
54 30 W
54 00 W
53 30 W
53 00 W
GANDER ZONE
AVALON ZONE
GANDER PENINSULA
DAVIDSVILLE GROUP
GANDER RIVER ULTRAB SE BELT
LOOKERS REACH
PITT SOUND REACH
BLOODY REACH FAULT
DOVER FAULT
LAKE
SOUND
SALMON POND
CLUCK
THORBURN
HORSES COVE FAULT
BONAVISTA PENINSULA
TRINITY BAY
RANDOM ISLAND
0 10 20
km
49 00 N
48 30 N
48 00 N

were accreted to the miogeocline during the Ordovician Taconic Orogeny (Williams and Hatcher, 1982). The Avalon Zone consists mainly of Precambrian (meta)volcanics and (meta)sediments, originating from rift related volcanism and associated sedimentation (Strong, 1979), which accreted during the mid-Palaeozoic Acadian Orogeny (Williams and Hatcher, 1982). The granitic intrusions common in the study area (Fig. 1.2) range in age from Precambrian within the Avalon Zone (O'Brien, 1987; Colman-Sadd et al., 1990) to Devonian/Carboniferous, primarily within the Gander Zone (i.e. Bell and Blekinsop, 1975; Blackwood, 1976).

1.2.1 Avalon Zone

The Avalon Zone is a folded and faulted Precambrian volcanic/sedimentary belt which is largely made up of (from oldest to youngest) the Love Cove Group (Jenness, 1957), Connecting Point Group (Hayes, 1948) and Musgravetown Group (Hayes, 1948). Also present in the Avalon Zone are Cambrian to early Ordovician platformal sediments of the Random Formation (Christie, 1950) and Adeytown and Harcourt Groups (Jenness, 1963) (Fig. 1.2). The division of Avalon Zone rocks into groups has long been controversial, due to complex deformational histories and lithologic similarities throughout (Dal Bello, 1977).

The Love Cove Group of metavolcanics and metasediments are the oldest rocks in the study region (Jenness, 1963).

Two bands, trending NNE/SSW and up to 15 kilometres (km) wide, extend north into Lockers Reach and Alexander Bay on the west side of Bonavista Bay (Fig. 1.2). The Love Cove Group consists of subaqueous to subaerial, Precambrian felsic to mafic volcanics from a volcanic arc (Strong, 1979; Knight and O'Brien, 1988; Dec et al., 1989), along with minor associated sediments (Colman-Sadd et al., 1990). Rocks of this group display regional greenschist facies metamorphism and great variability over short distances (Jenness, 1963). In the regions to the north and south of Clode Sound and south of Salmon Pond are an undifferentiated series of chlorite and sericite schists interbedded with volcanics (Jenness, 1963). The remainder of the rocks of the Love Cove Group vary from felsic lavas and pyroclastics in the eastern belt to intermediate lavas, pyroclastics and minor interbedded sediments in the western belt. Chlorite epidote schists are common and may have resulted from alteration of mafic volcanics (Jenness, 1963).

Rocks of the Love Cove Group are strongly foliated, with a near vertical schistosity which trends NNE-SSW and parallels the outcrop pattern of the group (Jenness, 1963). Tight to isoclinal folding is common, generally trending NE (Dallmeyer et al., 1983). The contacts between the Love Cove Group and younger Avalon Zone rocks were considered by Jenness (1963) to be high angle faults in almost all cases. Other authors have proposed a number of scenarios for

specific areas, ranging from conformable contacts (Hussey, 1979) to thrust faulting (Reusch and O'Driscoll, 1987). The western boundary of the Love Cove Group, the Dover Fault, is characterised by mylonitic rocks (Blackwood and Kennedy, 1975)

Rocks of the Connecting Point Group extend north from Trinity Bay to form the mouth of Clode Sound, most of Newman Sound and many of the islands in Bonavista Bay (Fig. 1.2). The group is comprised of marine volcaniclastic sediments, largely of turbiditic origin, which were deposited in a basin to the east of the Love Cove Group volcanic arc (Knight and O'Brien, 1988). Dark gray and black argillites are common, with minor gray and green-gray argillites. A slaty cleavage is generally present. Interbedded repetitively are thin ($\leq$ 1 cm) siltstones and cross-bedded feldspathic graywackes (Jenness, 1963; Dal Bello, 1977). Some carbonate content (greater than 5%) was noted within localized areas (Jenness, 1963). There are minor occurrences of red cherty quartzites thinly interbedded with shales and slates, comprising the only rocks of this colour within the predominantly green-gray to black sequence of the Connecting Point Group (Jenness, 1963). Felsic to intermediate lavas and pyroclastics are interbedded with slates within the upper part of the group (Jenness, 1963). Intrusive diabase dykes and sills were noted by Hussey (1979) in his study area near the mouth of Clode Sound.

Rocks of the Connecting Point Group have experienced less deformation than those of the Love Cove Group and are broadly folded (Jenness, 1963). Regional greenschist metamorphism is generally of lower grade than within rocks of the Love Cove Group (Dec et al., 1989; Dallmeyer et al., 1983).

The Musgravetown Group consists of coarse terrestrial red and green clastic sediments and interbedded volcanics (O'Brien, 1987). It occurs within the study area as three NE-SW trending bands of variable width, one of which forms the NE tip of the Bonavista Peninsula (Fig. 1.2). The most common rocks within the Musgravetown Group are red and green conglomerates, sandstones and shales, with localized occurrences of graywacke, arkosic sandstones and mafic to felsic volcanics and pyroclastics (McCartney, 1958, 1967; Jenness, 1963; O'Brien, 1987). Rocks of the Musgravetown Group have been broadly folded, with fold axes trending NNE (Jenness, 1963). Metamorphic alteration is of low grade and is variable throughout the group (Jenness, 1963; Blackwood and Kennedy, 1975).

Cambrian to Ordovician marine shelf sediments of the Random Formation and the Adeytown and Harcourt Groups overlie the Musgravetown Group (Jenness, 1963; Colman-Sadd et al., 1990). They are limited to occurrences: i) between Random Island and southern Bonavista Bay, ii) in the north of the Bonavista Peninsula near the town of Keels and iii)

on two islands within Lockers Reach (Fig. 1.2). The outcrop near Keels has been interpreted by Haworth et al. (1985) as the SW tip of a NE trending, 13 by 50 km oval outcrop of Cambrian sediments which forms part of the offshore bedrock geology.

The Random Formation is a thin (110 m) transitional zone between the late Precambrian Musgravetown Group and early Cambrian rocks of the Adeytown Group. It consists of a variety of siliceous sediments, including white quartzite, greenish gray to gray sandstones and pink cross-bedded quartz sandstones and quartzites (Jenness, 1963). Unconformably overlying the Random Formation is the Adeytown Group, consisting of red, green and gray shales and slates, with some interbedded pink, gray and green limestones. Folding and faulting are common, along with cleavage development in the shales and slates (Jenness, 1963). The Harcourt Group, conformably overlying the Adeytown, consists mainly of dark gray and black shales, silty shales, siltstones and minor grey limestones. Fossils are abundant within the lower 30 m of the Harcourt Group (Jenness, 1963). Deformation of Cambrian sediments is generally limited to broad folding, although strong folding and faulting occur in some areas. Metamorphic alteration is limited and mostly low grade (Jenness, 1963; Parsons, 1987).

1.2.2 Gander Zone

The Gander Zone lies to the west of the Dover Fault (Blackwood and Kennedy, 1975) and contains marine metasediments, gneisses and minor volcanics of Cambrian to Ordovician age (Jenness, 1963; Williams, 1976; Colman-Sadd et al., 1990). These rocks, along with the granitic intrusions common within the Gander Zone, form the western coastline of Bonavista Bay and much of the regional geology to the SW and west of the study region (Fig. 1.2). The Gander Zone has been divided into two gneissic belts and the Gander Group of metasediments (McGonigal, 1973; Blackwood and Kennedy, 1975; Blackwood, 1976).

The Hare Bay Gneiss is the easternmost of the two belts (Blackwood, 1976). It is composed largely of crudely banded biotite migmatite and tonalite gneiss with inclusions of paragneiss xenoliths. This belt is a "granitic" gneiss, with the paragneiss xenoliths perhaps being derived from the western Square Pond Gneiss. Therefore, the Hare Bay Gneiss may represent two periods of gneiss development (Blackwood, 1976, 1978). The Square Pond Gneiss to the west is composed of semi-pelitic and psammitic paragneisses, with minor phyllitic and migmatitic zones (Blackwood, 1978).

The Gander Group includes polydeformed, gray arenaceous to argillaceous metasediments and sediments with some interbedded volcanics (Jenness, 1963; Blackwood, 1976, 1978). Other rocks less commonly present include pebble

conglomerates, quartzites, black pelites and a pyritiferous slate (Jenness, 1963; Blackwood, 1978). Intercalated mafic volcanics and pyroclastics occur near the western boundary of the group (Jenness, 1963; McGonigal, 1973). A gradational increase in metamorphic grade from greenschist to upper amphibolite facies occurs eastward from the Gander Group across the two gneissic belts (Blackwood, 1976, 1978).

West of the Gander Group are Cambro-Ordovician ultramafic and mafic rocks of the Gander River Ultrabasic Belt (Jenness, 1958b) and sediments of the Davidsville Group (Kennedy and McGonigal, 1972) (Fig. 1.2). These rocks mark the eastern edge of the Dunnage Zone (Williams et al., 1972). They are not discussed in a separate section, due to their distance from the study area. The ultramafic and mafic rocks of the Gander River Ultrabasic Belt consist of gabbro, pyroxenite, serpentinite and carbonate schists (from alteration of pyroxenite and serpentinite) (Jenness, 1963). The Davidsville Group, farther west, consists largely of marine siliciclastic sedimentary rocks, including slates, shales, siltstones, sandstones and conglomerates (Colman-Sadd et al., 1990).

1.2.3 Intrusive Rocks

Granitic intrusions are very common in the area, occurring mainly within the Gander Zone (Fig. 1.2), where they are generally of Silurian and Devonian/Carboniferous

age (Bell and Blekinsop, 1975; Bell et al., 1979; Blekinsop et al., 1976). Blackwood (1978) defined three categories of granite in the Gander Zone: The first includes coarse-grained megacrystic granites with a NE trending foliation. These occur as linear features within the Hare Bay Gneiss. The second consists of medium to coarse-grained, two-mica leucocratic granites. These are occasionally porphyritic, have varying degrees of foliation and occur throughout the Gander Zone. The third and most extensive category is made up of undeformed coarse-grained megacrystic granites. The Ackley Batholith, extending into the south of the study area, belongs in this category (Blackwood, 1978) (Fig. 1.2). In the Avalon Zone, granitic intrusions of late Precambrian age commonly occur within the Love Cove Group (O'Brien, 1987; Colman-Sadd et al., 1990). An exception is the Terra Nova Granite, the largest intrusion within the western band of the Love Cove Group, which is of Devonian/Carboniferous age (Blackwood, 1976) and is genetically tied to the Ackley Batholith to the south (Jenness, 1963). Minor mafic intrusions of gabbro and diorite occur between the Love Cove and Musgravetown Groups, south of Alexander Bay (O'Brien, 1987) (Fig. 1.2).

1.2.4 Structural Geology

The NE trending fjords and peninsulas characteristic of the coastline of Bonavista Bay are suggestive of glacial

erosion by NE advancing ice (O'Brien, 1987) (Fig. 1.1). While such processes probably played a role in coastal development, a large part of the physiography is likely related to structural patterns and deformation in the region (Fig. 1.2). These are characteristically large scale upright folding, shear zones and faulting, the cause and timing of which are generally uncertain (O'Brien, 1987).

The oldest Avalon Zone rocks, the Love Cove and Connecting Point Groups, were likely first deformed during the Precambrian, at the same time as movement began along the Dover Fault (O'Brien, 1987). The majority of metamorphism, folding and faulting within these two groups may have occurred either during the Precambrian (O'Brien, 1987) or during the Devonian Acadian Orogeny (Dallmeyer et al., 1983), at which time all Avalon Zone rocks, including the terrestrial sediments and volcanics of the Musgravetown Group and shallow water, platformal Adeytown and Harcourt Groups were affected (Dallmeyer et al., 1983). The Acadian Orogeny likely saw the accretion of the Avalon Zone to the Gander Zone, with juxtaposition along the Dover Fault (Williams and Hatcher, 1982). Some of the faulting within the Avalon Zone may have occurred later than the Acadian deformation (O'Brien,, 1987)

The majority of the faults in the Avalon Zone are high angle, trending NE to NNE (Jenness, 1963; O'Brien and Knight, 1988) (Fig. 1.2). The Dover Fault is a near

vertical to high angle reverse feature (Blackwood and Kennedy, 1975). Acadian movement was likely strike slip (Blackwood, 1977). The Howses Cove and Bloody Reach Faults are both high angle and may have experienced significant vertical movement, along with strike slip motion (O'Brien, 1987; O'Brien and Knight, 1988). Abundant cross faulting, with an E-W trend, was noted by O'Brien (1987) and O'Brien and Knight (1988) in their map areas north of Newman Sound.

Large scale faulting is not common within the Gander Zone. Deformation has been primarily in the form of ductile shearing (Hanmer, 1981), which occurred during both the Ordovician Taconic Orogeny and the Devonian Acadian Orogeny (Williams and Hatcher, 1982).

1.3 Quaternary Geology

The Quaternary geology of the study area has been examined by Christie (1950), Jenness, (1960, 1963), Dyke (1972), Brookes, (1984, 1989) and personnel of the Newfoundland Department of Mines and Energy (DME) (Butler *et al.*, 1984; Vanderveer, 1988 and Kirby *et al.*, 1988). The only studies to encompass the entire region surrounding Bonavista Bay have been those of Jenness (1960, 1963). All others workers have studied limited areas.

Jenness (1960) identified two "drift zones" (the inner and outer) throughout eastern Newfoundland, separated by a discontinuous end moraine (Fig. 1.3). The inner drift zone

Figure 1.3. Compilation map of terrestrial glacial indicators within the study region (data from Jenness, 1963; Butler et al., 1984; Vanderveer, 1988; Kirby et al., 1988 and Brookes, 1989).

Legend

⟶ = Glacial striae (direction known).

⟷ (direction unknown).

⟶ = Crag and tail features.

⌐~⌐ = Meltwater channels.

—— = Drumlinoid landforms.

»»» = Eskers.

⊸ = Streamlined till mounds.

---· = End moraine (Jenness, 1963).

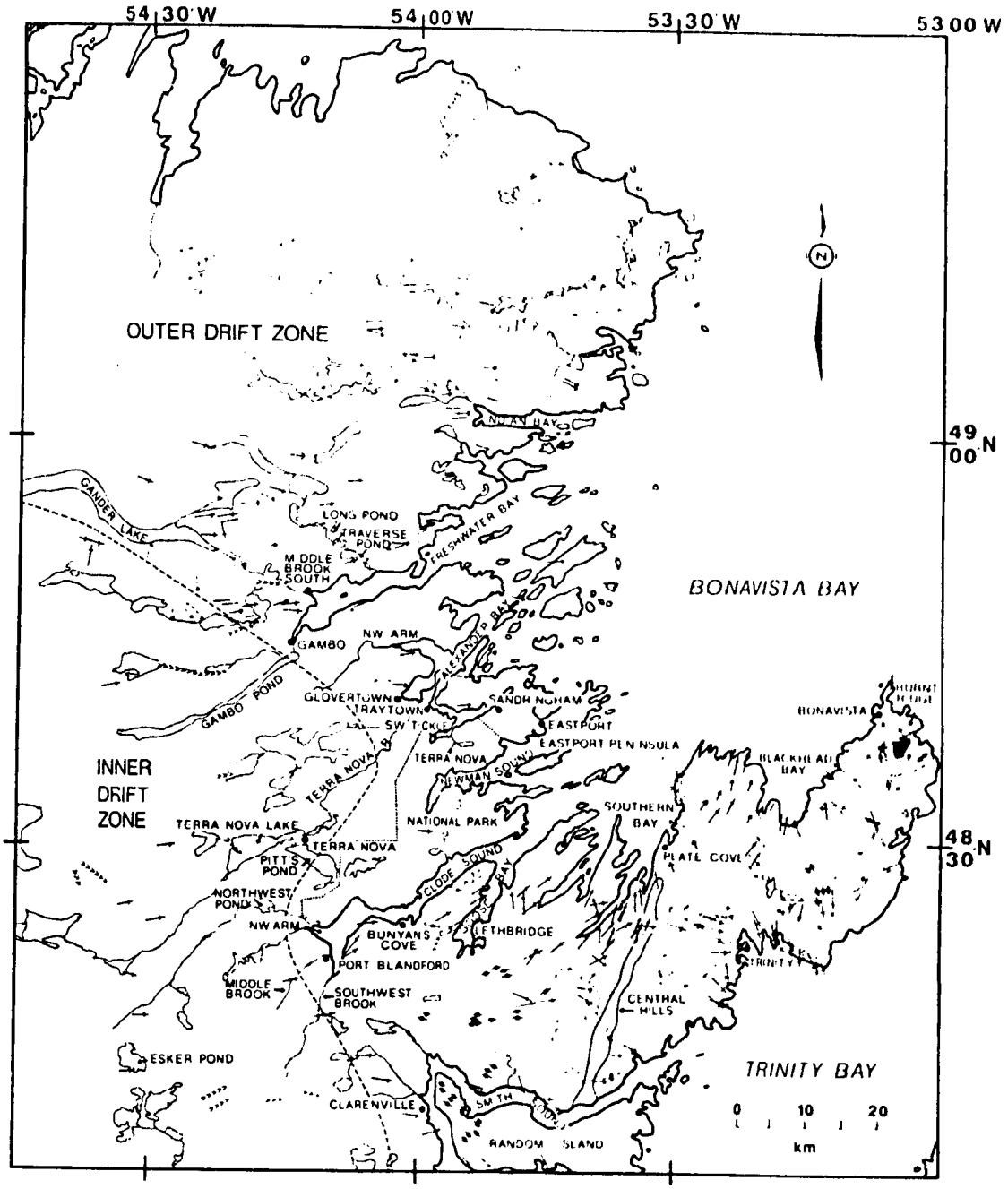
54 30 W
54 00 W
53 30 W
53 00 W
49 00 N
48 30 N
OUTER DRIFT ZONE
INNER DRIFT ZONE
BONAVISTA BAY
TRINITY BAY
N
GANDER LAKE
LONG POND
TRAVERSE POND
FRESHWATER BAY
MIDDLE BROOK SOUTH
GAMBO
NW ARM
GAMBO POND
GLOVERTOWN
TRAYTOWN
SANDY NOGHAM
SW TICKLE
EASTPORT
EASTPORT PENINSULA
BONAVISTA
BLACKHEAD BAY
TERRA NOVA
NEWMAN SOUND
TERRA NOVA LAKE
NATIONAL PARK
SOUTHERN BAY
PLATE COVE
PITTS POND
NORTHWEST POND
CLODE SOUND
NW ARM
BUNYANS COVE
LETHBRIDGE
PORT BLANDFORD
TRINITY
MIDDLE BROOK
SOUTHWEST BROOK
CENTRAL HILLS
ESKER POND
CLARENVILLE
SMITH SOUND
RANDOM ISLAND
0 10 20
km

contains ground moraine (till), moraines, eskers, kames and kame terraces. The outer drift zone contains eroded "residual ground moraine" deposits, with occasional large outwash deposits found in river valleys (Jenness, 1963). The end moraine which separates the zones is inconspicuous and was identified by Jenness (1960) on the basis of the pattern of associated outwash deposits and boulder strewn hillocks. Support for its inferred position was taken from the change in the presence of landforms (i.e. eskers) at the line. The end moraine is not distinguished on maps by Vanderveer (1988) or Kirby et al. (1988). A road-cut into the moraine displayed large (up to 6 m) boulders in a matrix of finer, poorly-sorted and unstratified material (Jenness, 1963).

1.3.1 Inner Drift Zone

The inner drift zone contains a number of landforms in association with a thin covering of till. The till is extensive and compositionally similar to the underlying bedrock (Jenness, 1963). Limited mapping in the zone by the DME indicates eroded and hummocky till or till veneer (Vanderveer, 1988; Kirby et al., 1988). The highest density of landforms within the inner drift zone occurs in a 50 km wide belt of eskers near Esker Pond. Most trend NE-SW or E-W (Jenness, 1963). Eskers also occur near Terra Nova Lake and north of Gambo Pond. Striae, where present in the inner

drift zone, indicate ice flow towards the east and NE (Fig. 1.3). An incised glaciofluvial terrace occurs at the mouth of the Terra Nova River, where it enters the SW end of Terra Nova Lake. Glaciofluvial sediments are also abundant between Terra Nova and Pitt's Ponds (Jenness, 1963; Vanderveer, 1988; Kirby et al., 1988).

1.3.2 Outer Drift Zone

The outer drift zone is host to sporadic deposits of residual till and glacial outwash. The majority of the zone contains patchy till cover, often as hummocky and eroded zones amongst abundant rock outcrops and vegetation (Vanderveer, 1988; Kirby et al., 1988). The primary deposits in the outer drift zone consist of eroded outwash deposits of sand and gravel within river valleys extending from the vicinity of the end moraine towards the coast (Jenness, 1960). Those within the study area are summarized briefly:

i) The westernmost deposit extends eastward from Gander Lake to the community of Middle Brook South in Freshwater Bay. It consists of isolated deposits of well stratified sand and gravel originating from the Gander Group to the west. A delta at Middle Brook South has an upper surface elevation of 30 m (Jenness, 1963).

ii) Well stratified and cross-bedded sands and gravels extend from Gambo Pond towards Alexander Bay, terminating in

NW Arm as a delta with a surface elevation of 30 m above sea level (Jenness, 1963).

iii) Outwash deposits along the Terra Nova River terminate in a 30 m high sandy delta at Traytown, Alexander Bay (Jenness, 1963).

iv) An outwash train leading into SW Tickle (Alexander Bay) may be linked with extensive outwash deposits on the Eastport Peninsula (Jenness, 1963). Extensive glaciofluvial/deltaic sequences, consisting of well stratified and cross-bedded fine sands, overlain by coarser sand and boulders, occur near the town of Sandringham on the Eastport Peninsula (Christie, 1950; Jenness, 1963; Dyke, 1972). Dyke (1972) described a glaciolacustrine sequence in places overlying these deposits. From 55 m elevation, the delta surface decreases in height eastward to reach elevated deltas at 30 m above sea level at Eastport and Sandy Cove (Dyke, 1972). The latter faces Newman Sound, which was surveyed for the present study.

v) Two deltaic deposits occur at the southern end of Clode Sound (Jenness, 1963). The first, near Port Blandford, is 30 m high and originated from either the valley of Southwest Brook (Jenness, 1963) or Middle Brook (Kirby et al., 1988). Along the side of the Trans-Canada Highway in the valley of Southwest River are thick deposits of red shaley gravel. The second delta, in NW Arm, has an upper surface elevation of 15 m. At its base are rhythmic

sequences which were interpreted by Jenness (1963) as varved clays. The sands comprising the delta consist mostly of quartz and pink feldspar, with minor biotite, epidote and chloritic schists. This feature may have developed subsequent to nearby deltas with higher surface elevation. (Jenness, 1963).

vi) There are a number of remaining outwash deposits in the outer drift zone, including valley deposits near Glovertown, river valley deposits leading into Newman Sound, a deltaic deposit with a 30 m elevation at Plate Cove and many small glaciofluvial deposits around the bay (Jenness, 1963; Kirby et al., 1988).

Christie (1950) described a series of glacial sediments in the region between Lethbridge (Goose Bay) and Smith Sound, Trinity Bay. At Lethbridge, a bluish/buff coloured "glacial clay" underlies organic soil. Towards Smith Sound are a number of gravel pits, in which a large component of the gravel is either red or green fractured shale clasts. Mixing of the two is rare. Overlying the gravel are granitic erratics (Christie, 1950).

Directional indicators in the south of the outer drift zone generally indicate an ice flow to the east or NE. Striae at the base of the Bonavista Peninsula indicate northeasterly ice flow, with some localized north and northwesterly trends near Goose and Southern Bays (Jenness, 1963; Vanderveer, 1988; Kirby et al., 1988; Brookes, 1989)

(Fig. 1.3). East of the Central Hills, indicators point to ice movement radiating outwards from the centerline of the Bonavista Peninsula. In the north of the outer drift zone, directional indicators generally suggest ice movement to the east, towards Bonavista Bay. Exceptions to this trend occur towards the center of the Gander Peninsula, where ice flow is indicated to have been northerly. Meltwater channels, where present, usually extend into ponds or low lying land (Butler et al., 1984; Vanderveer, 1988).

1.4 Previous Quaternary Studies

Many previous Quaternary studies from the region of Bonavista Bay and beyond are relevant to the present study. These include terrestrial studies of the region around the bay, marine studies from the NE Newfoundland shelf and the large scale (minimalist/maximalist) theories on the glacial history of the eastern Canadian continental margin. All of the studies discussed here deal with glaciation during some period of the Wisconsinan glacial stage. Most researchers use Early, Middle and Late Wisconsinan divisions which correspond closely with the recognition of oxygen isotopic stages by Shackleton and Opdyke (1973). The Early Wisconsinan, 75-64 ka BP (thousand years before present), corresponds with isotopic stage 4. The Middle Wisconsinan, from 64-23 ka BP, corresponds with isotopic stage 3 and part of stage 2 (from 32-23 ka BP). The Late Wisconsinan, from

23-10 ka BP, corresponds with isotopic stage 2. The Holocene, from 10 ka BP to present, corresponds with isotopic stage 1.

1.4.1 Study Area

The primary studies of terrestrial Quaternary geology in the study area (Christie, 1950; Jenness, 1960, 1963; Dyke, 1972; Brookes, 1984, 1989) all discuss position(s) of glacial ice within the study region at stages of the last glaciation. Few attempts have been made to place the maximum position of the ice front. Only the large scale theories of Wisconsinan glaciation, such as those of Ives, 1978 and Flint, 1971, discussed in the following section, provide indications of the possible maximum glacial extent in the region.

The presence of E-W and NE-SW trending directional indicators inland of Bonavista Bay (Fig. 1.3) led Christie (1950), Jenness (1960, 1963) and Brookes (1984, 1989) to interpret that a Late Wisconsinan ice sheet advanced northeastward from central Newfoundland towards Bonavista Bay, perhaps extending beyond the present coastline. Striae at the base of the Bonavista Peninsula have been interpreted to indicate a northerly diversion of ice into Clode Sound, Goose Bay, and Southern Bay (Christie, 1950; Brookes, 1989). Beyond these interpretations, individual workers have generally examined more limited regions of the study area.

Christie (1950) made the majority of his observations in the area south of Goose Bay. He interpreted that "glacial action" in that region was limited, on the basis of the non-mixing of red and green shale fragments within glacial sediments and attributed this to the diversion of ice into Bonavista and Trinity Bays. Christie (1950) also used the presence of erratics overlying finer glacial sediments to indicate that "glacial ice did not remove the overburden but rode over it". He did not directly suggest that the underlying glacial sediments originated from a previous glaciation. Given that subsequent workers (Jenness, 1960, 1963; Brookes, 1989) have found no evidence of pre-Late Wisconsinan glaciations in this region, the erratics may have been derived from an ice re-advance during the last glaciation.

Jenness' (1960, 1963) theories on the glaciation of the study area developed from his definition of the inner and outer drift zones and location of the dividing end moraine. The moraine was interpreted to define an important stage during Late Wisconsinan deglaciation; a stillstand or re-advancement which followed a rapid ice front retreat (based upon the poorly-sorted and unstratified till cover over much of the outer drift zone). Subsequent deglaciation produced the large scale outwash trains within river valleys. The presence of what were interpreted to be varved clays beneath deltaic sands and gravel at the SW end of Clode Sound led to

the suggestion that freshwater lakes were created during final deglaciation (Jenness, 1960, 1963).

Dyke's (1972) study was limited to the Eastport Peninsula, where he disputed Jenness' (1963) interpretation of deglacial events. Dyke (1972) suggested that the abundant outwash debris was not associated with the inner drift zone, nor the speculated end moraine, but originated from an ice front sitting near or upon the peninsula. Dyke (1972) considered that cross-bedded sands, silt and clay near Sandringham were deposited in an ice marginal lake, which was subsequently over-ridden by a small scale glacial re-advance. The ice front then retreated westward, as opposed to the SW movement indicated by Jenness (1963).

Brookes (1989) concentrated upon the Bonavista Peninsula, where he argued for the Late Wisconsinan existence of a separate ice dome, separated from the larger ice cap to the west. The contact between the two was positioned along a line between Southern Bay and the town of Trinity (Fig. 1.3). As well as the radiating pattern of directional indicators on the peninsula, Brookes (1989) used till pebble lithologies to support his model. Till to the west of the Central Hills contains igneous pebbles, whereas till on the remaining eastern part of the peninsula generally does not. Igneous intrusions are common to the west of the Bonavista Peninsula (Fig. 1.2), while there are none within the sediments of the Musgravetown Group upon the

peninsula. Ice from this separate dome (the Bonavista Ice Divide) flowed coastward from high ground in the middle of the peninsula. Ice from the main Newfoundland Ice Cap may have been drawn down into Bonavista Bay through the inner fjords and perhaps extended well offshore, perhaps continually during the Early to Late Wisconsinan. A small plateau on the northeastern tip of the peninsula (Burnt Ridge) may have existed as a nunatak during Late Wisconsinan glaciation (Brookes, 1989) (Fig. 1.3).

Relatively fewer studies have provided data from the Gander Peninsula. Grant (1974) modelled the presence of a Late Wisconsinan remnant ice cap upon the peninsula, following the initial deglaciation of the Newfoundland Ice Cap. This interpretation was supported by Butler et al., (1984), as a way of explaining the evidence of radial ice flow upon the peninsula. Brookes (1989), however, proposed that an ice divide, connected with the Newfoundland Ice Cap, developed on the Gander Peninsula during glacial maximum.

The elevations of the emerged deltas discussed in Section 1.3.2 and similar indicators of relative sea level (RSL) changes along the coast of Bonavista Bay have led to the defining of isobases for the region to tie in with others on the island of Newfoundland. Isobases trend SW-NE within the study area (i.e.: Jenness, 1960; Grant, 1980). The isostatic uplift in the eastern region of Bonavista Bay is between 15 m (Jenness, 1960) and 25 m (Grant, 1980;

Rogerson, 1982). In the west of the bay it is approximately 30-35 m (Jenness, 1960; Grant, 1980; Rogerson, 1982).

A number of Quaternary studies have been conducted to the west of the study area which have implications for the present study. South of Notre Dame Bay (Fig. 1.1), Lundqvist (1965) identified a possible equivalent to the end moraine mapped by Jenness (1960, 1963). While he could not locate a specific morainal feature, Lundqvist (1965) did map a line along which till thickness changed suddenly and from which a number of deltas emanated. Sediments seaward of this line have provided a number of radiocarbon dates, indicating minimum ages of deglaciation. Marine shells have been dated at 11,500 to 11,900 y BP (years before present) at the head of Green Bay (Dyck and Fyles, 1963). Samples associated with a delta at Springdale have provided ages of 11,800 and 12,000 y BP. (Blake, 1983, 1987 and Tucker, 1974). Macpherson and Anderson (1985) reported a total organic matter (TOM) radiocarbon date of 13,200 y BP from lake sediments on a peninsula extending into Notre Dame Bay, with palynological evidence of a subsequent reversion to colder conditions and a return to the post-glacial warming trend by 10,500 y BP. These data indicate that an ice front to the west of the study area was near or inland of the position of the "line of (ice) retardation" (Lundqvist, 1965) by 12-13,000 y BP. The dates from outwash deltas suggest that relative sea level was above present sea level

at this time. If the end moraine within the study area is genetically equivalent to this line, then a similar chronology may be indicated for the Bonavista Bay region (Brookes, 1989).

Offshore, a number of previous studies from beyond the study area have provided insights into the glacial history of the NE Newfoundland shelf. Dale and Haworth (1979), Dale (1979), Mudie and Guilbault (1982) and Scott et al. (1984) all examined cores from the Notre Dame Channel, north of Notre Dame Bay. Cores from 50 km north of the coast contained till (Dale and Haworth, 1979) and, more specifically, lodgement till (Mudie and Guilbault, 1982) at their bases. Continuous deposition was inferred from the till to glaciomarine and Holocene sediments (Dale and Haworth, 1979). The till was correlated with a seismostratigraphic unit which is widespread across the shelf (Dale, 1979; Dale and Haworth, 1979). Four TOM radiocarbon dates were acquired from one of these cores (Dale, 1979; Mudie and Guilbault, 1982). The lowermost, from the top of a laminated sequence of greyish-red silt and clay, 1 m above the till, provided a date of 25,490 y BP (Dale, 1979). This was corrected by Mudie and Guilbault (1982) to between 18-19,000 y BP to account for older carbon. Another date, 40 cm above, was corrected to 16,980 y BP (Mudie and Guilbault, 1982). Amino racimization age estimation at this level indicated an age no greater than

15,000 y BP (Dale, 1979). From micropalaeontological and palynological evidence, Scott et al. (1984) interpreted that the till originated during ice recession in isotopic stage 3 (Middle Wisconsinan), followed by a warming interval, a return to glacial conditions (perhaps permanent floating ice cover) and finally transition into Holocene conditions. This model assumed that the TOM date of 25,490 y BP (Dale, 1979) is correct. Scott et al. (1984) acknowledge that this may not be so, and note that the warming sequence may represent Late Wisconsinan fluctuations, as suggested by the corrected dates of Mudie and Guilbault (1982).

Recent seismic surveys across the Northeast Newfoundland Shelf, east-northeast of Bonavista Bay, have provided evidence of Wisconsinan glaciation of the entire shelf (G. Fader, pers. communication, 1990). Huntec DTS and airgun data collected on cruise 89-006 of CSS Dawson indicate the presence of till tongues (King and Fader, 1986) and moraines on the shelf. From the relationship of till to glaciomarine sequences, G. Fader (pers. communication, 1990) has interpreted that a glacial retreat of probable Late Wisconsinan age occurred within the region.

Miller et al. (1985) and Miller (1987) interpreted the glacial to post-glacial palaeoceanography of the NE Newfoundland shelf, north and NE of Bonavista Bay, from foraminiferal data from nine cores at five sites. One core, from 180 km north of the Gander Peninsula, contained four

benthonic foraminiferal assemblages which were interpreted to represent a gradual transition (from base to top) from an ice marginal late Pleistocene environment to the present day Holocene, Inner Labrador Current environment. At the remaining sites, 100 km NE of Bonavista Bay, late Holocene assemblages were interpreted to unconformably overlie a late Pleistocene ice margin/cold shelf fauna (Miller, 1987). Macpherson (1988), however, argued from palynological evidence for continuous late Pleistocene to Holocene sedimentation, but with erosion of late Holocene sediments from some of the cores. Holocene sediments in most of the cores comprise a thin (< 0.5 m) package (Macpherson, 1988).

1.4.2 Regional Studies

As is the case elsewhere along the coast of Newfoundland, the timing and extent of the last glacial maximum in the region of Bonavista Bay are uncertain. Possible models for the study area are linked to the minimum and maximum views of Late Wisconsinan ice extent on the eastern Canadian continental margin (i.e.: Ives, 1978 and Flint, 1971 respectively). Relatively few models of glaciation prior to the Late Wisconsinan exist (i.e.: King and Fader, 1986).

Flint (1940, 1971) proposed the greatest coverage of Late Wisconsinan ice sheets across the island of Newfoundland, with Labrador-based ice inundating the island

and much of the continental shelf. The island may have been host to separate ice caps before being over-ridden. Within Flint's (1971) model, much of the Grand Banks, to the present day 200 m isobath, was ice covered at glacial maximum. The ice sheet occupied Bonavista Bay and extended approximately 20 km beyond the mouth of the bay. Flint (1971) allowed that the actual position of the margin anywhere on the coast was probably determined largely by calving rates. Many view this model as extreme (i.e.: Ives, 1978; Rogerson, 1982), although the maximalist viewpoint is nonetheless supported by a number of researchers (i.e.: CLIMAP Project Members, 1976; Hughes et al., 1977; Mayewski et al., 1981; Denton and Hughes, 1981a; Hughes et al., 1985). Within the maximum model of Denton and Hughes (1981a), the ice sheet extended approximately 100 km NE of Bonavista Bay. Mayewski et al. (1981) modelled an ice sheet of up to 1 km thickness over Bonavista Bay which extended 40 km NE of the bay. Recent work on the Scotian Shelf (King and Fader, 1988; Gipp, 1989; Gipp and Piper, 1989) does support the premise that a large amount of the continental shelf of eastern Canada was covered by grounded ice during the Late Wisconsinan.

The minimalist views have been typically represented by the work of Grant (1977), Ives (1978) and Dyke and Prest (1987). In these models, one or more separate ice caps existed on the island of Newfoundland, perhaps fronting

against the Laurentide Ice Sheet to the west. Ice extent on the continental shelf was limited. In NE Newfoundland, Ives (1978) modeled Late Wisconsinan ice from the center of the island extending across the southern portion of Bonavista Bay and ice from an Avalon Peninsula-based ice cap upon the Bonavista Peninsula. This model depicted parts of the Bonavista and Gander Peninsulas as coastal nunataks and a very large area in the eastern part of present day Bonavista Bay as being sub-aerially exposed. Grant (1977), with a similar ice distribution, proposed that the NE tips of the Bonavista and Gander Peninsulas were nunataks during the Late Wisconsinan and that the majority of Bonavista Bay was ice free. The model of Dyke and Prest (1987) mapped an ice front across the mouth of Bonavista Bay, with only the northeasternmost tip of the Bonavista Peninsula existing as a nunatak. The minimalist viewpoint has been supported by the theoretical isostatic modelling of Quinlan and Beaumont (1981, 1982).

Models such as those presented above generally deal with grounded ice on the continental shelf at the time of glacial maximum. Mayewski *et al*. (1981) and Denton and Hughes (1981b) have speculated that floating ice shelves may have played a large role in the Late Wisconsinan glaciation. As well, recent ideas on ice sheet dynamics have suggested that early deglaciation may have produced surging ice streams in the marine environment as early sea level rise

caused development of floating ice shelves. Reduced basal friction may have allowed a drawing down of ice from terrestrial sheets into the marine environment and the development of ice streams (Ruddiman and McIntyre, 1981; Mayewski et al., 1981; Denton and Hughes, 1983; Hughes, 1987).

Glaciations preceding the Late Wisconsinan have been discussed by relatively few authors (i.e.: Grant and King, 1984; King and Fader, 1986 and Andrews, 1987). During the Early Wisconsinan, the Laurentide Ice Sheet may have had equal or greater extent than during the Late Wisconsinan. On the eastern Canadian continental margin the boundaries of Early Wisconsinan ice have been modelled by Vincent and Prest (1987) as similar to those of the Late Wisconsinan maximalist model of Denton and Hughes (1981a), but with slightly greater ice coverage on the Grand Banks.

The Middle Wisconsinan, although generally considered to have been an ice recessional period, may have seen continued glaciation of much of northern and eastern Canada (Dredge and Thorleifson, 1987; Andrews, 1987). Three hypothetical models for Middle Wisconsinan glaciation were presented by Dredge and Thorleifson (1987), all of which display an ice cap on the island of Newfoundland which extended to just beyond the present coastline. In a different scenario, Grant and King (1984) speculated that a Middle Wisconsinan ice cap may have developed on the

continental shelf to the south of Newfoundland, advancing northward into Placentia Bay on the SW coast.

King and Fader (1986) presented a model in which glaciation of the eastern Canadian continental margin was continuous throughout the Wisconsinan. Their primary study area was the Scotian Shelf, although similar conditions were interpreted for the Grand Banks of Newfoundland. The Scotian Shelf/Grand Banks advance in the Early Wisconsinan saw development of a grounded, dry-based ice sheet across the shelf, between 70 and 50 ka BP. Increasing relative sea levels produced ablation, an ice shelf which was buoyant in deep basins by 46 ka BP and deposition of blanket till and lift-off moraines. Oscillations in the buoyancy line between 46-32 ka BP resulted in development of wedge-shaped till tongues at shelf edge and within basins. The ice shelf retreated between 32-16 ka BP to present day coastal areas (King and Fader, 1986). Much of the chronology for this model was based upon TOM radiocarbon dates. Recent studies on the Scotian Shelf, incorporating radiocarbon dates from shells, have indicated that the last major ice advance occurred on the Scotian Shelf at approximately 24 ka BP, with retreat occurring between 18-12 ka BP (King and Fader, 1988; Gipp, 1989; Gipp and Piper, 1989), altering significantly the chronology of King and Fader (1986).

1.5 Bathymetry

Bonavista Bay over most of its area is broad, open, and of variable depth (Fig. 1.4). Along the west and SW coast of the bay are a number of narrow, deep fjords. With the exception of these fjords, the majority of the bay is exposed to the North Atlantic. A slight rise in the seabed (to <250 m) in the NE serves to separate the bay from the deeper North Atlantic. In one northwestern area of this rise, a channel of between 250-300 m depth extends into the deeper region offshore (Figs. 1.4, 1.5).

The outer part of Bonavista Bay consists of both an open region, containing the broad Eastern and Western Basins (Fig. 1.4), and a series of inlets (or "reaches") between islands in the west of the bay. The Eastern and Western Basins are generally between 300 and 350 m deep and are separated by a broad rise at approximately 300 m depth. The Eastern Basin is 5-6 km wide and approximately 35-40 km long. It shallows from a maximum depth of over 320 m at its middle, becoming indistinct from the surrounding bathymetry in the NE. The Western Basin is poorly defined, with variable width and depths. Its SW end contains a narrow depression of up to 400 m depth which shallows and broadens to the NE. The middle of the basin is near 300 m depth and is largely recognizable as a continuation of this feature on the basis of seismic profiles rather than the present surface morphology. The basin deepens to 350 m to the NE,

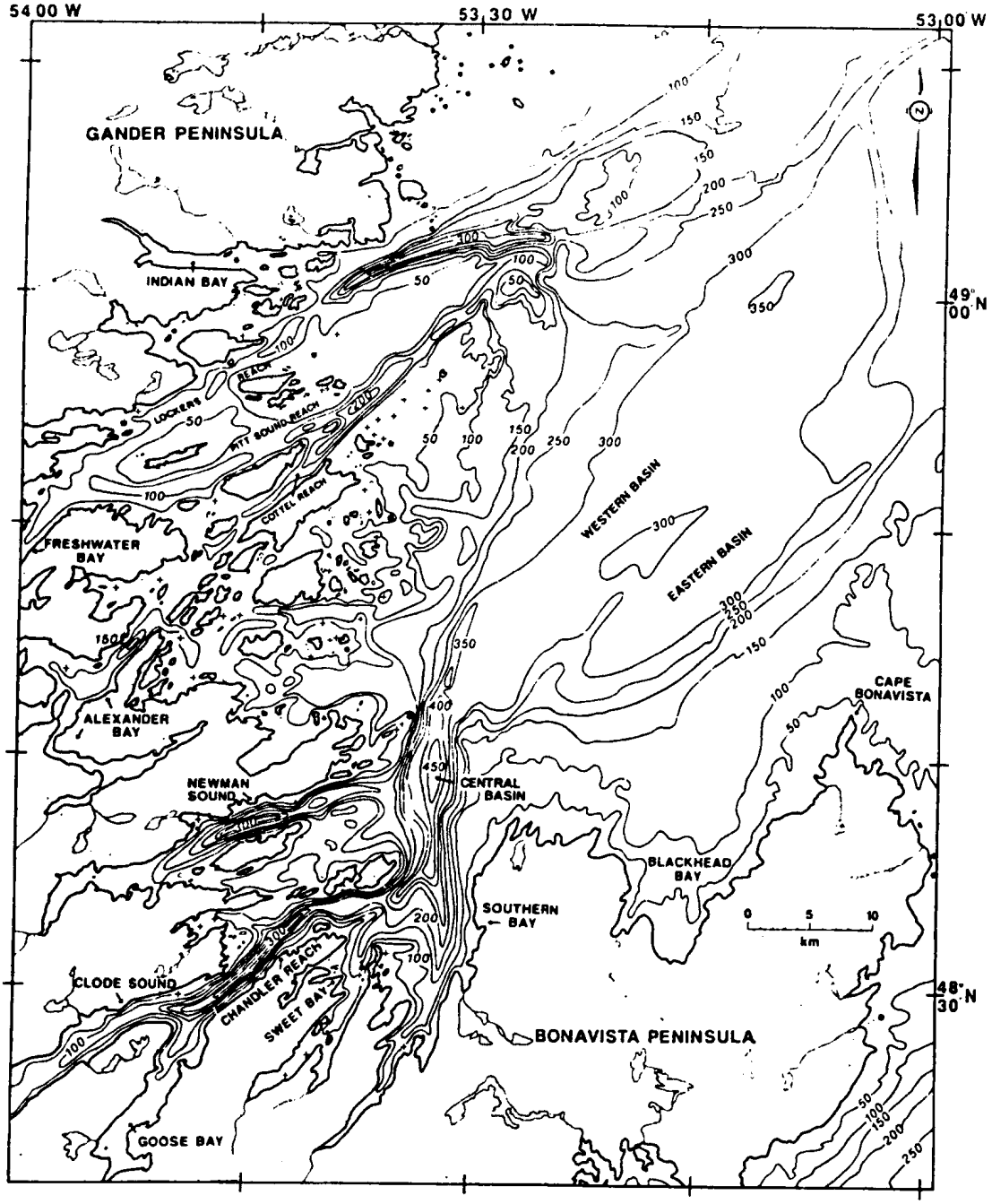

Figure 1.4. Bathymetric map of Bonavista Bay.

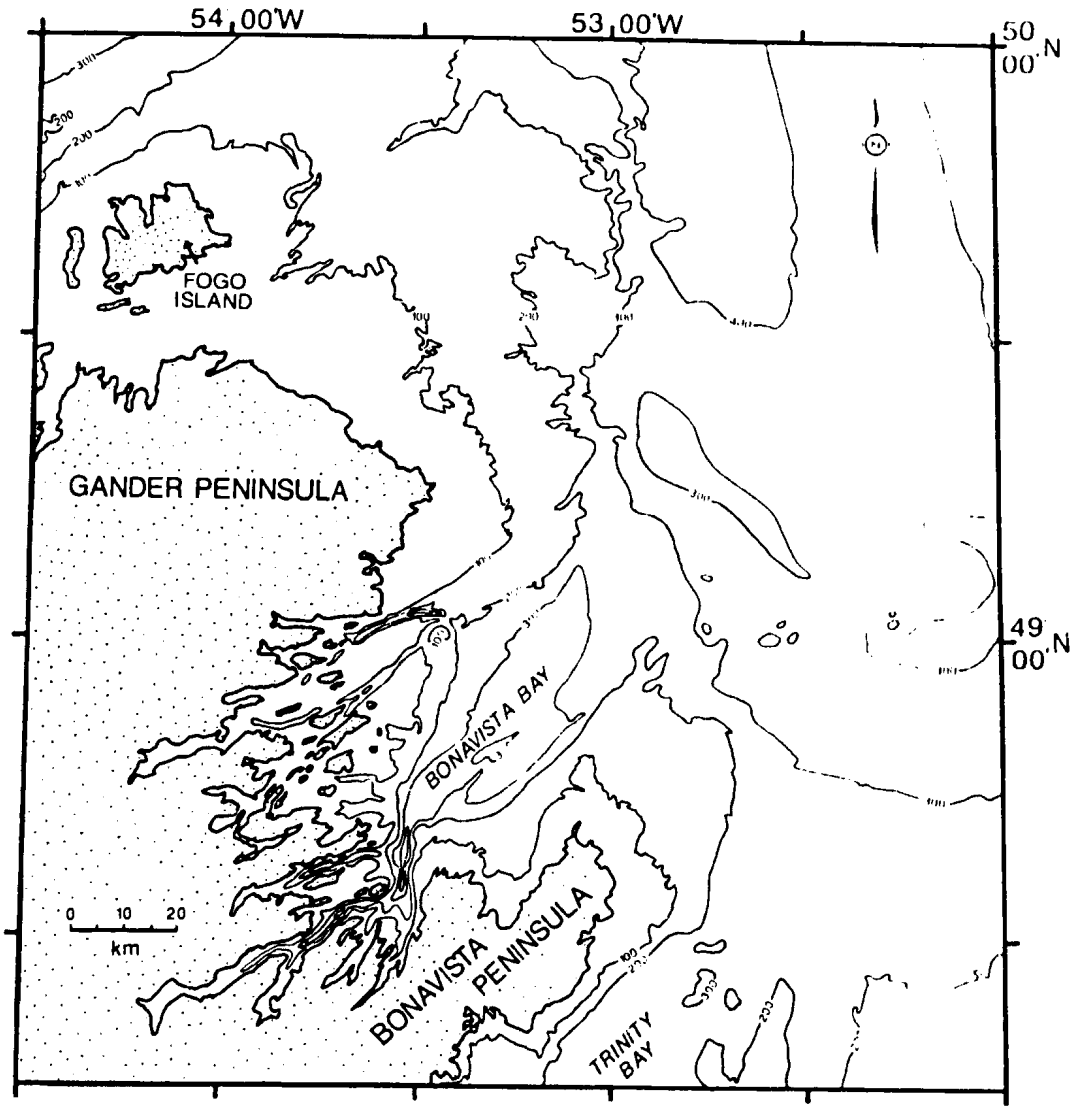

Figure 1.5. Bathymetric map of the Northeast Newfoundland Shelf in the region of the study area.

before becoming separated from the North Atlantic by the shallow rise to 250 m depth (Fig. 1.4).

The region to the west of the Western Basin is generally shallower than 100 m, especially in the vicinity of the numerous islands. There are, however, a number of inlets, two of which are especially deep and extensive. These extend to the SW and WSW and are over 200 and 300 m deep respectively (Fig. 1.4).

The inner area of the bay contains a number of narrow fjords which extend far into the coastline. These reach depths of >300 m and are separated from the rest of the bay by sills. This is evidenced in those fjords which have been surveyed for this study, namely Newman Sound and Clode Sound/Chandler Reach. The bathymetric map (Fig. 1.4) does not have the resolution to display these sills.

Between the fjords and the outer bay is the 450 m deep Central Basin (Fig. 1.4). A small sill at 350 m depth, observed within the seismic data, separates this feature from the outer bay (Western Basin).

1.6 Scientific Objectives

The objective of the present study is to address some of the uncertainties about the Late Quaternary history of Bonavista Bay which are described within Section 1.4. Specifically, the scientific objectives of the thesis are as follows: i) to establish a seismic stratigraphic framework

within Bonavista Bay through the interpretation of high-resolution seismic reflection data, ii) to identify lithofacies within piston cores and correlate them with the seismic stratigraphy, iii) to use AMS radiocarbon dates to establish a chronostratigraphy, iv) to interpret the glacial and sedimentary history of Bonavista Bay and v) to compare this model with existing models of glaciation(s) within the region and on the eastern Canadian continental margin.

CHAPTER 2

DATA COLLECTION AND ANALYSIS

2.1 Field Studies.

Seismic reflection data and piston cores were collected during cruises 86-026 and 87-030 of CSS Dawson and cruise 87-033 of CSS Hudson to Bonavista Bay. The survey of greatest extent was conducted during cruise 86-026, when approximately 430 line km of continuous seismic data were collected, using a 3.5 kHz Oceans Research Equipment sub-bottom profiler and a 40 cubic inch (in^3) airgun with a Benthos multi-element streamer (Fig. 2.1). Average ship's speed was 5.5 knots.

During cruise 86-026, a network of gravity readings was also collected on a grid of 5.6 km spacing throughout and north of Bonavista Bay. Continuous operation of the 3.5 kHz system provided a large volume of data between stations (Fig. 2.2). Although of substantially lower quality than the main seismic lines, these data provided indications of sediment thicknesses and distribution over a very large area. Rapid speed variations, from 0 to 13 knots, however, made accurate mapping of this information difficult.

Positioning during cruise 86-026 was accomplished by a "Mini Ranger" system with three transponders, Loran "C", satellite navigation and radar fixes. The transponders were situated at known sites along the coast by a geophysical

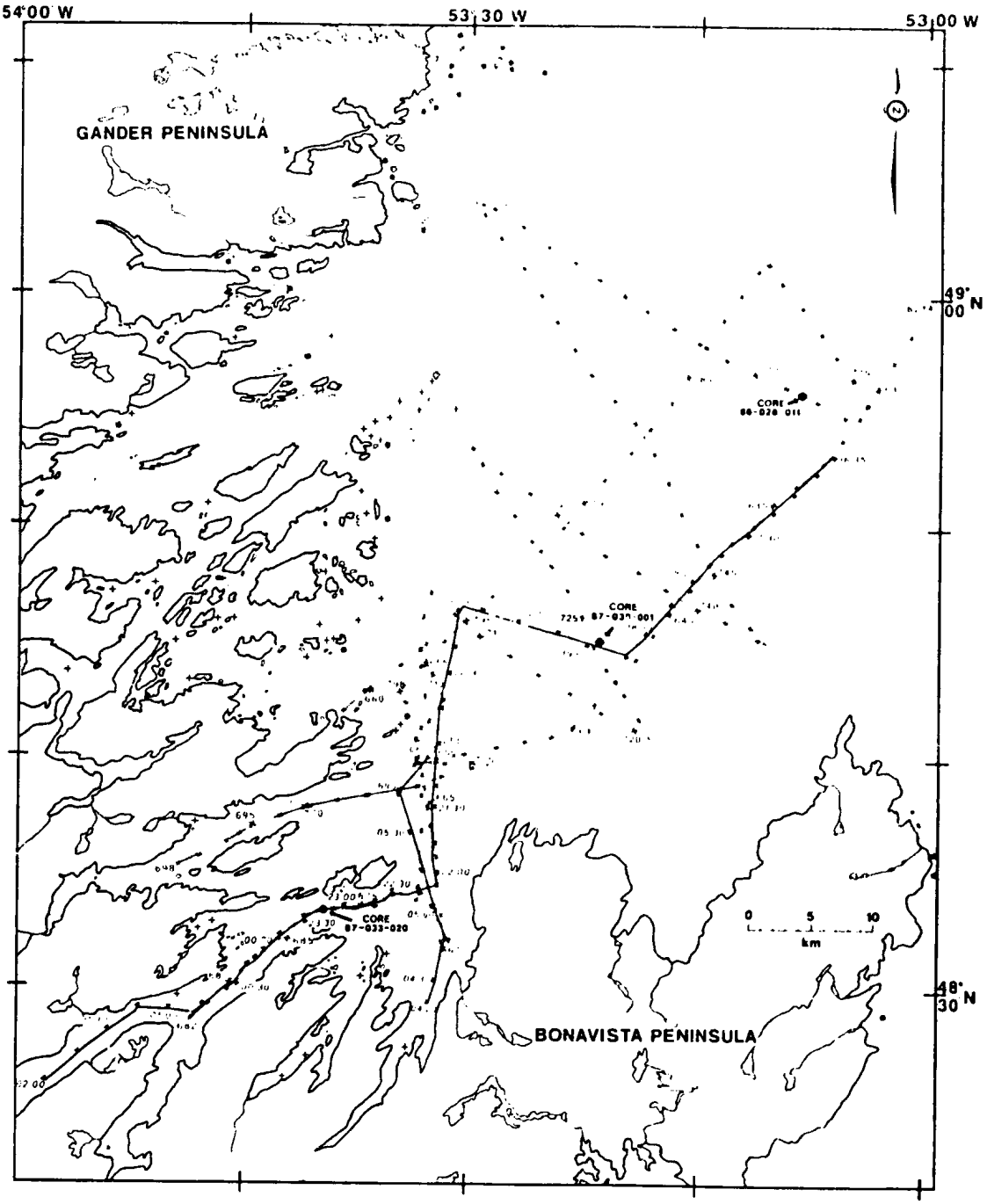

Figure 2.1. Map of the primary seismic survey coverage and core sites within the study area.

= Dawson 86-026 survey grid; (3.5 kHz and airgun data).

= Hudson 87-033 survey lines; (Huntec and airgun data).

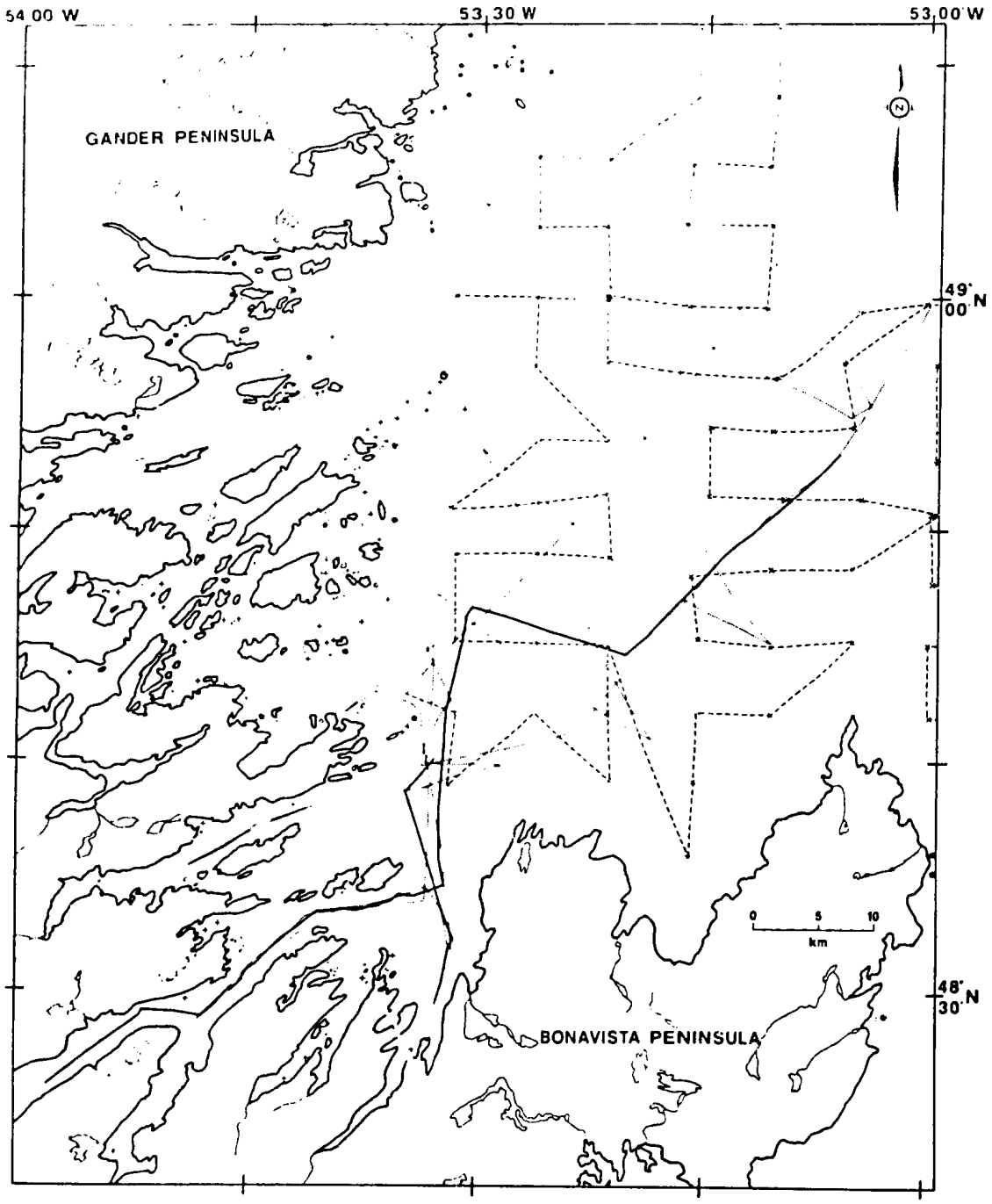

Figure 2.2. Map of secondary 3.5 kHz data coverage, superimposed on primary seismic survey grid.

x = gravity station.

---------- = 3.5 kHz high speed data.

land party. Where triangulation was achieved, fixes from this system provided accuracy to within 10 m. In topographically sheltered regions, such as Chandler Reach and Newman Sounds, radar fixes were generally the only means of positioning, with an accuracy considered to have been between 300-500 m. Loran "C", used in intermediate situations and when transponders were not operational, is normally considered accurate to within 50 m (95 % confidence). Satellite navigation fixes were received sporadically and were used to check the positioning.

Seismic data was recorded on EPC graphic recorders. A half second sweep rate with variable delays was used for both the 3.5 kHz and airgun surveys. The records were annotated every fifteen minutes and upon changes of course. Separate notation was made of ship's speed and heading, distance from start of survey, watchkeepers, operational systems and when available, transponder ranges. The positions of each fix were calculated upon completion of the survey, when a track plot was generated (Fig. 2.1). The mean distance between fixes was 2.5 km. In cases where fixes were not available from any of the navigational systems, fix locations were interpolated on the basis of heading and distance covered since the previous fix. Such positions were checked back with inverse bearings from later fixes and with seismic cross-overs where possible.

During CSS Dawson cruises 86-026 and 87-030, two 5.6 m

long Benthos piston cores (86-026-011; 87-030-001) were collected from the mid/outer region of Bonavista Bay (Fig. 2.1).

During CSS Hudson cruise 87-033, 115 line km of additional seismic data were collected using a Huntec Deep Towed System (DTS) (Hutchins et al., 1976) as well as a 10 in^3 airgun and Bedford Institute of Oceanography 25', 100' and Benthos multi-element streamers (Fig. 2.1). The Huntec DTS utilized both an internal hydrophone and an external streamer, the input from each being recorded on separate EPC recorders. Coverage from this survey repeated certain segments of the main seismic lines from the previous year for comparison of the Huntec DTS data with existing 3.5 kHz and airgun data. The Huntec DTS data was recorded at a quarter second sweep (250 ms), while the airgun was recorded at a 1 second sweep. Average ship's speed was 6 knots. Automatic record annotations were made every five minutes. Navigation relied on Loran "C" in the outer regions of the bay and on radar fixes in the inner reaches.

During cruise 87-033, a 14.5 m long wide diameter core (87-033-020) was collected from Chandler Reach using the Long Core Facility (LCF) system (Fig. 2.1).

2.2 Seismic Data Analysis.

The seismic data, contained on rolls of EPC paper, were reproduced as transdex copies at a 50 % reduction. Diazo

blueline working copies were produced from these.

The seismic data were analyzed using both reflection correlation and sequence stratigraphic methods (i.e.: Vail et al., 1977; King and Fader, 1986). As discussed in Chapter 3, seismic sequences within individual basins in the study area cannot be directly correlated. Within each basin, "seismic units" were defined on the basis of the presence or lack of coherent reflections within a unit (either acoustically stratified or acoustically transparent), reflection intensity (low, moderate or high), reflection continuity and spacing. For example, a sequence of continuous, moderate intensity reflections would constitute a seismic unit, as long as this character was distinct from over and underlying sequences. The upper and lower boundaries of a unit generally correspond to an individual continuous or semi-continuous reflection, which was correlated throughout each individual basin.

Depths are measured in milliseconds, two-way-travel-time (ms). Multiplication of millisecond values by 0.75 will provide an approximate conversion to metres, assuming an acoustic velocity of 1500 metres per second.

2.3 Laboratory Analysis.

2.3.1 Magnetic Susceptibility Testing

Whole core magnetic susceptibility measurements were

carried out on core 87-033-020 by Frank Hall of the University of Rhode Island, immediately following collection. This data provided support for later identification of lithofacies within the core.

2.3.2 Core Description

All three cores were immediately split in the laboratory into working and archive halves. The surface of the working half was cleaned with a spatula and X-rayed. The cores were described in terms of lithology, internal structure, colour and bioturbation, utilizing both the cleaned surface and X-radiographs. Colours were classified on the basis of the Rock Colour Chart distributed by the Geological Society of America.

2.3.3 Sampling.

The working halves of the cores were sampled for sedimentological, mineralogical and palynological analyses. Cores 86-026-011, 87-030-001 and 87-033-020 were systematically sampled at 100 cm, 50 cm and 75 cm intervals, respectively. Sampling density was increased near distinct lithological boundaries. Sub-samples were occasionally collected in laminated core sections. A 1 m interval was chosen for 86-026-011 because of the apparent homogeneity of sediment throughout the core. Core 87-033-020, 14.5 m long, was sampled every 75 cm, rather than every 50 cm, to limit

the number of samples for processing. Two separate samples were taken at each level for i) general sedimentological and mineralogical analyses and ii) palynological analysis. Ten to 25 cubic centimetres (cc) of sediment was removed from the cores for general sedimentological and mineralogical analyses. Three to 10 cc samples were collected for palynological analyses using a syringe with the needle tip removed. Both sets of samples were oven dried for a day at 30°C and weighed.

Six additional samples in the form of rectangular slabs (average dimensions: 4 x 2 x 0.8 cm) were collected from between 0.8 and 3.3 m depth in core 87-030-001 for the purpose of thin-section preparation.

2.3.4 Sampling for Radiocarbon Dating

Seven samples were selected for submission to laboratories for radiocarbon dating. Six of the seven consisted of shells or shell fragments, all of which required accelerator mass spectrometry (AMS) techniques. One shell sample was found to be too small for analysis. The seventh was a bulk sediment sample submitted for TOM dating which was found to contain insufficient carbon. The shells were all removed with a spatula, washed in tap water, dried and weighed. The five shell samples which yielded dates all were reported to have had problem-free analyses. Three of the five were submitted to Beta Analytic Inc. of

Coral Gables, Florida, while two were submitted to Isotrace Laboratory at the University of Toronto.

2.3.5 Sedimentological/Mineralogical Processing and Analyses.

Samples were first treated with hydrogen peroxide to destroy organic material. They were then disaggregated in water with 10 cc of 1% Calgon (sodium hexametaphosphate) and wet sieved through a 63 μm screen. The coarse fraction was oven dried and weighed, while the fine fraction was contained in one litre graduated cylinders. Additional, measured amounts of Calgon were added to completely disaggregate the silt and clay-sized fractions. At this point, water was added to the cylinders to bring the level to the one litre mark.

Grain size analysis of the <63 μm fraction was carried out using the pipette technique described by Carver (1971) and Piper (1974). The >63 μm size fractions were wet sieved, dried and weighed. The weight percentage of each phi (Φ) interval was then calculated.

Following the pipette analyses, the fluid level was returned to the one litre mark on the graduated cylinders with the addition of water and additional Calgon. They were stirred vigorously and allowed to settle for sixteen hours, prior to siphoning off the upper 20 cm of liquid. Flocculation of the sediment in this removed liquid (clay-size fraction) was induced by the addition of 10 cc of

saturated $MgCl_2$ solution. After settling was complete, much of the overlying clear water was decanted and samples were transferred to 250 cc centrifuge tubes, where they were spun at 3000 rpm for ten minutes. The clay was finally transferred to 50 cc vials.

Samples were prepared for x-ray diffraction analysis by smearing a small amount of clay over glass slides using a piece of acetate film. The slides were initially air dried and then placed in a desiccator for a minimum of one day. All analyses conducted used a Phillips x-ray diffractometer with a Cu tube. The desiccated slides were run from 2° to 32° 2θ at 1° 2θ per minute, 1000 or 2000 counts s^{-1} (cps) and a paper speed of 600 mm/hour. This produced a diffractogram where the vertical scale was either 1000 or 2000 cps and the horizontal scale was 1 cm per degree 2θ. The slides were re-run from 24° to 26° 2θ at 1/4° 2θ per minute. Slow scans allow a distinction between ~3.54 Å chlorite and ~3.58 Å kaolinite peaks (Biscaye, 1965). The slides were subsequently glycolated in an oven for 24 hours at 60°C and re-run from 2° to 32° 2θ at 1° 2θ per minute. Semi-quantitative calculations of the relative abundances of smectites, illite, chlorite, kaolinite, quartz, plagioclase and K-feldspars, amphiboles, calcite and dolomite were made using weighted peak areas and the appropriate intensity factors (as per Piper, 1974).

2.3.6 Thin-Section Preparation.

Six dried samples from core 87-030-001 were impregnated with epoxy resin. The samples were placed in an evacuated chamber in a bath of ultra-low viscosity epoxy resin (L.R. White; London Resin Co.) until no bubbles could be seen to escape the samples. The chamber was placed overnight in an oven at 60° C to cure the resin. The samples were cut, mounted on glass slides and polished.

2.3.7 Palynological Processing and Analyses.

Twenty four samples were processed for palynological analysis using the methodology of Dr. E. Burden of Memorial University of Newfoundland and with the assistance of Mr. Brian Sears, also of Memorial. Six lycopodium tablets were initially introduced as a pollen standard to each sample, providing easily recognizable grains and a known standard pollen concentration. Any carbonates present were destroyed using 2.7M cold HCl (hydrochloric acid) for two hours. The samples were repeatedly cleaned by rinsing and centrifuging. The silicates were next removed by concentrated cold HF (hydrofluoric acid), with the samples allowed to stand in solution overnight. Slides were prepared on three occasions for each sample: the first slide was prepared immediately following the above procedure. The samples were next sieved through 10 μm sieve cloth and then placed back in HF. The residues were cleaned and the second

slides made. Cellulose material and iron sulphides were then removed by use of $HC_2H_3O_2$ and HNO_3, respectively. Upon final cleaning, three more slides were made for each sample, bringing the total number to five.

Slides from the final stage were examined to determine the relative abundances of pollen/spores and dinoflagellates to standard exotic lycopodium spores for each sample. A Reichert "Zetopan" microscope set up for palynological work was utilized. For the purposes of this part of the study all pollen/spores were grouped together, as were all dinoflagellates. A count of 200 lycopodium grains was considered the minimum acceptable for each slide.

CHAPTER 3

SEISMIC STRATIGRAPHY

3.1 Sediment Distribution.

Regions of Bonavista Bay in which water depth exceeds 200 m are usually host to accumulations of sediment overlying the acoustic basement. The thickness of this sediment ranges from less than 10 milliseconds two-way-travel-time (ms) to over 250 ms, dependant on location within the bay. Shallower regions contain only isolated pockets of sediment over acoustic basement.

The majority of sediments are confined to a number of basins within Bonavista Bay (Fig. 3.1). These basins are best defined by the topography of the underlying acoustic basement, although most are also apparent in present day bathymetry (Fig. 1.4). The seismic sequence observed in each basin is isolated from neighbouring basins, making direct correlation difficult.

The "inner" region of the bay (defined here as lying SW of a line between Great Black Island and Western Head; Fig. 3.1), is characterized by narrow (<3 km wide), deep basins in which sediment thickness often exceeds 150 ms. The sediments in these basins often abut sharply against sills and side walls, a morphology best defined within the surveyed fjords of Newman Sound and Chandler Reach. The Central Basin, between the fjords and outer bay, is a deep,

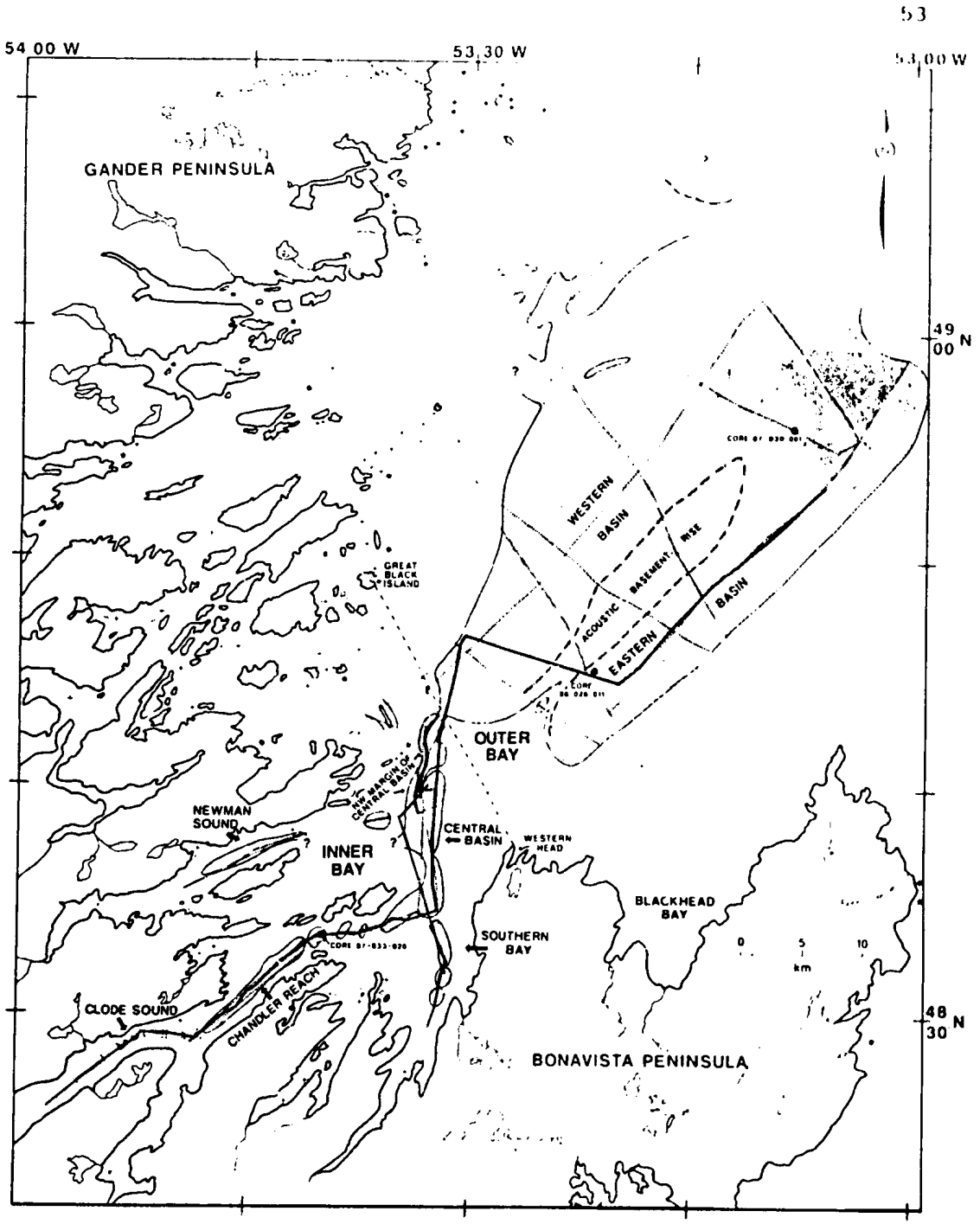

Figure 3.1. Location map of basins discussed in text, superimposed upon the track plot of primary seismic coverage. The outer boundary of the basins corresponds with the <2 ms contour of total sediment thickness maps (Chapter 5; figures 5.1, 5.2)

largely infilled depression with apparently semi-continuous ledges along its margin, defined by acoustic basement and generally host to substantial sediment accumulations. At the northern end of the Central Basin, a broad acoustic basement rise forms the boundary between the inner and the outer bay. At the mouth of Southern Bay (south of the Central Basin) are three shallow basins, separated by low rises in acoustic basement (Fig. 3.1).

The "outer" region of the bay is characterized by a broad depression with maximum sediment thickness of 70 ms. The sediments largely occur within the NE-SW oriented Eastern and Western Basins (Fig. 3.1). These are separated by a shallow acoustic basement rise, across which a thinned sediment package (average thickness of 20 ms) extends.

To the N-NW of the outer region, sediment cover extends almost to two deep, narrow troughs which occur on the western side of the bay. Sediments within these troughs were observed during a single traverse west of the primary survey region. A spoon-shaped zone furthest north within the study area, east of the Gander Peninsula, contains thin (<20 ms), patchy deposits which have been tentatively mapped on the basis of 3.5 kHz data collected at high speed.

The shape and continuity of basins shown in figure 3.1 are approximate. Some smaller, low relief depressions are undefined by the contour interval of the hydrographic charts (Fig. 1.4), especially where they are largely infilled.

3.2 Acoustic Basement

Acoustic basement is defined as the horizon where total reflection of the energy of the seismic reflection systems occurs and no deeper internal structure is revealed. The depth to acoustic basement varies with the frequency of the survey equipment used. Of the three types utilized, the system with the highest frequency, lowest energy and least penetration is the 3.5 kHz O.R.E. sub-bottom profiler. This system is commonly unable to penetrate a compacted glacial till (i.e.: Bell *et al.*, 1987). Therefore, if a compacted till were present, acoustic basement would likely be interpreted along its upper surface. The Huntec DTS acoustic pulse has greater penetration and can be expected to define bedrock beneath several metres of till. The airgun system has the greatest penetration, although resolution is greatly reduced. Acoustic basement has been interpreted from the airgun data unless otherwise noted in the discussion.

Within the basins of the outer bay, acoustic basement is undulatory, with moderately rounded highs of up to 12 ms relief possibly forming NE-SW trending linear ridges. If so, they parallel strike of regional bedrock and are likely bedrock related. In the inner region of the bay the acoustic basement is irregular, with abundant peaks of over 100 ms height forming sills between and occasionally within basins. Acoustic basement defines a ledge along the side

walls of the Central Basin. This feature has been infilled with sediment (Fig. 3.2) and occurs with variable continuity and scale on either side of the basin, although it is most common on its western side.

3.3 Seismic Units

Sediments within individual basins in the study area cannot be directly correlated. Sequences observed in each basin are therefore divided into "seismic units" and discussed separately. As outlined in Section 2.2, a seismic unit is defined primarily on the basis of its acoustic character and, to a lesser extent, on its relationship to surrounding seismic units. Differentiation into seismic units is easiest with the 3.5 kHz data, although the units appear on data from all three survey systems. In comparison, Huntec DTS data coverage is limited, while the airgun data does not resolve units as clearly. Therefore the acoustic stratigraphy is described mainly on the basis of the 3.5 kHz data, with reference to Huntec DTS and airgun data where possible.

3.3.1 Morphological Description

The morphology of a seismic unit is an important part of its description, as it is an indicator of possible depositional processes. Unit morphology incorporates the shape and thickness of units relative to variations in the

Figure 3.2. East-West 3.5 kHz profile of the Central Basin, displaying ledges commonly associated with this feature. The western ledge is often present elsewhere in the basin, while the eastern ledge is absent. Acoustic basement in mid-basin is defined on the basis of airgun data. V.E. = vertical exaggeration. Depth in milliseconds two-way-travel-time.

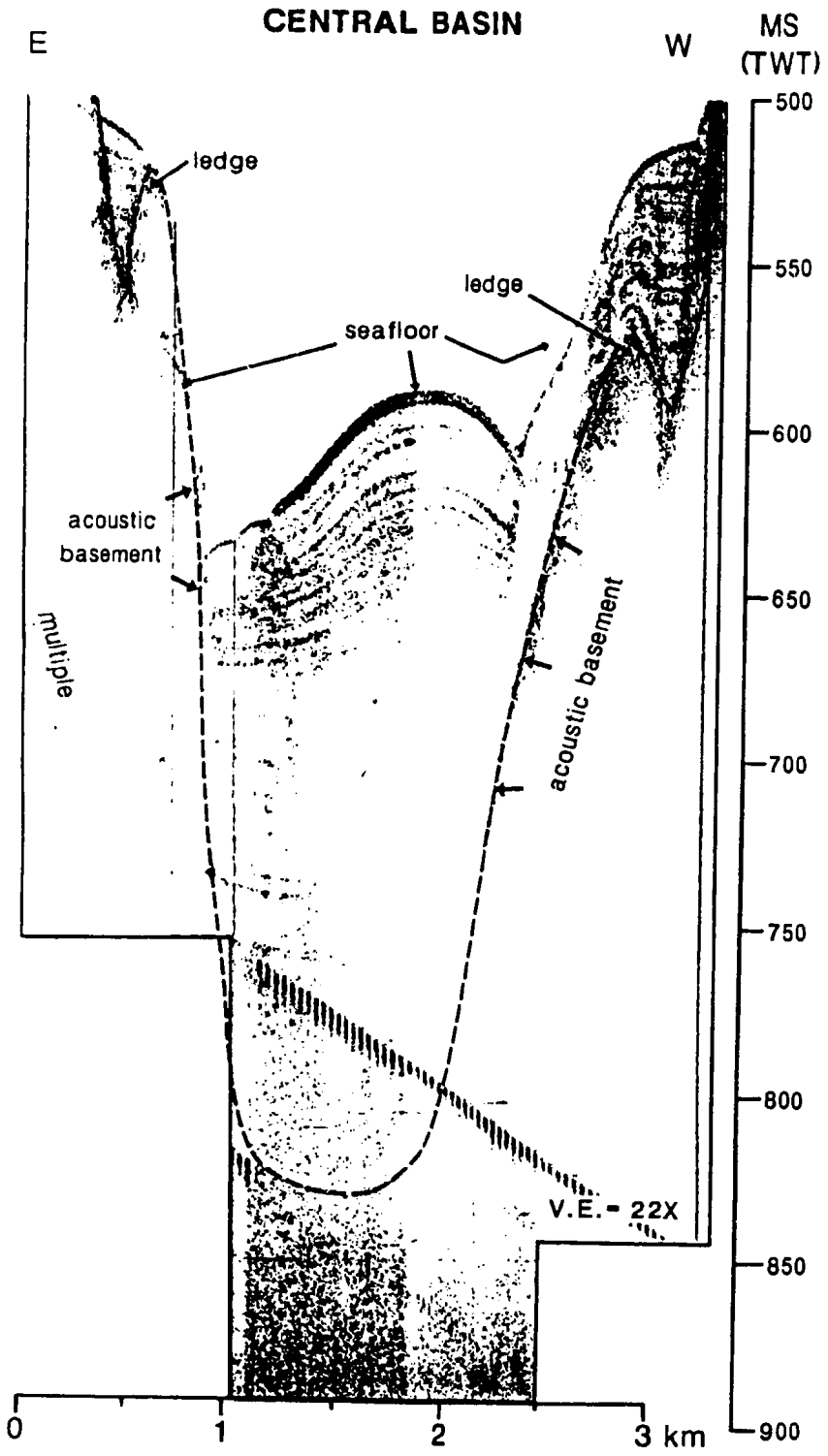
CENTRAL BASIN
E
W
MS
(TWT)
500
550
600
650
700
750
800
850
900
ledge
ledge
seafloor
acoustic
basement
multiple
acoustic basement
V.E. = 22X
0
1
2
3 km

surface on which they lie, as well as the relationship of reflections within a unit to other reflections and to the unit boundaries. In the case of an acoustically transparent sequence, the unit morphology is defined by the upper and lower boundaries. The morphological terms used, with one exception, are those of Barrie and Piper (1982) and Syvitski et al. (1987) (Fig. 3.3).

A unit which has a conformable morphology is ideally of equal thickness within and outside of a basin. Reflections within the unit do not onlap the underlying surface or converge. A unit with draping basin-fill morphology may display converging reflections (perhaps onlapping other reflections within the unit), or reflections onlapping the underlying surface as thinning occurs on the basin margins. "Draping basin-fill" has been substituted for "onlapping basin-fill" (Barrie and Piper, 1982) to avoid the implication that onlapping reflections are always present. A ponded morphology indicates that reflections abut an underlying surface at the basin margins and are confined to within the basin.

Differentiation of unit morphologies is occasionally dependant on the ability of the seismic systems to resolve the reflections as they converge or onlap. The Huntec DTS is theoretically able to resolve reflections spaced as closely as 6-8 cm (Hutchins et al., 1976). In reality this is partially dependant on the printing resolution of the EPC

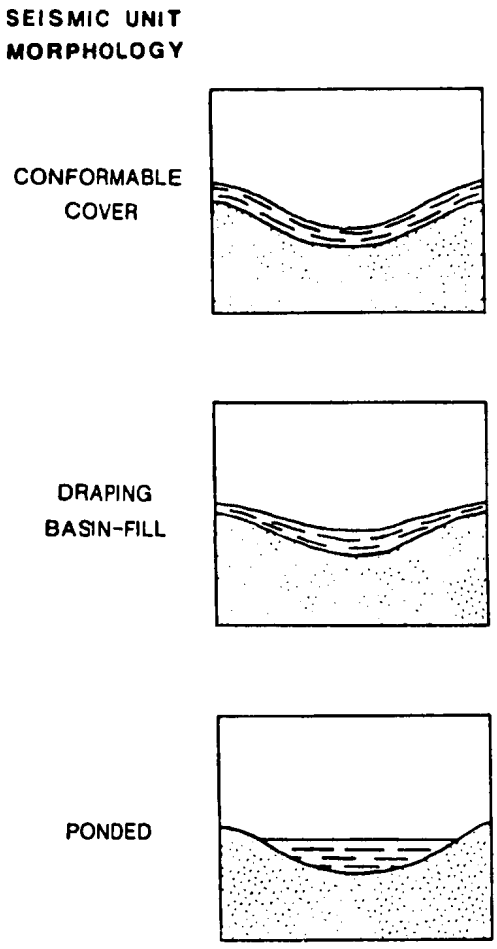

Figure 3.3. Idealized representations of the seismic unit morphologies discussed in text. Modified from Barrie and Piper (1982) and Syvitski et al., (1987).

recorder (Gipp, 1989). The 3.5 kHz system has a theoretical resolution of half the signal wavelength, which is equivalent to 21 cm at an acoustic velocity of 1500 m/s. The resolution of the airgun is much less.

3.4 Individual Basin Descriptions

The locations of seismic reflection profiles presented within this section are displayed in figure 3.4, with the exceptions of figures 3.5, 3.11 and 3.12, each of which contain profiles from more than one basin. The discussion is divided into two parts; the first dealing with basins in the outer bay, the second with basins in the inner bay. As mentioned in Section 3.3, the acoustic character is described from the 3.5 kHz data unless otherwise noted.

3.4.1 Outer Bay

There are three seismic units (1 to 3) in each of the Eastern and Western Basins in the outer bay. These are tentatively correlated between the two basins on the basis of their acoustic character and morphology (Fig. 3.5).

Unit 1, the basal unit, is generally <15 ms thick and acoustically incoherent. A number of low to moderate intensity reflections of variable continuity are often present. It has a draping basin-fill morphology, although uppermost reflections occasional , abut the 3.5 kHz acoustic basement at the basin margins. Therefore, unit 1 on the

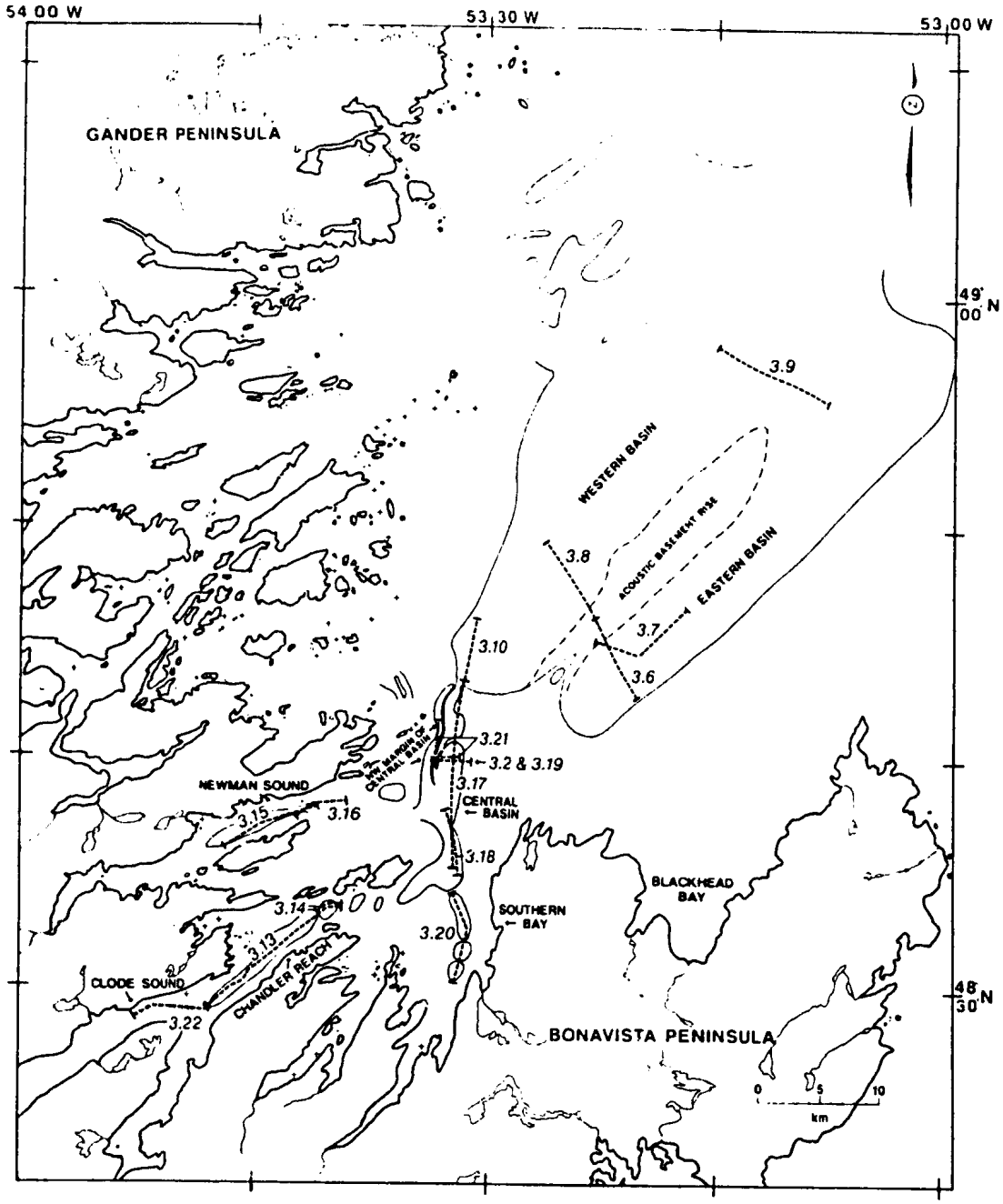

Figure 3.4. Index map displaying the locations of seismic reflection profiles presented in figure 3.2 and figures 3.5 to 3.21 (excluding figures 3.5, 3.11 and 3.12).

Figure 3.5. Tentative correlation of seismic units observed within the main basins of outer Bonavista Bay. Basin locations illustrated in figure 3.1. Acoustic basement on the airgun data is deeper than that of the 3.5 kHz data by 8 ms and 5 ms in the Eastern and Western Basins respectively. Note the greater extent of unit 1 upon the basin margins as displayed on the airgun data. Dashed line denotes tentative seismic unit boundaries. 3.5 kHz and airgun data from C.S.S Dawson cruise 86-026. V.E. = vertical exaggeration. Depth in milliseconds two-way-travel-time.

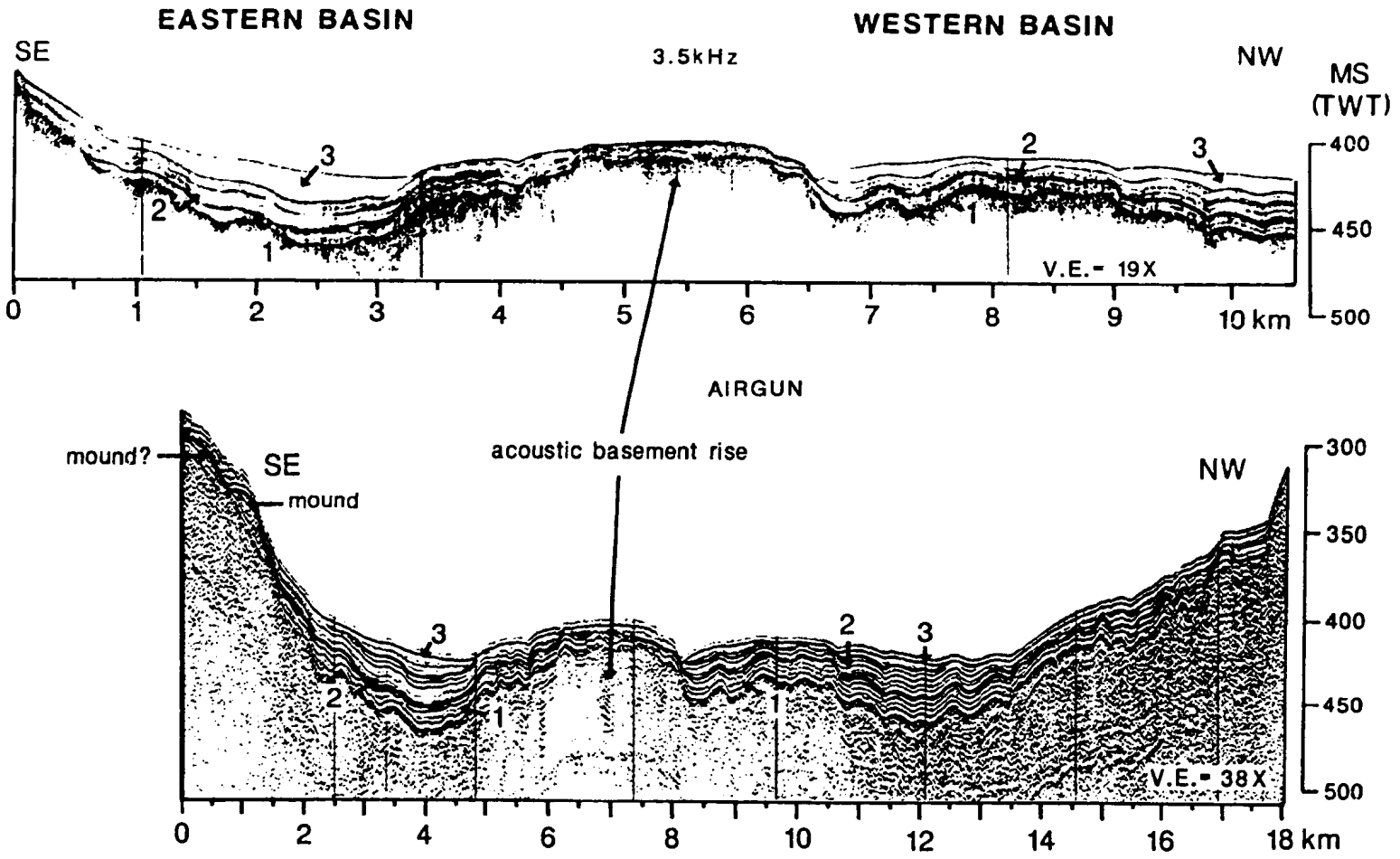
EASTERN BASIN
WESTERN BASIN
SE
3.5kHz
NW
MS
(TWT)
400
450
500
V.E.- 19X
0
1
2
3
4
5
6
7
8
9
10 km
AIRGUN
mound?
SE
mound
acoustic basement rise
NW
300
350
400
450
500
V.E.- 38X
0
2
4
6
8
10
12
14
16
18 km

3.5 kHz data appears ponded in some areas. Airgun data reveals an acoustic basement 5 to 8 ms deeper than that of the 3.5 kHz and Huntec DTS data, with the interval between containing one or more high intensity, continuous coherent reflections. Also included in unit 1 are acoustically incoherent lens-shaped mounds (Fig. 3.5; airgun data) which overlie the acoustic basement identified on the Huntec DTS data, but which the 3.5 kHz system is unable to penetrate.

Unit 2 is acoustically stratified and composed of moderate to high intensity, parallel, continuous, coherent reflections. It is commonly 15-20 ms thick. Unit 2 has a draping basin-fill morphology, extending onto the basin margins and across the rise between the two main basins. Individual reflections cannot be traced between the basins.

Unit 3 is acoustically transparent, with the characteristic exception of one or more low to moderate intensity reflections near mid-package. It is between 10 and 20 ms thick in the center of the basins. Although the present distribution appears largely limited by erosion to the central regions of the basins and pockets on the margins, the morphology of unit 3 most closely resembles draping basin-fill.

EASTERN BASIN

Unit 1 occurs throughout the Eastern Basin. It is acoustically incoherent, but contains a number of low to

moderate intensity reflections of variable continuity (Fig. 3.6). Unit thickness averages 15 ms in the center of the basin, but varies over undulations in acoustic basement and at the basin margins. On the 3.5 kHz data, reflections within the unit occasionally abut the 3.5 kHz acoustic basement (i.e.: Fig. 3.6; 5 km along track). This is most consistently observed in a low intensity, semi-continuous reflection, 2 to 4 ms above this acoustic basement. In some regions of the basin, the uppermost surface of unit 1 onlaps the basin margin, so that unit 1 on the 3.5 kHz data is limited to within the basin and has a ponded morphology (Fig. 3.6; 1.5 km along 3.5 kHz track). Commonly, basal reflections on the airgun data extend further out of the basin (Fig. 3.6), indicating a draping basin-fill morphology for the overall unit. Within the 3.5 kHz data, the entire seismic sequence becomes indistinct on the basin margin and over the acoustic basement rise between basins, making it difficult to discriminate the individual units (i.e.: Fig. 3.6; 5.5 km to end of 3.5 kHz track).

There are a number of distinct mounds and lens-shaped zones within unit 1 (Figs. 3.7, 3.6 and 3.5). The majority are acoustically incoherent, lens-shaped mounds overlying the acoustic basement on the Huntec DTS data and over which reflections of unit 1 conformably drape. These mounds are not resolved on the 3.5 kHz data (Fig. 3.6). There are also downwardly concave, lens-shaped zones (Fig. 3.7). Some are

Figure 3.6. 3.5 kHz and airgun profiles within the Eastern Basin. Location shown in figure 3.4. Seismic units 1 to 3 are discussed in text. Note the greater extent of unit 1 upon the basin margins as displayed within the airgun data. Dashed line denotes tentative seismic unit boundaries. V.E. = vertical exaggeration. Depth in milliseconds two-way-travel-time.

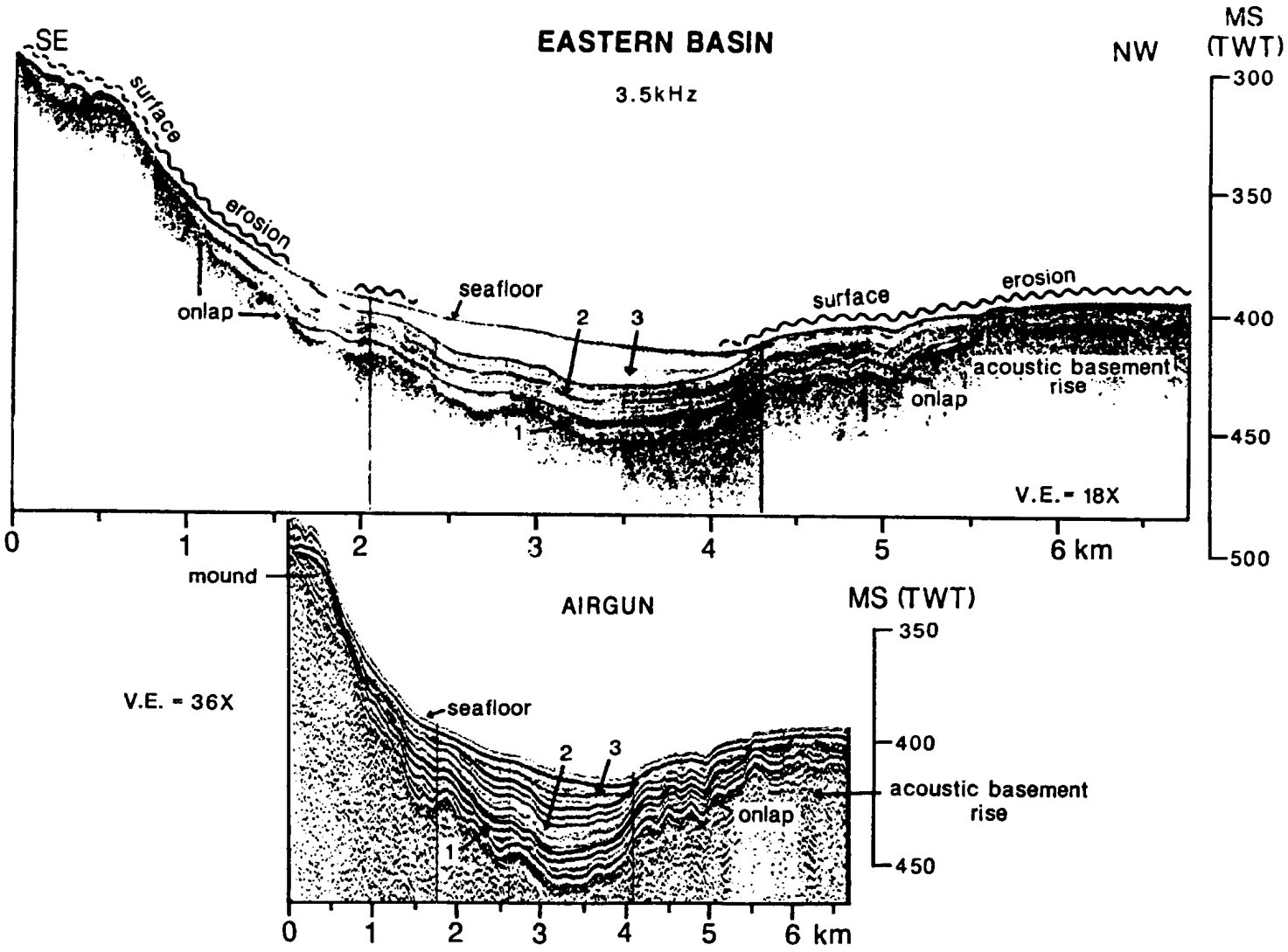
EASTERN BASIN
3.5kHz
SE
NW
MS (TWT)
300
350
400
450
500
surface
erosion
onlap
seafloor
2
3
1
surface
erosion
acoustic basement rise
onlap
V.E.= 18X
0
1
2
3
4
5
6 km
mound
AIRGUN
MS (TWT)
350
400
450
V.E. = 36X
seafloor
2
3
1
onlap
acoustic basement rise
0
1
2
3
4
5
6 km

Figure 3.7. Huntec DTS profile within the Eastern Basin. Location shown in figure 3.4. Seismic units 1 to 3 are discussed in text. V.E. = vertical exaggeration. Depth in milliseconds two-way-travel-time.

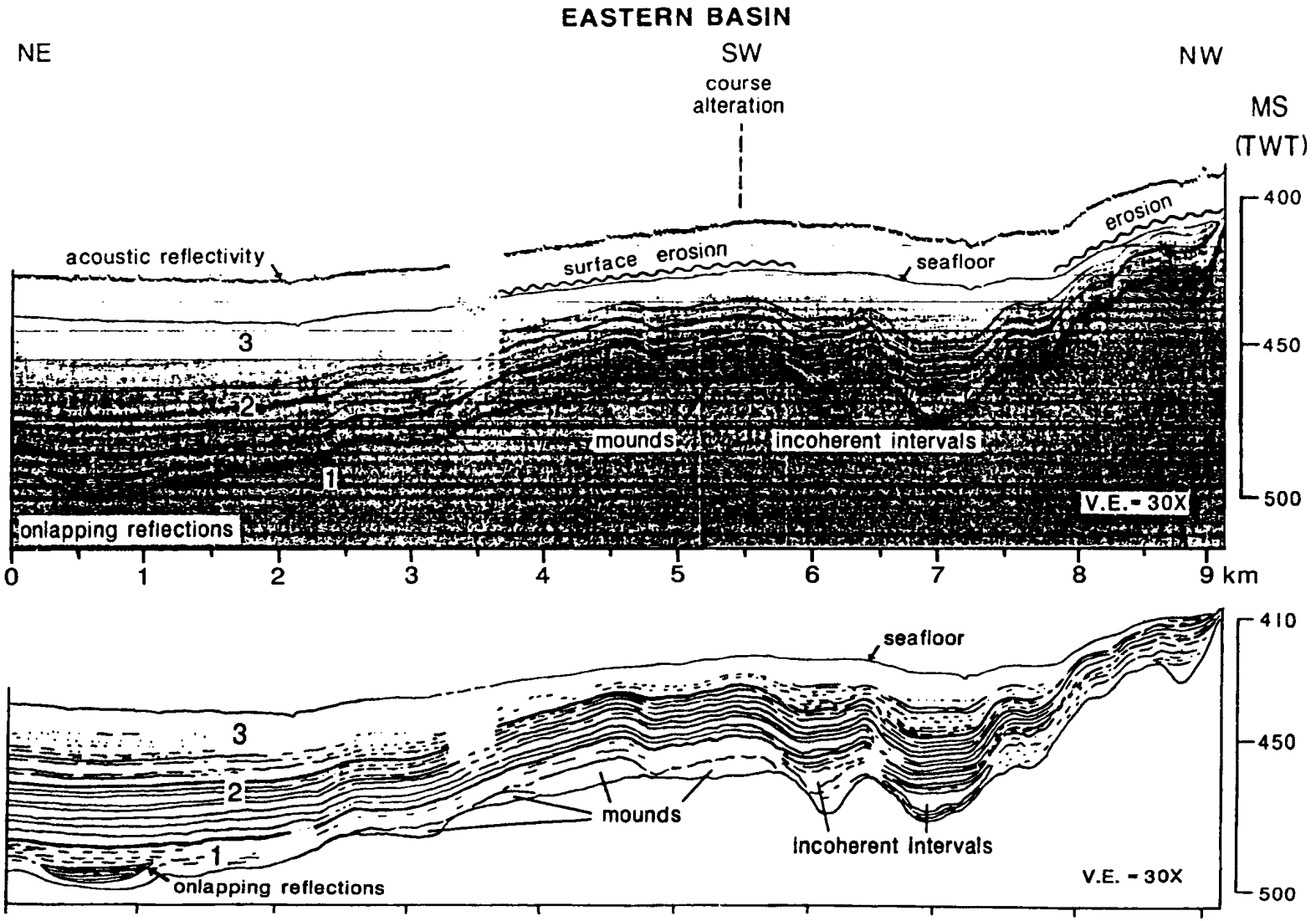
EASTERN BASIN
NE
SW
NW
course alteration
MS (TWT)
400
450
500
acoustic reflectivity
surface erosion
seafloor
erosion
3
2
1
mounds
incoherent intervals
V.E. = 30X
onlapping reflections
0
1
2
3
4
5
6
7
8
9 km
seafloor
410
450
500
3
2
1
mounds
incoherent intervals
onlapping reflections
V.E. = 30X

acoustically incoherent and interfinger with the surrounding, more acoustically stratified interval (Fig. 3.7; at 6 and 7 km along track). One zone, however, consists of moderate to high intensity reflections onlapping an acoustically incoherent package (Fig. 3.7; 0.2 to 1 km along track). Both the mounds and downwardly concave zones overlie the lowermost reflections revealed by the airgun data.

Unit 2 is present throughout the Eastern Basin. It consists of moderate to high intensity, continuous coherent reflections and has a draping basin-fill morphology, extending across the rise between the two main basins and onto the basin margins (Fig. 3.6). It is generally between 15 and 20 ms thick in the center of the Eastern Basin. Where thinning occurs on the basin margin, there appears to be onlapping and occasional offlap of reflections within the unit. Also, the overall acoustic character generally becomes incoherent. Erosion of upper reflections occurs on the rise separating the Western and Eastern Basins (Fig. 3.6). In this area, poor resolution of reflections within unit 2 makes correlation with the Western Basin difficult.

Unit 3 is acoustically transparent, with the characteristic exception of one or more moderate intensity reflections near the middle of the package. In the Eastern Basin the unit is up to 20 ms thick (Fig. 3.6). Present distribution appears to be largely limited by erosion to the

central regions of the basins and pockets on the margins.

WESTERN BASIN

Unit 1 is acoustically incoherent, with the exception of a few low to moderate intensity reflections of variable continuity. It is an average of 15 ms thick in the center of the Western Basin. As in the Eastern Basin, the unit on the 3.5 kHz data can exhibit either a ponded or draping basin-fill morphology (Figs. 3.8, 3.9, respectively). Similarly, basal reflections interpreted from the airgun data display greater lateral extent in areas where uppermost reflections of unit 1 onlap the basin margin (Fig. 3.8; 6.3 km along track). At the northern end of the basin, apparent erosion of unit 1 occurs within a depression in acoustic basement. A pocket of reflections onlaps the partially eroded unit 1 (Fig. 3.9; 1 km along 3.5 kHz track). Nearby (but not seen in figure 3.9) are lens-shaped, acoustically incoherent mounds of unit 1 immediately above the basal airgun reflections, similar to those observed within the Eastern Basin. It is possible that some of the undulatory rises in the airgun acoustic basement in the outer basins are similar to these mounds. Low intensity reflections within the airgun data beneath acoustic basement cannot be clearly identified and likely originate within underlying Precambrian to early Palaeozoic strata.

Unit 1 is generally present on the NW margin of the

Figure 3.8. 3.5 kHz and airgun profiles within the Western Basin. Location shown in figure 3.4. Seismic units 1 to 3 are discussed in text. Dashed line denotes tentative seismic unit boundaries. V.E. = vertical exaggeration. Depth in milliseconds two-way-travel-time.

WESTERN BASIN

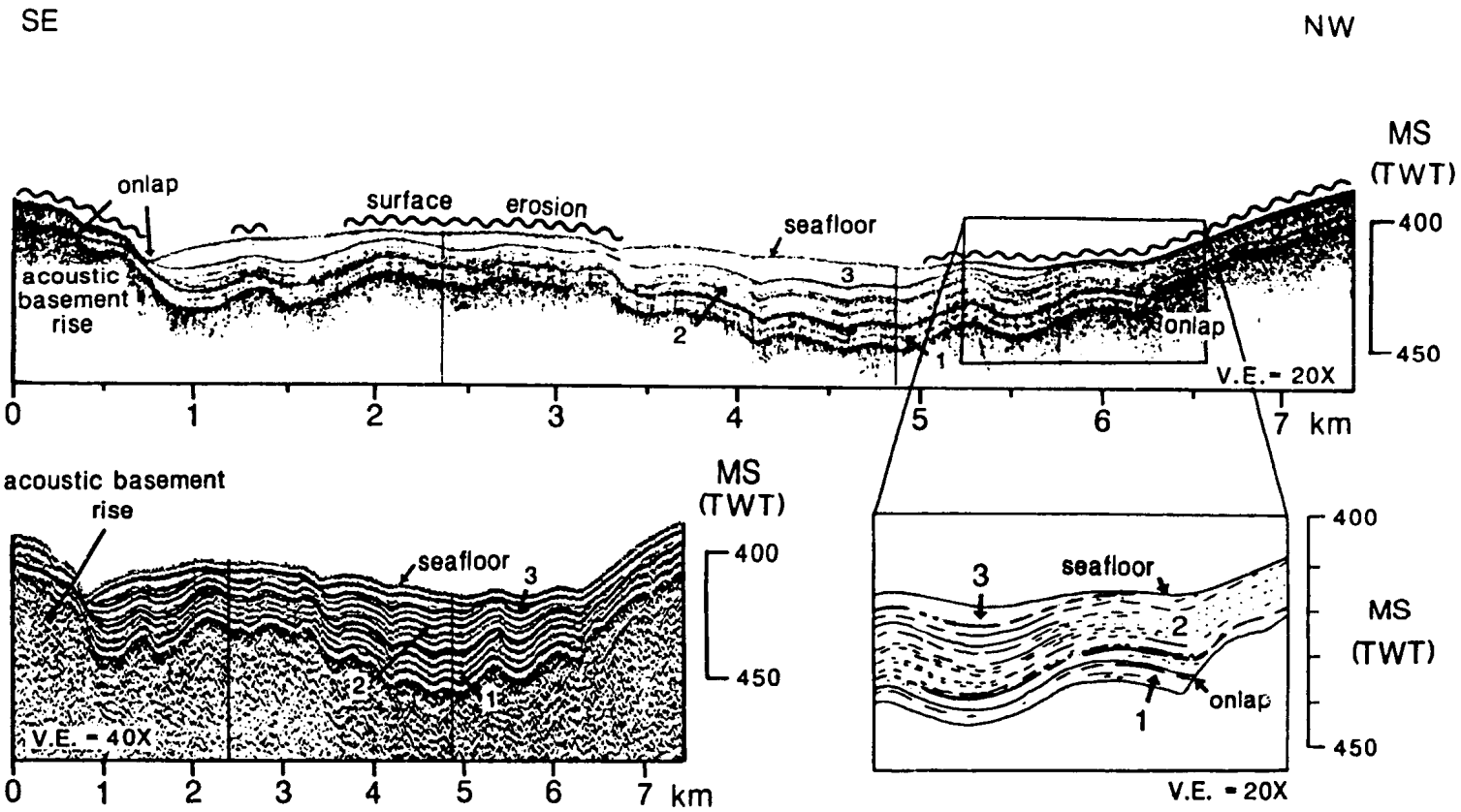

Figure 3.9. 3.5 kHz and airgun profiles within the Western Basin. Location shown in figure 3.4. Seismic units 1 to 3 are discussed in text. Dashed line denotes tentative seismic unit boundaries. V.E. = vertical exaggeration. Depth in milliseconds two-way-travel-time.

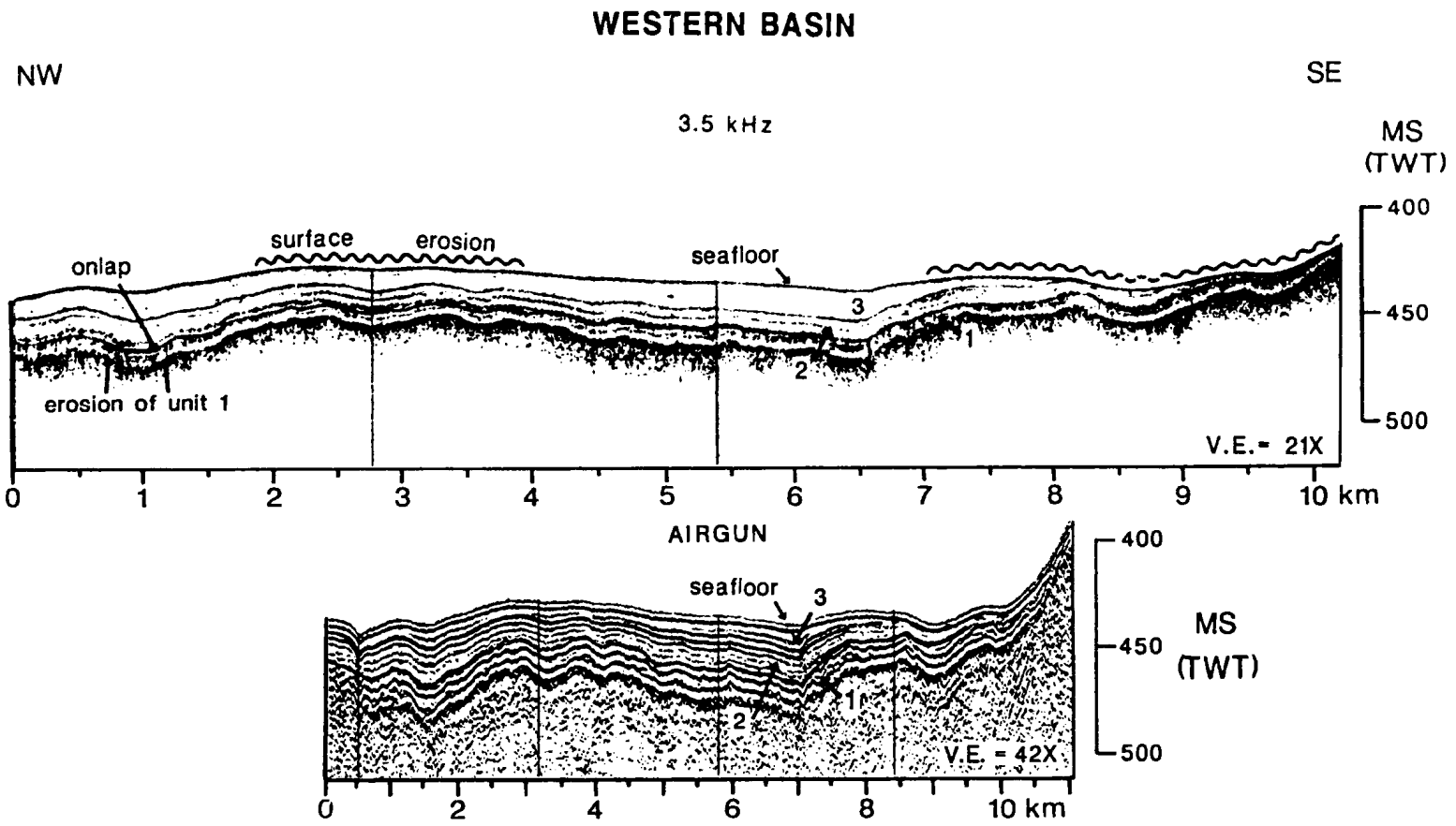
WESTERN BASIN
NW
SE
3.5 kHz
MS
(TWT)
400
450
500
surface
erosion
onlap
seafloor
3
1
2
erosion of unit 1
V.E.= 21X
0
1
2
3
4
5
6
7
8
9
10 km
AIRGUN
seafloor
3
2
1
V.E. = 42X
0
2
4
6
8
10 km

basin, thinly draping basement rises or as ponded pockets in many outlying small depressions in acoustic basement. It may also be present in one of the narrow, deep troughs on the western side of the bay.

Huntec DTS and airgun data from the SW end of the Western Basin display a seismic sequence which is difficult to correlate with data elsewhere in the bay (Fig. 3.10). In this region the basin depth is increasing towards the sill dividing inner and outer bays. There is no clear equivalent of unit 1 in this area, but a lowermost sequence of pinching and swelling, transparent and acoustically stratified complex reflections, which is at least 50 ms thick in the deepest part.

Unit 2 consists of moderate to high intensity, continuous coherent reflections with a draping basin-fill morphology (Figs. 3.8-3.10). Unit thickness in the center of the basin center averages 15 ms. To the NW this unit is occasionally extensive on the basin margin (Fig. 3.8; 6.3 km to end of track), where it averages 15 ms in thickness. Erosion of upper reflections in unit 2 often occurs on the margins (Figs. 3.8, 3.9). As in the Eastern Basin, reflections within the unit converge as it thins and the acoustic character of unit 2 often becomes incoherent outside the center of the basin.

A thick pocket of sediment occurs in the NW of the Western Basin. This deposit lies between the two primary

Figure 3.10. Huntec DTS profile within the Western Basin. Location shown in figure 3.4. Seismic units 1 to 3 are discussed in text. V.E. = vertical exaggeration. Depth in milliseconds two-way-travel-time.

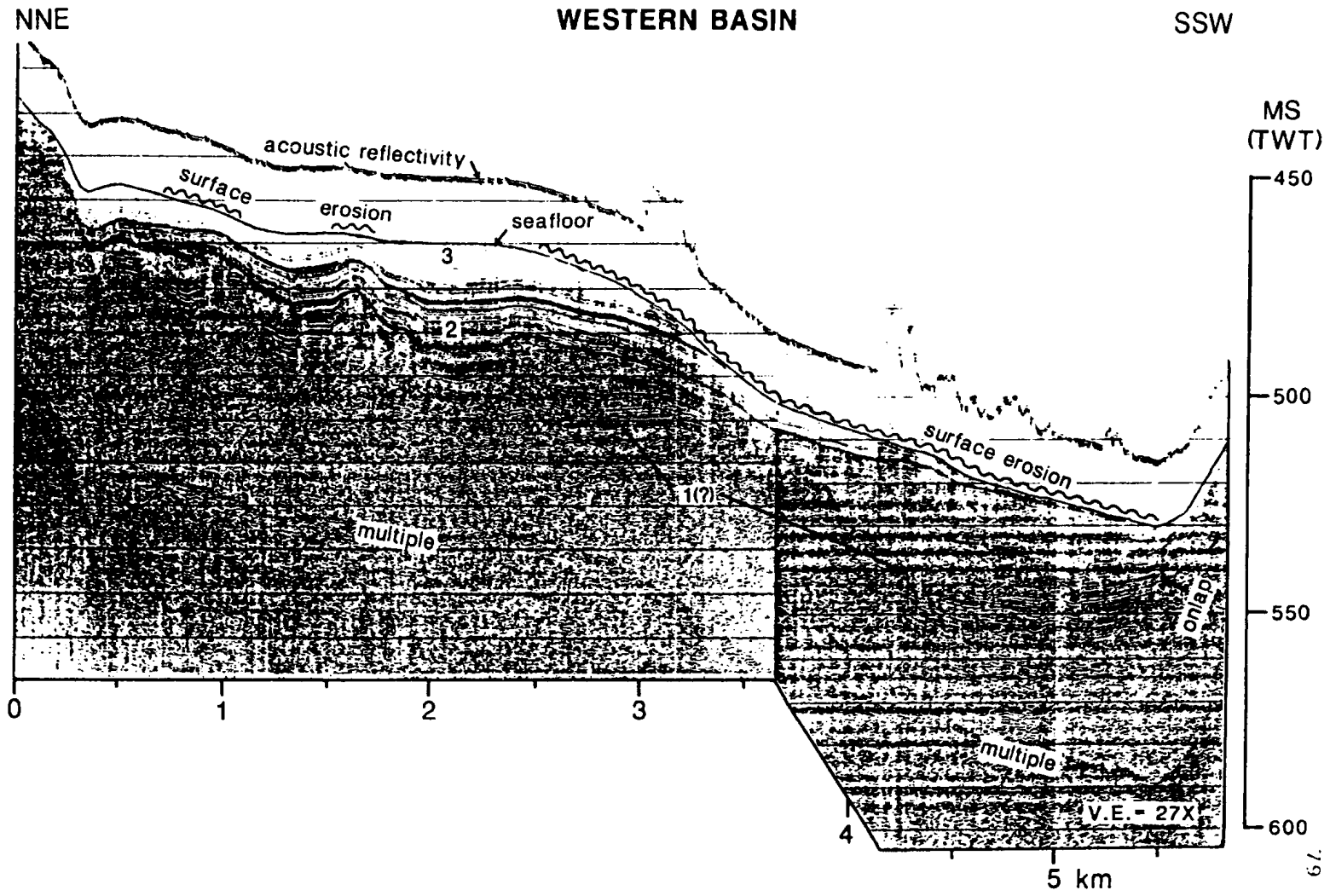
NNE
WESTERN BASIN
SSW
MS
(TWT)
450
500
550
600
acoustic reflectivity
surface
erosion
seafloor
3
2
1(?)
surface erosion
multiple
onlap
multiple
V.E. - 27X
0
1
2
3
4
5 km

survey lines which extend furthest NW, and is evident only within the 3.5 kHz data which was collected at high speed (Fig. 2.2). Units 2 and 3 are present and are 50 and 20 ms thick respectively. Unit 1 may be present, but is not clearly defined.

In the SW of the Western Basin, unit 2 conformably overlies the intercalated lower sequence (Fig. 3.10). Unit 2 is 10 ms thick over most of the profile, but has been completely eroded at the southern end (Fig. 3.10; 5.4 km along track).

Unit 3 in the Western Basin has a lower intensity and less continuous middle section reflection than in the Eastern Basin (Figs. 3.8, 3.9). The unit is acoustically transparent overall and has a morphology suggestive of draping basin-fill, but with erosion limiting distribution to the basin center and isolated pockets. The thickness of unit 3 is generally less than 10 ms, with the exception of the deeper areas in the NE and SW of the basin. In the NE, the unit reaches 17 ms in thickness. In the SW end of the basin (Fig. 3.10) unit 3 ranges up to 20 ms thick and has undergone erosion at both the upslope end and in the deeper area immediately adjacent to the SW bounding sill (Fig. 3.10; 3.5 to 5.5 km along track). This erosion appears in a number of profiles which cross this margin.

3.4.2 Inner Bay

Four seismic units (A to D) occur in each of the main basins of Chandler Reach, Newman Sound and Central Basin. These are tentatively correlated on the basis of acoustic character, unit morphology and stratigraphic position (Figs. 3.11, 3.12).

Unit A, lowermost of the four, is generally an acoustically incoherent package which often exhibits continuous, coherent high intensity reflections and occasional discontinuous reflections of variable intensity. Within the airgun data the unit contains a range of reflection intensities and continuities. The morphology of the unit is ponded, with reflections abutting against the acoustic basement at the basin margins.

Unit B is acoustically transparent, with occasional low intensity, continuous to discontinuous reflections. This unit is generally not as distinct on the airgun data as on the 3.5 kHz or Huntec DTS data. Unit morphology is generally ponded.

Unit C is characterized by moderate to high intensity, generally continuous, parallel reflections. In some areas the unit is ponded, while in others it displays a draping basin-fill morphology.

Unit D is acoustically transparent but contains one or more moderate intensity, continuous reflections near mid-sequence. It usually has a draping basin-fill morphology.

Figure 3.11. Tentative correlation of seismic units observed within the main basins of inner Bonavista Bay. Basin locations illustrated in figure 3.1. Data from Huntec DTS and 3.5 kHz presented for Chandler Reach; 3.5 kHz data only for Newman Sound and Central Basin. Dashed line denotes continuation of acoustic basement on the basis of airgun data. Seismic units A and B are not resolved within the northern end of the Central Basin. V.E. = vertical exaggeration. Depth in milliseconds two-way-travel-time.

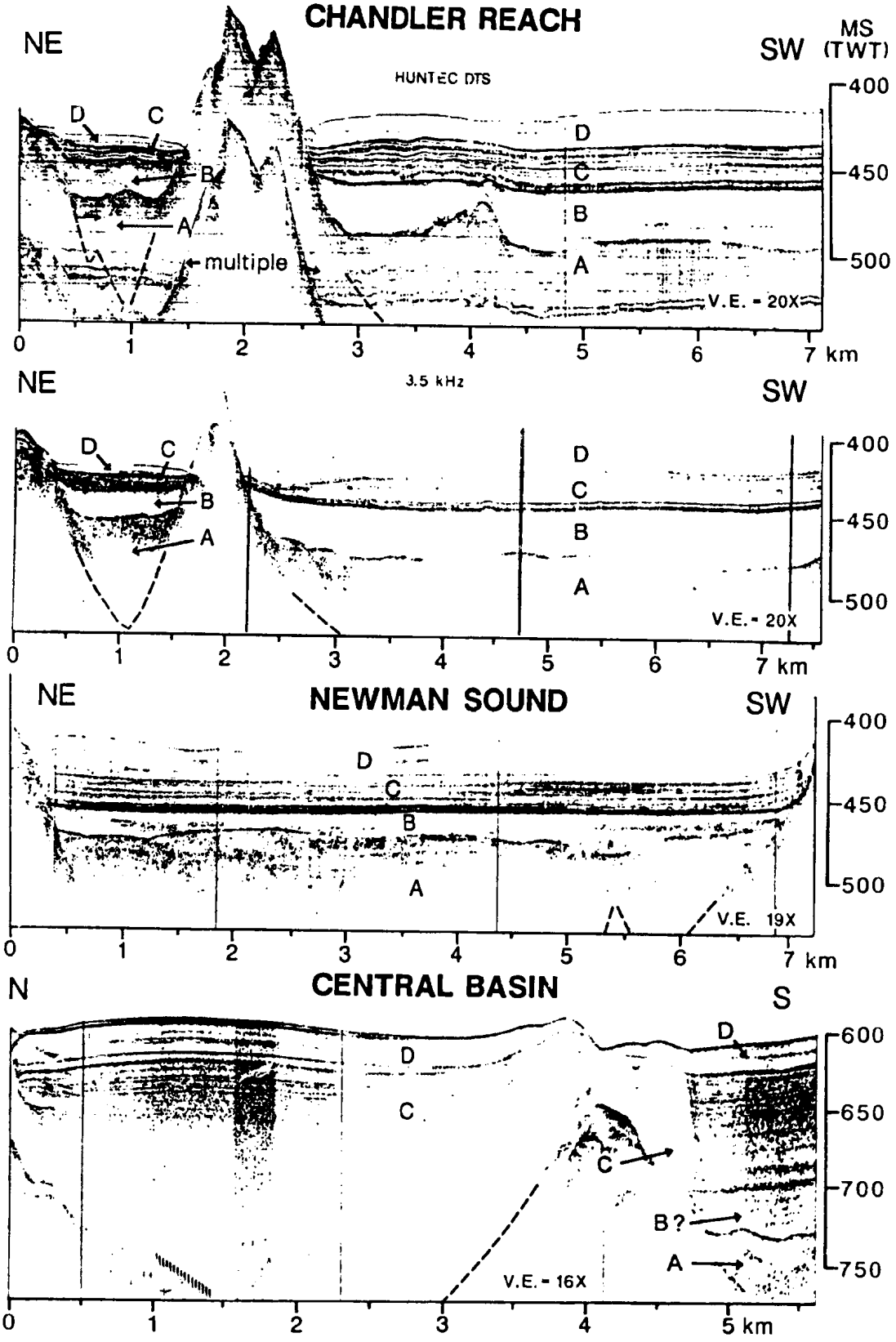
CHANDLER REACH
NE
SW
MS (TWT)
HUNTEC DTS
D
C
B
A
multiple
V.E. - 20X
400
450
500
0
1
2
3
4
5
6
7 km
NE
3.5 kHz
SW
D
C
B
A
V.E. - 20X
400
450
500
0
1
2
3
4
5
6
7 km
NE
NEWMAN SOUND
SW
D
C
B
A
V.E. 19X
400
450
500
0
1
2
3
4
5
6
7 km
N
CENTRAL BASIN
S
D
C
B?
A
V.E. - 16X
600
650
700
750
0
1
2
3
4
5 km

Figure 3.12. Tentative correlation of seismic units observed in airgun data from the main basins of inner Bonavista Bay. Basin locations illustrated in figure 3.1. Chandler Reach and Newman Sound data from C.S.S Dawson cruise 86-026; Central Basin data from C.S.S. Hudson cruise 87-033. V.E. = vertical exaggeration. Depth in milliseconds two-way-travel-time.

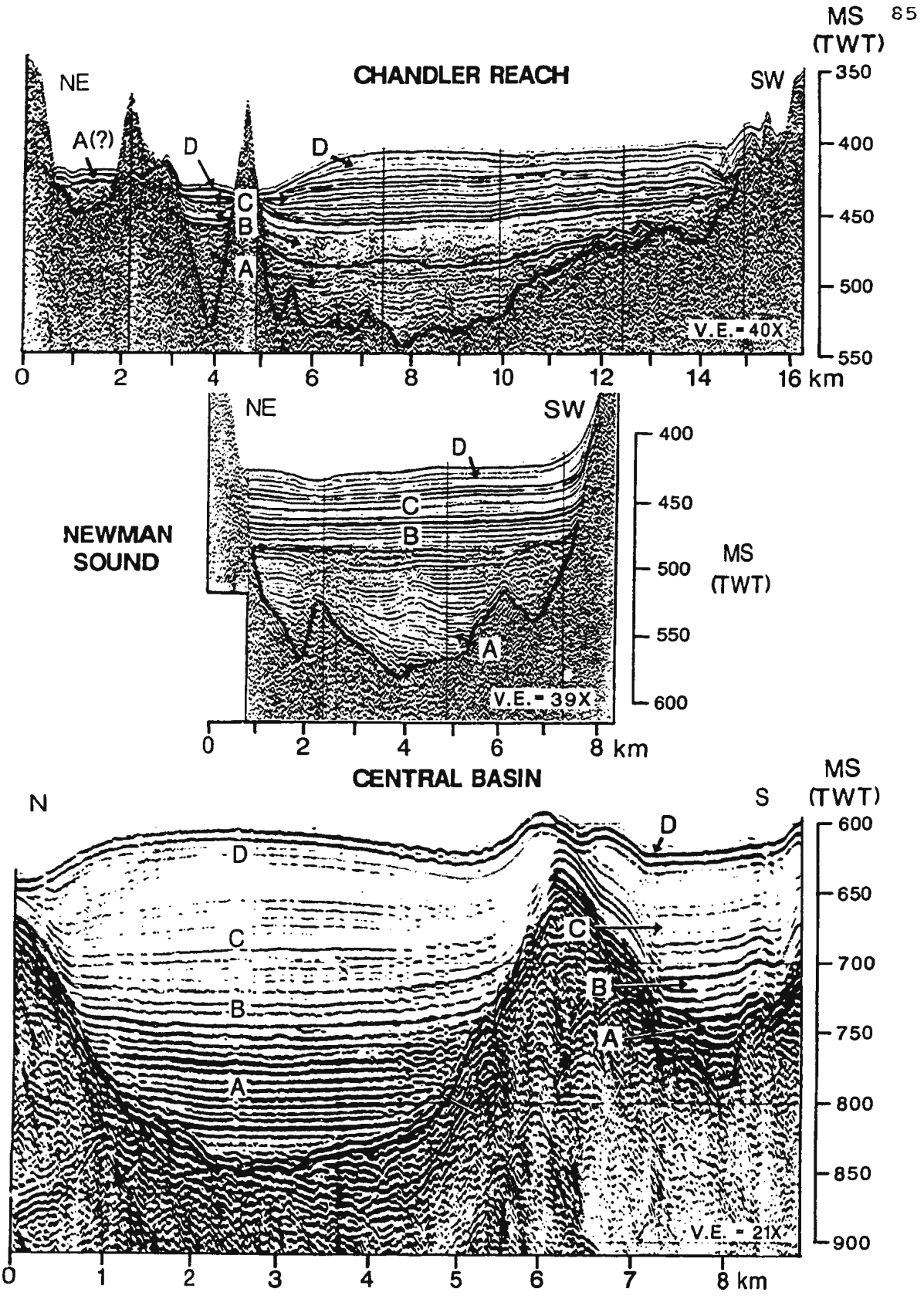
CHANDLER REACH
NE
SW
MS (TWT)
A(?)
D
D
C
B
A
V.E. - 40X
350
400
450
500
550
0
2
4
6
8
10
12
14
16 km
NEWMAN SOUND
NE
SW
D
C
B
A
V.E. - 39X
400
450
500
550
600
MS (TWT)
0
2
4
6
8 km
CENTRAL BASIN
N
S
MS (TWT)
D
D
C
C
B
B
A
A
V.E. - 21X
600
650
700
750
800
850
900
0
1
2
3
4
5
6
7
8 km

CHANDLER REACH

Huntec DTS, 3.5 kHz and airgun seismic reflection data are all available from this area. Core 87-033-020 was collected from the NE end of the basin. As indicated in figure 3.1, there is one large basin within Chandler Reach and three smaller, outer basins. The small basin immediately to the NE may not actually be a separate feature (Fig. 3.13; 0 to 1.5 km along track) and may be connected to the larger basin. The two outermost basins (one is displayed in figure 3.12; Chandler Reach, at 1 km along track) are addressed following the discussion of the largest basin and its NE neighbour.

Unit A is acoustically incoherent with occasional low intensity semi-continuous reflections (Fig. 3.13). The unit has an average thickness of 50 ms in the basin and a ponded morphology. The upper boundary of unit A is gradational, with acoustically incoherent zones and reflections (especially evident on the Huntec DTS data) intermixed with the acoustically transparent sequence of unit B above. Downlapping semi-continuous reflections at the SW end of the main basin define at least one wedge-shaped zone at the upper boundary of unit A (Fig. 3.13; 9.5 to 12 km along track), as well as a depression in unit A beneath this wedge (10.2 km along track). In this area, the upper boundary of unit A displays low relief mounds. Only the airgun data is able to penetrate more than 20 ms into unit A, displaying a

Figure 3.13. Huntec DTS and airgun profiles within Chandler Reach. Location shown in figure 3.4. The isolated seismic sequence in the left of the figure corresponds with the basin immediately to the NE referred to within the text. Seismic units A to D are discussed in text. V.E. = vertical exaggeration. Depth in milliseconds two-way-travel-time.

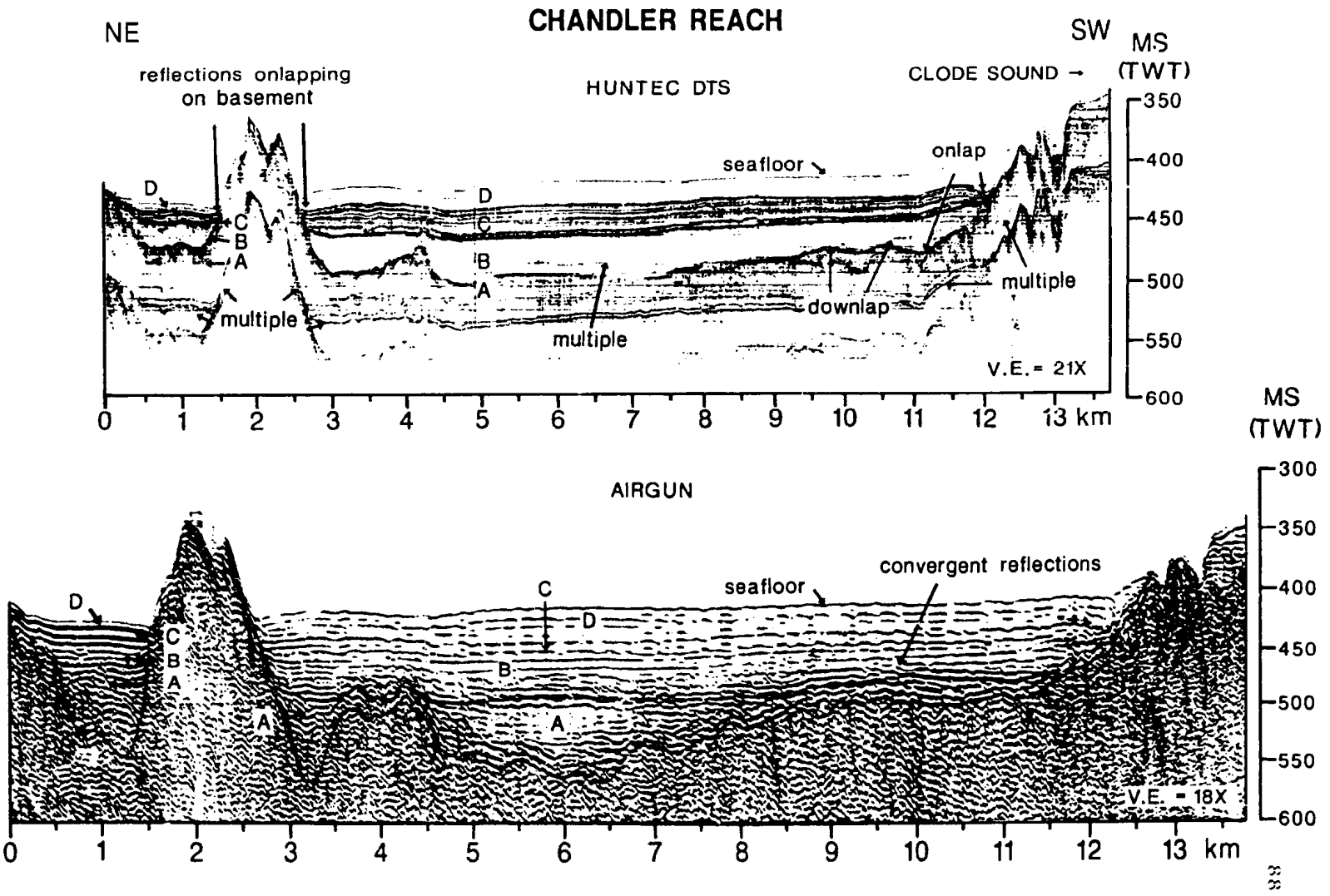
CHANDLER REACH
NE
SW
MS (TWT)
reflections onlapping on basement
HUNTEC DTS
CLODE SOUND →
seafloor
onlap
D
C
B
A
multiple
downlap
V.E. = 21X
0 1 2 3 4 5 6 7 8 9 10 11 12 13 km
350
400
450
500
550
600
AIRGUN
convergent reflections
V.E. = 18X
300

semi-continuous series of reflections of variable intensity (Fig. 3.13).

Unit B is acoustically transparent, ponded and an average of 27 ms thick (Fig. 3.13). Contact with the overlying sequence is sharp and is defined by a couplet of high intensity reflections. There are several low intensity, semi-continuous reflections within the unit which are most evident at the SW end of the basin. At least one of these downlaps onto unit A. The airgun data display moderate to low intensity reflections of variable continuity, some of which downlap and converge at the SW end of the basin (Fig. 3.13; 9.7 km along airgun track). In the small basin to the NE, unit B is approximately 20 ms thick and exhibits semi-continuous reflections (Huntec DTS data) in the upper 5 ms of the unit (Fig. 3.14). There is a depression immediately beneath the boundary with unit C which contains onlapping reflections (Fig. 3.14; 0.7 km along track). Unit B drapes slightly onto the NE basin margin.

Unit C is comprised of a series of moderate to high intensity, parallel, continuous reflections (Fig. 3.13). It has a ponded morphology, except where it drapes onto the eastern margin of the NE basin (Fig. 3.14). It is generally <25 ms thick, but pinches to <10 ms at the contact with the basin walls and within the NE basin. The boundary with the overlying unit is sharp. The Huntec DTS profile displays

Figure 3.14. Huntec DTS profile within the basin NE of the main basin in Chandler Reach. Location shown in figure 3.4 as parallel to figure 3.13, although this figure is an enlargement of the NE end of the same Huntec profile. Seismic units A to D are discussed in text. Dashed line denotes continuation of acoustic basement on the basis of airgun data. V.E. = vertical exaggeration. Depth in milliseconds two-way-travel-time.

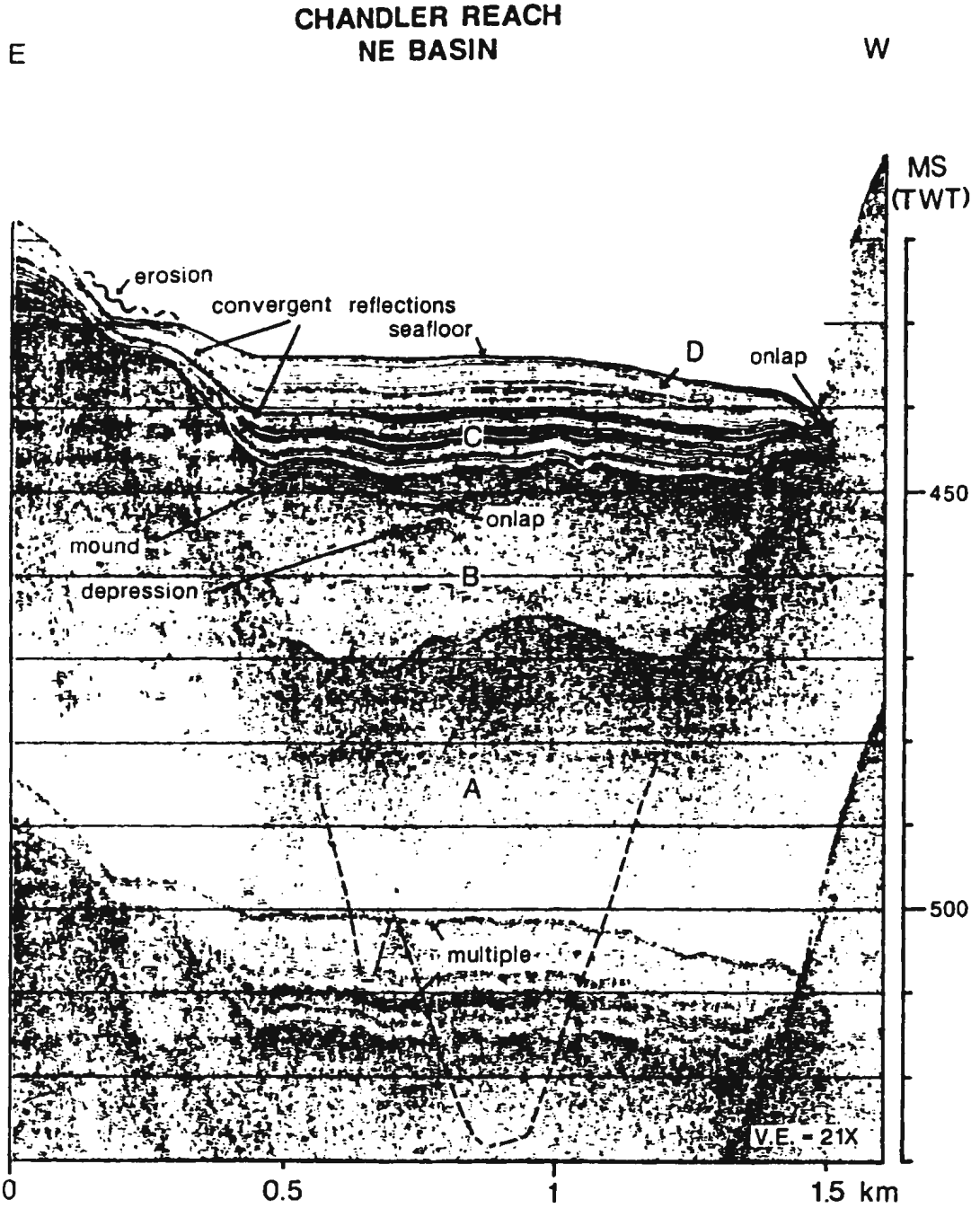
CHANDLER REACH
NE BASIN
E
W
MS
(TWT)
erosion
convergent reflections
seafloor
D
onlap
C
onlap
mound
depression
B
A
multiple
450
500
V.E. - 21X
0
0.5
1
1.5 km

some lateral variation in reflection intensity as well as acoustically incoherent zones in the interval between two high intensity reflections at the base of unit C. There are convergent reflections within the NE basin, as displayed in figure 3.14.

Unit D is acoustically transparent, with moderate to low intensity reflections near the middle of the package (Fig. 3.13). It generally has a draping basin-fill morphology and is an average of 20 ms thick. It pinches (or is eroded) to less than half this thickness and is ponded to the NE of the large basin. The thickness of unit D is much less (approximately 6 ms) in the basin immediately to the NE. It onlaps the rise separating the basins but drapes onto the outer margin, where it appears to be slightly eroded (Fig. 3.14).

Units A to D are observed only within the innermost, main basin and the basin immediately to the NE. The two outer basins at the mouth of Chandler Reach appear to contain only ponded packages of unit A, with an approximate thickness of 30 ms. One of the two basins is displayed in figure 3.12; at approximately 1 km along the track of the Chandler Reach profile. Unit D may, however, be present in these basins as a thin (<5 ms) veneer which is not resolved on the acoustic data.

NEWMAN SOUND

Unit A within Newman Sound ranges up to 95 ms thick (Fig. 3.15). It has a ponded morphology, with low intensity, discontinuous to continuous reflections. Within the middle of this unit are two, and possibly three, channel-shaped occurrences of moderate to high intensity, continuous reflections which onlap an underlying reflection. Beneath this reflection, the airgun data display ~10 ms thick zones of reflections which converge laterally. As in Chandler Reach, the upper boundary of unit A is gradational, with reflections interfingering with the overlying transparent sequence of unit B. The upper surface of unit A displays low relief mounds.

A small basin in the shallower region outside Newman Sound (Fig. 3.1) contains a 50 ms thick, ponded package of unit A.

Unit B is acoustically transparent, ponded and has an average thickness of 15 ms (Fig. 3.15). As in the main basin in Chandler Reach, the contact with the overlying unit C is sharply defined by a series of high intensity reflections. Recognition of unit B is more difficult on airgun than 3.5 kHz profiles. Low intensity reflections at the base of unit B downlap onto unit A (Fig. 3.15).

Unit C consists of high intensity, continuous reflections and has an average thickness of 20 ms (Fig. 3.15). It has a ponded morphology to the NE, but rises

Figure 3.15. 3.5 kHz and airgun profiles within Newman Sound. Location shown in figure 3.4. Seismic units A to D are discussed in text. V.E. = vertical exaggeration. Depth in milliseconds two-way-travel-time.

NEWMAN SOUND

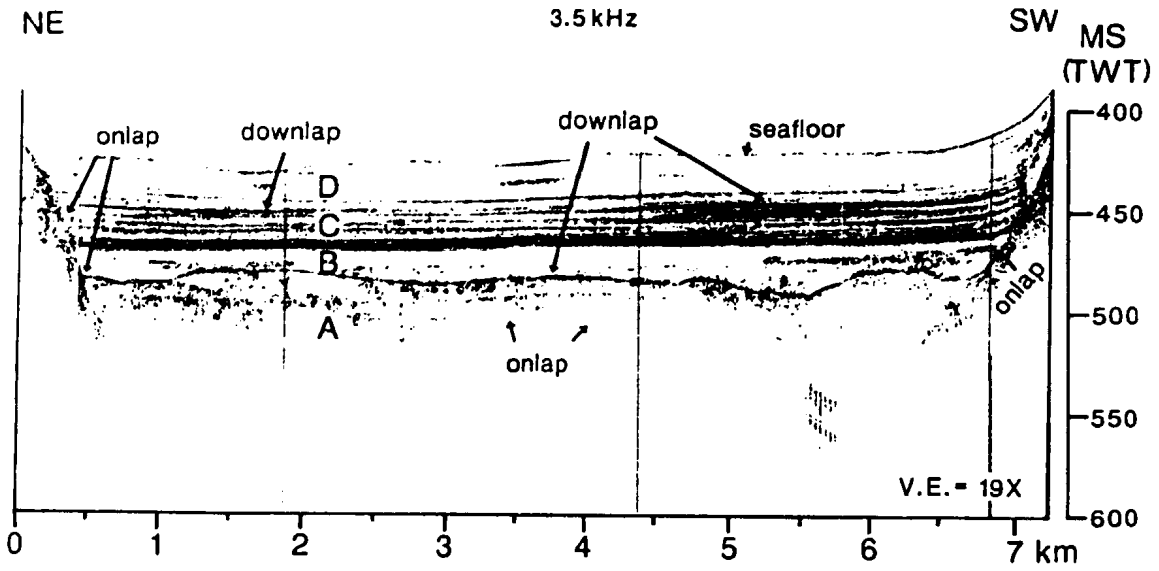

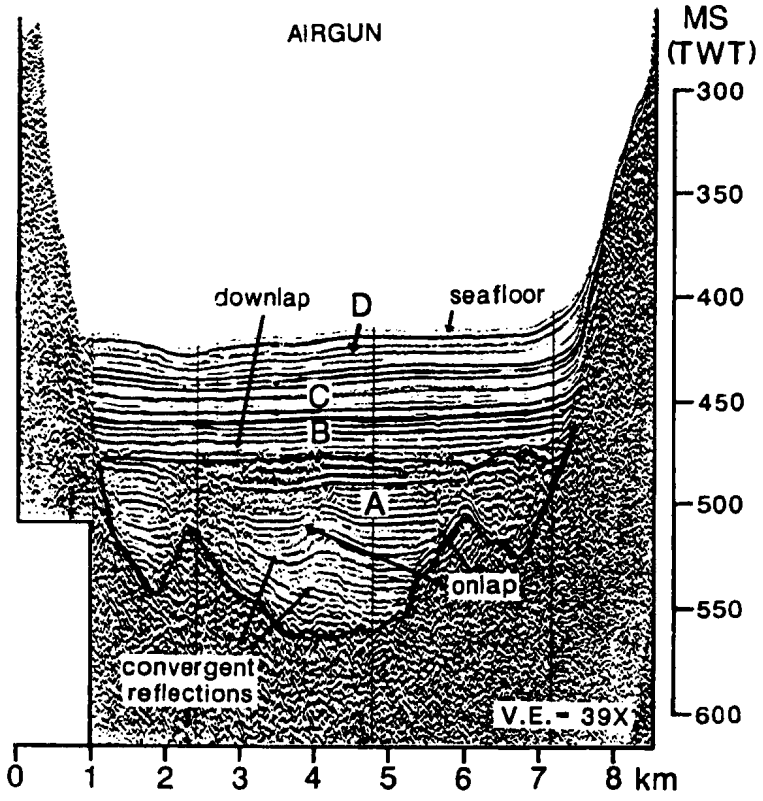

slightly onto the SW (landward) margin. The contact with unit D is gradational and marked by semi-continuous and low intensity reflections. There are downlapping reflections near the upper surface of the unit. A cross-sectional profile of the basin at its NE end displays an unconformable contact with unit D, with erosion of upper reflections in unit C on the SE side of the basin (Fig. 3.16). Reflections downlap at the base of unit C.

Unit D is acoustically transparent, with the exception of a number of moderate intensity, semi-continuous reflections near the middle of the unit. It has an average thickness of 20 ms (Fig. 3.15). As in Chandler Reach, the unit onlaps against the outer sill and drapes over the landward margin (Fig. 3.15).

CENTRAL BASIN

Unit A is evident in the majority of the Central Basin only on the airgun profiles, due to a total sediment thickness over acoustic basement which exceeds 230 ms (Fig. 3.17). The 3.5 kHz and Huntec DTS profiles can only penetrate to the uppermost surface of unit A at the southern end of the basin (Fig. 3.18; 2.5 to 3.5 km along track) and along the sidewall ledges (Fig. 3.19).

Within the middle and deepest part of the basin, unit A is up to 110 ms thick (Fig. 3.17). It exhibits a ponded morphology with high intensity, continuous reflections

Figure 3.16. 3.5 kHz profile across the NE end of Newman Sound. Location shown in figure 3.4. Ship's speed was increased during this section of the Newman Sound survey, relative to the data in previous figure, producing a greater degree of horizontal compression. Seismic units A to D are discussed in text. V.E. = vertical exaggeration. Depth in milliseconds two-way-travel-time.

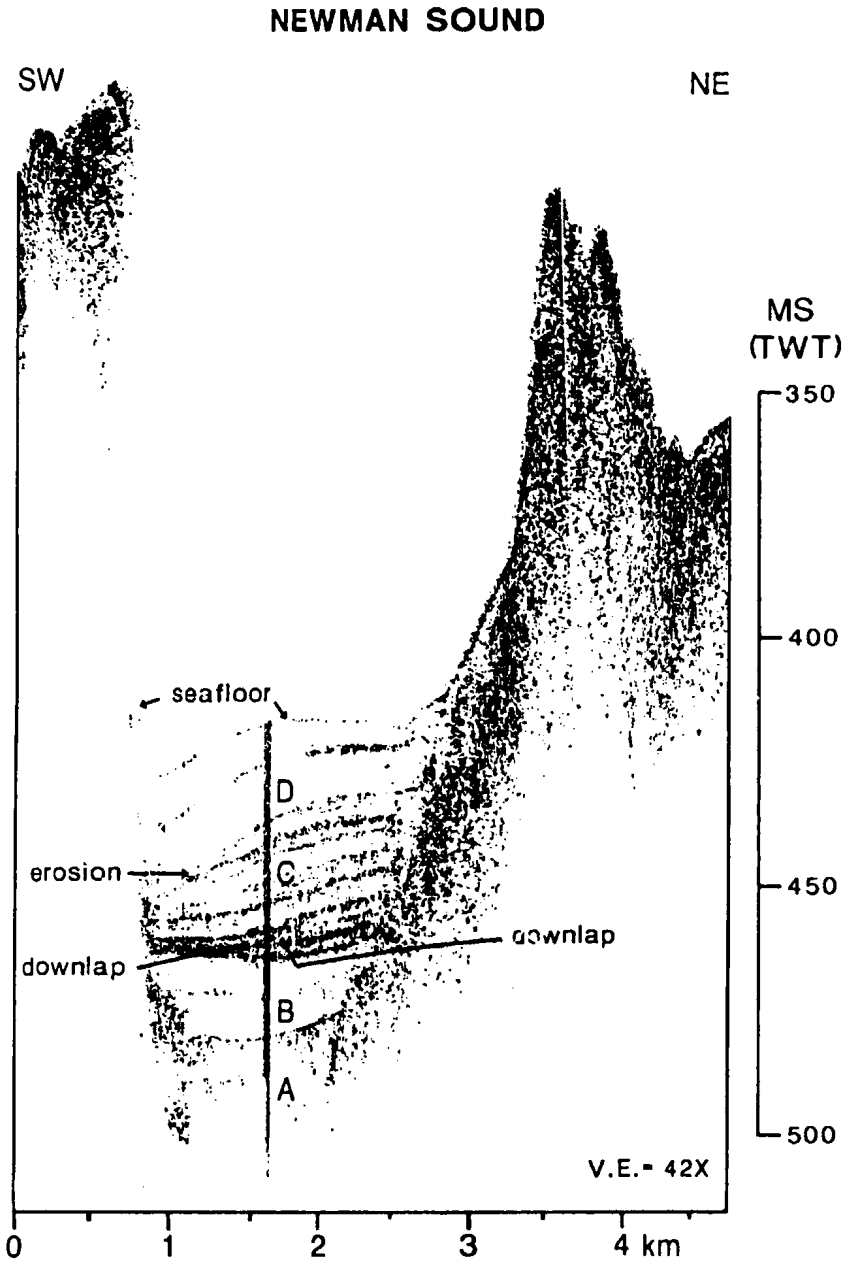
NEWMAN SOUND
SW
NE
MS
(TWT)
350
400
450
500
seafloor
D
C
B
A
erosion
downlap
downlap
V.E.- 42X
0
1
2
3
4 km

Figure 3.17. Airgun profile within Central Basin. Location shown in figure 3.4. Seismic units A to D are discussed in text. V.E. = vertical exaggeration. Depth in milliseconds two-way-travel-time.

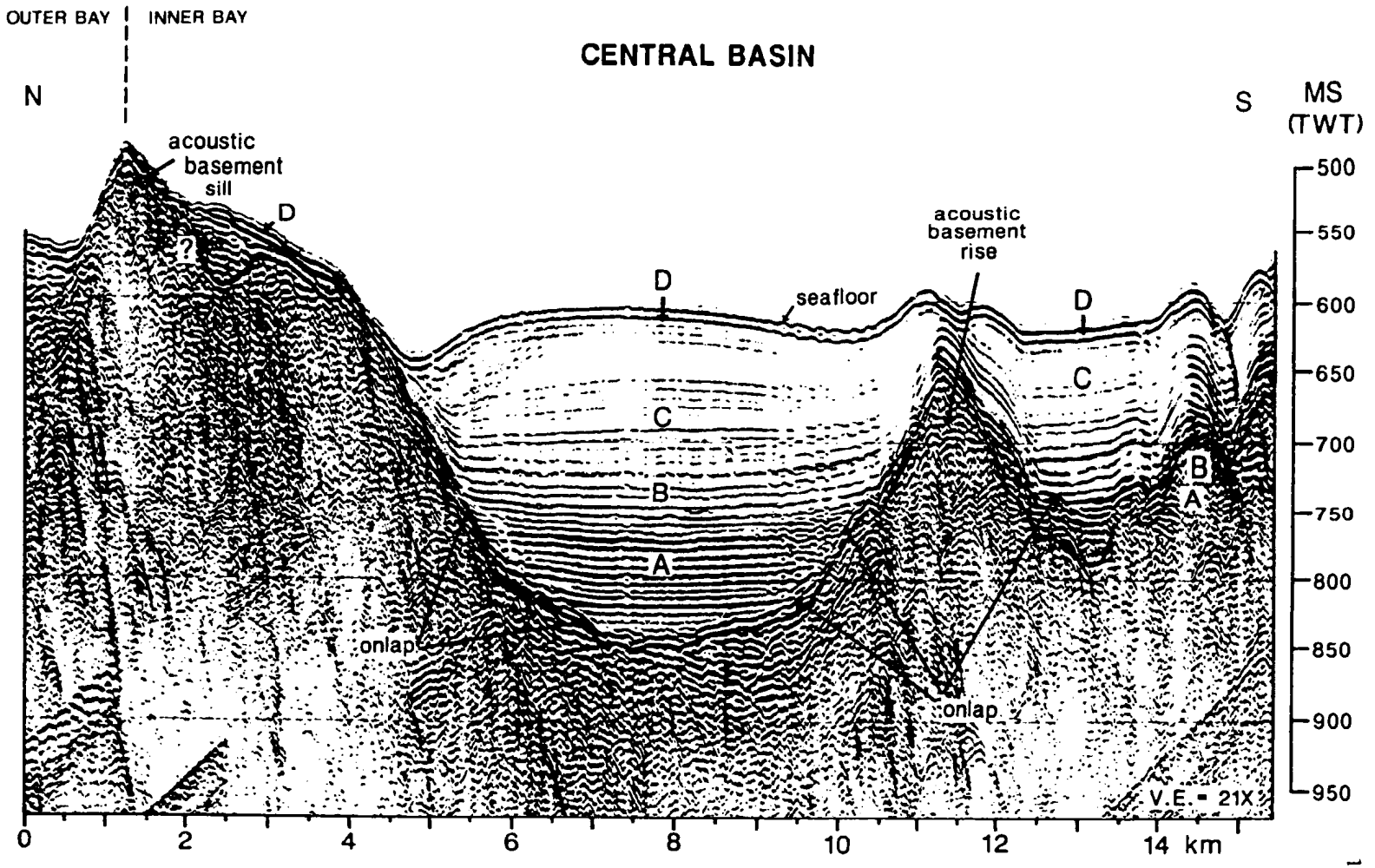
OUTER BAY
INNER BAY
CENTRAL BASIN
N
S
MS
(TWT)
acoustic
basement
sill
D
?
D
seafloor
acoustic
basement
rise
D
C
C
B
B
A
A
onlap
onlap
V.E. = 21X
500
550
600
650
700
750
800
850
900
950
0
2
4
6
8
10
12
14 km

Figure 3.18. 3.5 kHz profile within the southern end of Central Basin. Location shown in figure 3.4. Seismic units A to D are discussed in text. Dashed line denotes continuation of acoustic basement on the basis of airgun data. V.E. = vertical exaggeration. Depth in milliseconds two-way-travel-time.

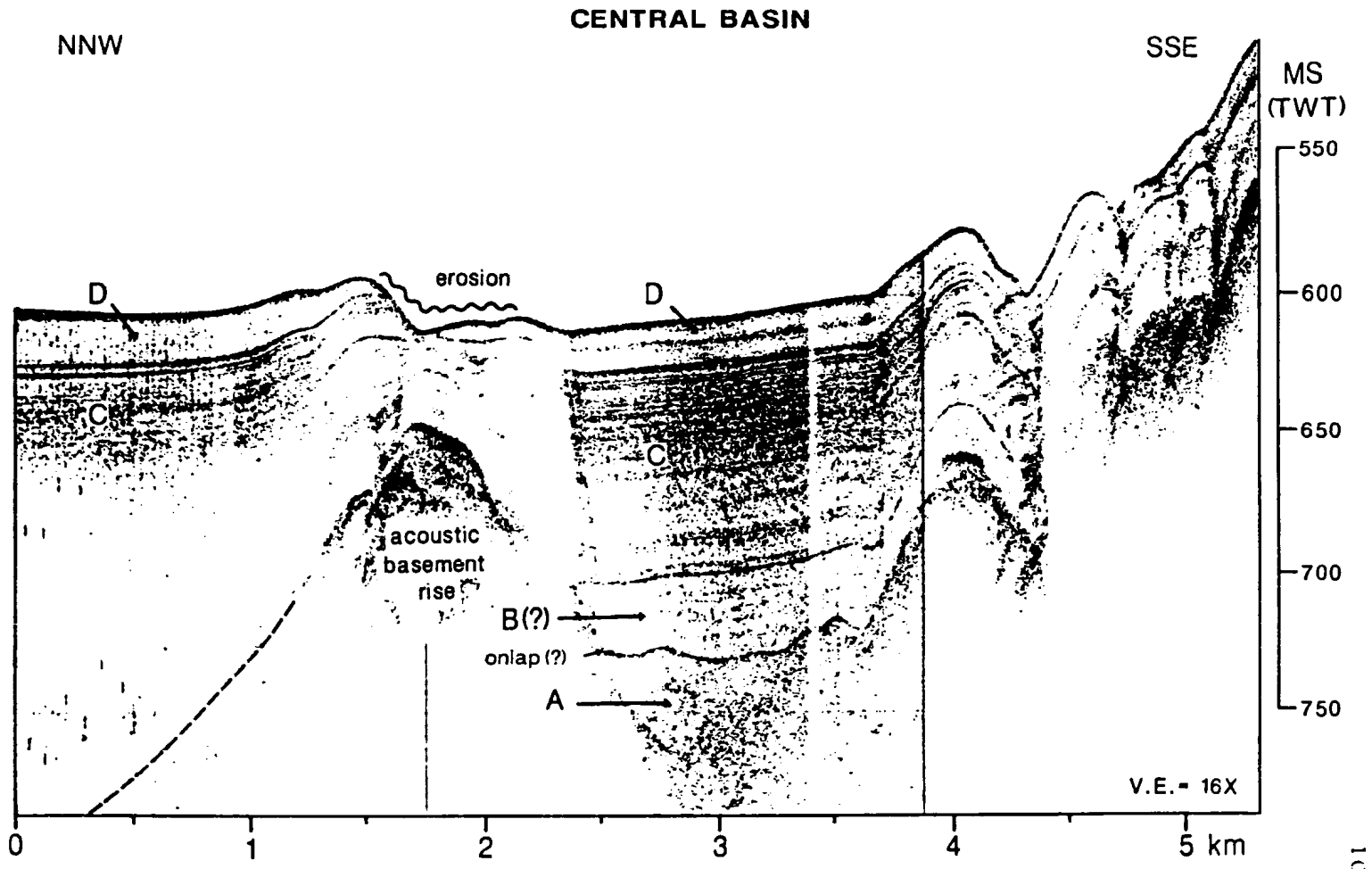
CENTRAL BASIN
NNW
SSE
MS
(TWT)
550
600
650
700
750
D
erosion
D
C
C
acoustic
basement
rise
B(?)
onlap (?)
A
V.E. = 16X
0
1
2
3
4
5 km

Figure 3.19. 3.5 kHz E-W profile within Central Basin. Location shown in figure 3.4. Seismic units A to D are discussed in text. Boundaries of units A and B are tentative within the main basin. Dashed line denotes continuation of acoustic basement on the basis of airgun data. V.E. = vertical exaggeration. Depth in milliseconds two-way-travel-time.

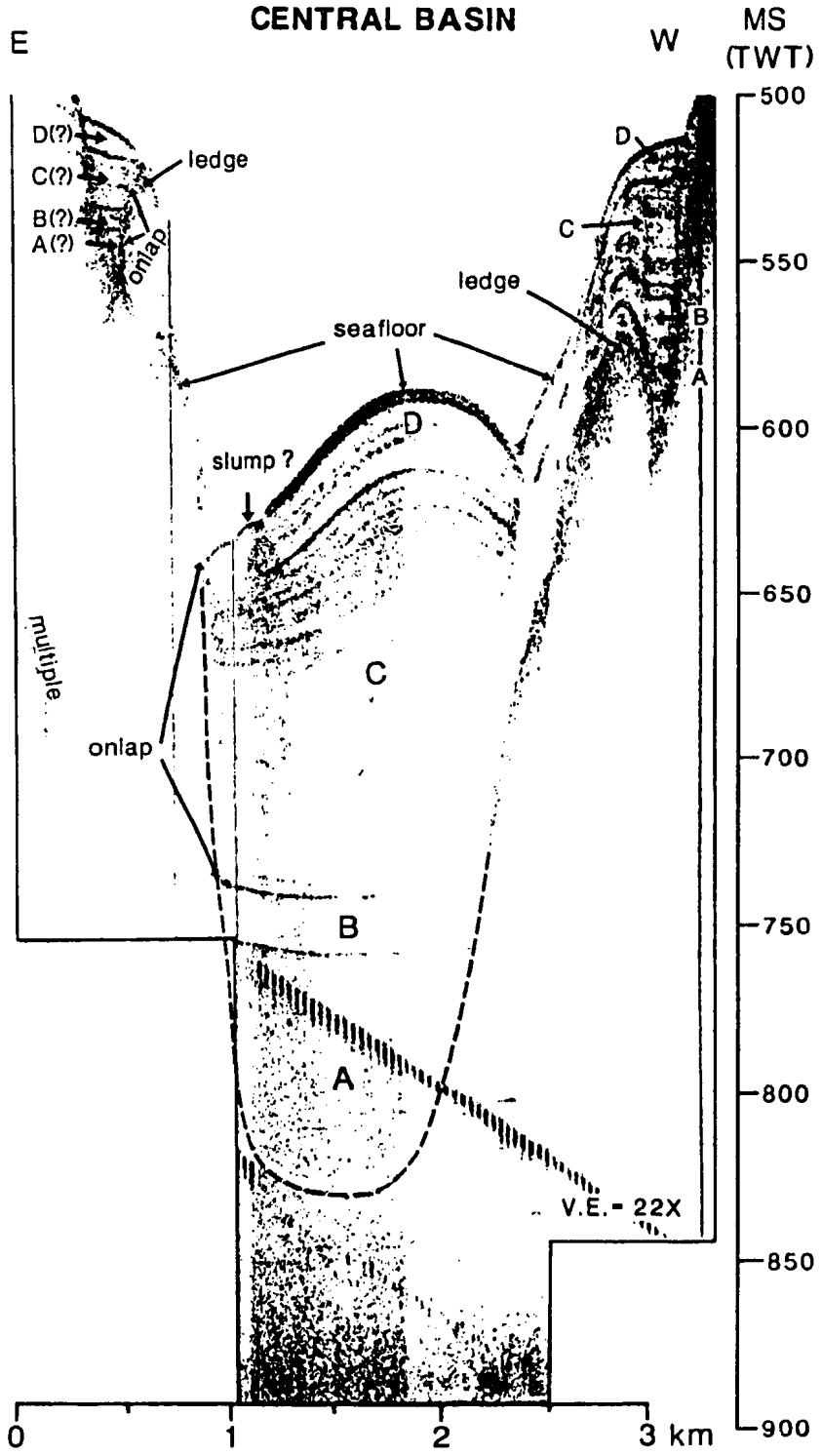
CENTRAL BASIN
E
W
MS
(TWT)
D(?)
C(?)
B(?)
A(?)
ledge
onlap
seafloor
ledge
D
C
B
A
slump ?
multiple
onlap
V.E. - 22X
500
550
600
650
700
750
800
850
900
0
1
2
3 km

onlapping the acoustic basement. Thin (~10 ms) lens-shaped zones occur 15 ms below the unit top, adjacent to the acoustic basement rise which occurs towards the southern end of the basin (Fig. 3.17; 9 to 10 km along track). South of this large basement rise, reflections are less parallel and are semi-continuous. 3.5 kHz data display an irregular upper surface of unit A, on which reflections of unit B appear to onlap (Fig. 3.18; 2.5 km along track).

Within the ledges on the margin of the basin, unit A is ponded and up to 30 ms thick (Fig. 3.19). There is no clear evidence that this unit extends out of the depressions and down into the deepest part of the Central Basin.

Unit B is an acoustically transparent sequence, but is not as clearly defined within the Central Basin as within Chandler Reach or Newman Sound. It is best observed in a cross-sectional profile of the Central Basin immediately outside Chandler Reach as a ponded 10-15 ms thick interval. The 3.5 kHz data in figure 3.18 faintly displays a ponded, 25-30 ms thick package over unit A which terminates in an upper, low to moderate intensity couplet of reflections. A similar interval in figure 3.19 is 15-20 ms thick. The airgun data display a lower intensity series of reflections above unit A (Fig. 3.17). This is similar to the airgun sequence observed in Newman Sound. A 10 ms thick interval of unit B is evident within the sediment package on the western ledge on the basin margin (Fig. 3.19). It drapes

over the ledge and into the main part of the basin.

Unit C in the Central Basin is an average of 90 ms thick and consists of parallel, continuous reflections of moderate intensity, with a few ~10 ms thick intervals of lower intensity reflections (Figs. 3.17, 3.18). Unit C has a draping basin-fill morphology. In E-W profile (Fig. 3.19), reflections of unit C appear to connect with a package of moderate intensity reflections within the ledge on the basin margin. The maximum observed thickness of unit C within the sidewall ledges is 40 ms, although it is variable between profiles. Reflections in the ledges onlap against acoustic basement. Erosion of the uppermost sediments within unit C has occurred over the large acoustic basement high within the Central Basin (Fig. 3.18; 1.5 to 2 km along track).

Unit D is acoustically transparent but has moderate intensity, discontinuous to continuous reflections near mid-unit. It is an average of 20 ms thick in the basin and commonly has a draping basin-fill morphology (Fig. 3.18). The unit extends onto the ledges, where it is present as a 10-15 ms package (Fig. 3.19). In the southern end of the basin, one profile displays the unit draping both sidewalls, although it is more commonly restricted to one side of the basin. Total erosion of the unit occurs at the acoustic basement rise near mid-basin and at the landward end of the basin. The unit pinches at the northern end of the basin

and thins as it rises onto the acoustic basement sill (Fig. 3.17; 4 to 5 km along track). Reflections of units C and D in the Central Basin dip northwards (~1° slope) within a 1 kilometre distance of the northern sill (Fig. 3.17).

ADDITIONAL SEISMOSTRATIGRAPHIC UNITS

A single Huntec DTS/airgun profile from the mouth of Southern Bay indicates the presence of three basins which host sediment packages (Fig. 3.20). The two southernmost basins contain a package of semi-coherent reflections which do not clearly resemble units A to D. An acoustically incoherent unit (A?), with a ponded to draping basin-fill morphology and variable thickness of 7 to 30 ms, occurs at the base of the succession. The upper surface of this unit is irregular. Overlying this is a 20-30 ms thick series of interfingered acoustically stratified and transparent intervals with an average individual thickness of 2-4 ms. Some of these intervals onlap either the acoustically incoherent unit below or acoustic basement. Sediments drape the landward margin to the south of the basins.

The outermost of the three basins contains units A to D (Fig. 3.20; 4 to 7 km along track). Unit A ranges up to 10 ms thick and appears to exist as pockets onlapping an irregular basement surface. A number of parabolic reflections have been generated by this surface, seen on both 3.5 kHz and Huntec DTS records. Unit B is 10 ms thick

Figure 3.20. Huntec DTS profile within Southern Bay. Location shown in figure 3.4. Seismic units A to D are discussed in text. Dashed line denotes continuation of acoustic basement on the basis of airgun data. V.E. = vertical exaggeration. Depth in milliseconds two-way-travel-time.

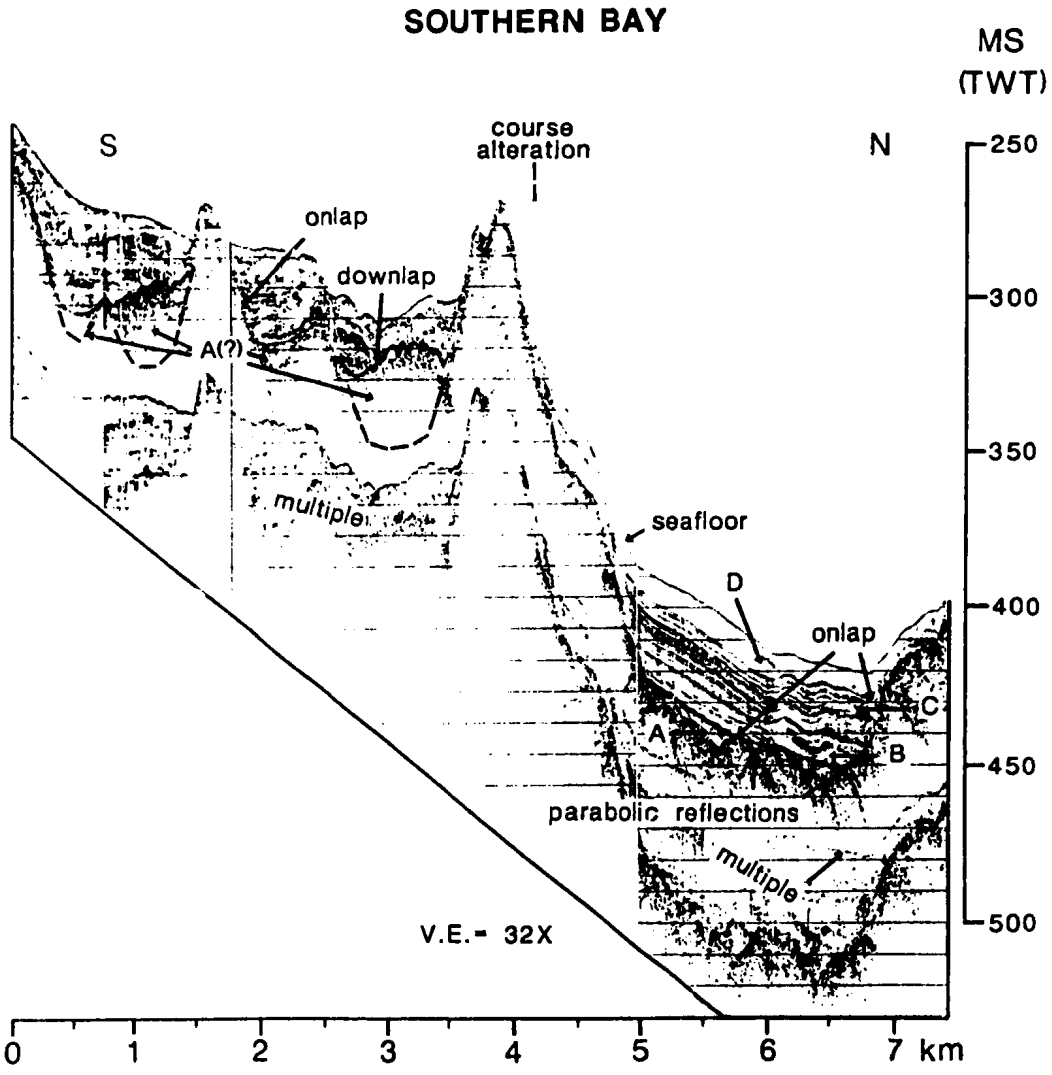
SOUTHERN BAY
MS
(TWT)
S
course
alteration
N
250
300
350
400
450
500
onlap
downlap
A(?)
multiple
seafloor
D
onlap
C
A
B
parabolic reflections
multiple
V.E.- 32X
0
1
2
3
4
5
6
7 km

and has a draping morphology, except at the northern edge, where it onlaps acoustic basement. Huntec DTS data shows convergent reflections and lens-shaped zones within this unit (Fig. 3.20). Unit C is an average of 12 ms thick. Although it has a draping basin-fill morphology, unit C is observed on the 3.5 kHz data to onlap rises of the underlying unit B. Unit D is up to 10 ms thick and has a draping basin-fill morphology.

The trough which parallels the NW end of the Central Basin in shallower water (and which may cross the sill to link with the outer bay sediments; Fig. 3.1) contains a package of unit A which is up to 50 ms thick, ponded and with a number of moderate intensity semi-continuous reflections (Fig. 3.21). Unit A's irregular upper boundary is gradational. While unit B is not clearly evident within figure 3.21, it is present in other profiles as a transparent, 5-10 ms ponded interval with low intensity, discontinuous reflections. Unit C is 10-20 ms thick and ponded, consisting of moderate intensity, semi-continuous reflections. Unit D has a variable distribution. In figure 3.21, unit D is up to 30 ms thick; whereas it is absent in other traverses across the trough. Some erosion of unit D has occurred (Fig. 3.21; 4 to 4.5 km along track). Unit morphology is both ponded and draping basin-fill. A small pocket of gas within units C and D is evident in figure 3.21, at approximately 6 km along track. This is the only

Figure 3.21. 3.5 kHz profile (E-W) across the Central Basin and then northward over the NW margin of the Central Basin. Location shown in figure 3.4. Seismic units A to D are discussed in text. Dashed line denotes continuation of acoustic basement on the basis of airgun data. V.E. = vertical exaggeration. Depth in milliseconds two-way-travel-time.

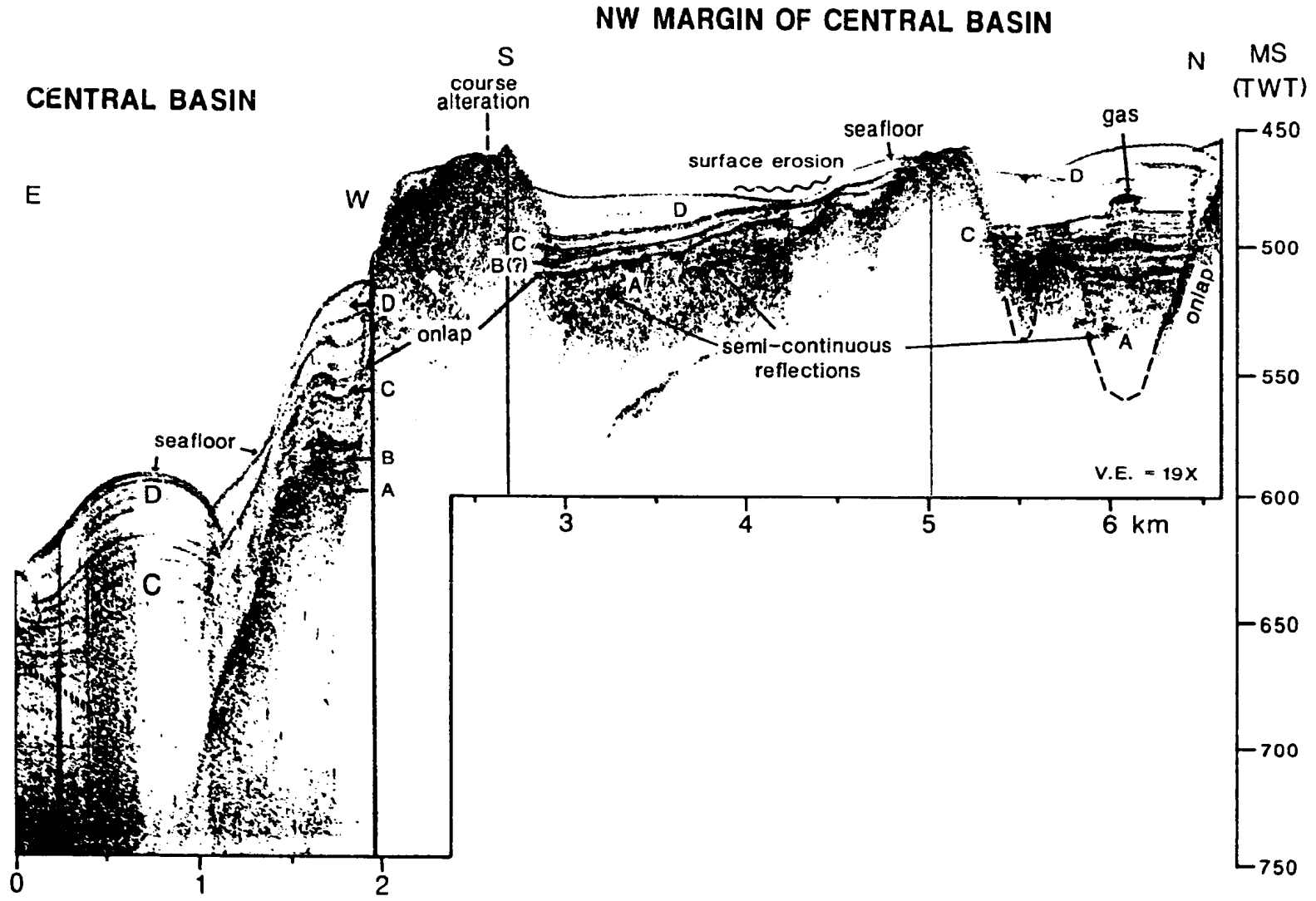
NW MARGIN OF CENTRAL BASIN
CENTRAL BASIN
E
W
S
N
course alteration
seafloor
surface erosion
gas
MS (TWT)
450
500
550
600
650
700
750
D
C
B(?)
A
onlap
semi-continuous reflections
B
V.E. = 19X
0
1
2
3
4
5
6 km

clear evidence of gas charging of sediments within Bonavista Bay.

Huntec DTS and airgun data from Clode Sound display a series of terraces which occur at decreasing depths into the fjord (to the SW) (Fig. 3.22). Some are formed by acoustically incoherent and stratified packages of sediment, over 40 ms thick, overlying and onlapping acoustic basement highs. Some of the stepped edges of these are defined by downcutting and erosion of the sediments. The seismic sequences beneath the terraces are not correlatable. They consist of intervals of moderate to high intensity, continuous reflections and intervals which are acoustically semi-transparent. Generally, the uppermost 2-4 ms consists of high intensity, continuous reflections, overlying a 10-15 ms thick semi-transparent interval. Erosion is very common, with downcutting of up to 30 ms defining the terraces and, in some cases, dissecting them (i.e.: Fig. 3.22; 3.8 km along track). The northeasternmost occurrence, at the transition into Chandler Reach, has three lens-shaped upper intervals which pinch out at their NE edge (Fig. 3.22).

Figure 3.22. Huntec DTS profile within Clode Sound. Location shown in figure 3.4. V.E. = vertical exaggeration. Depth in milliseconds two-way-travel-time.

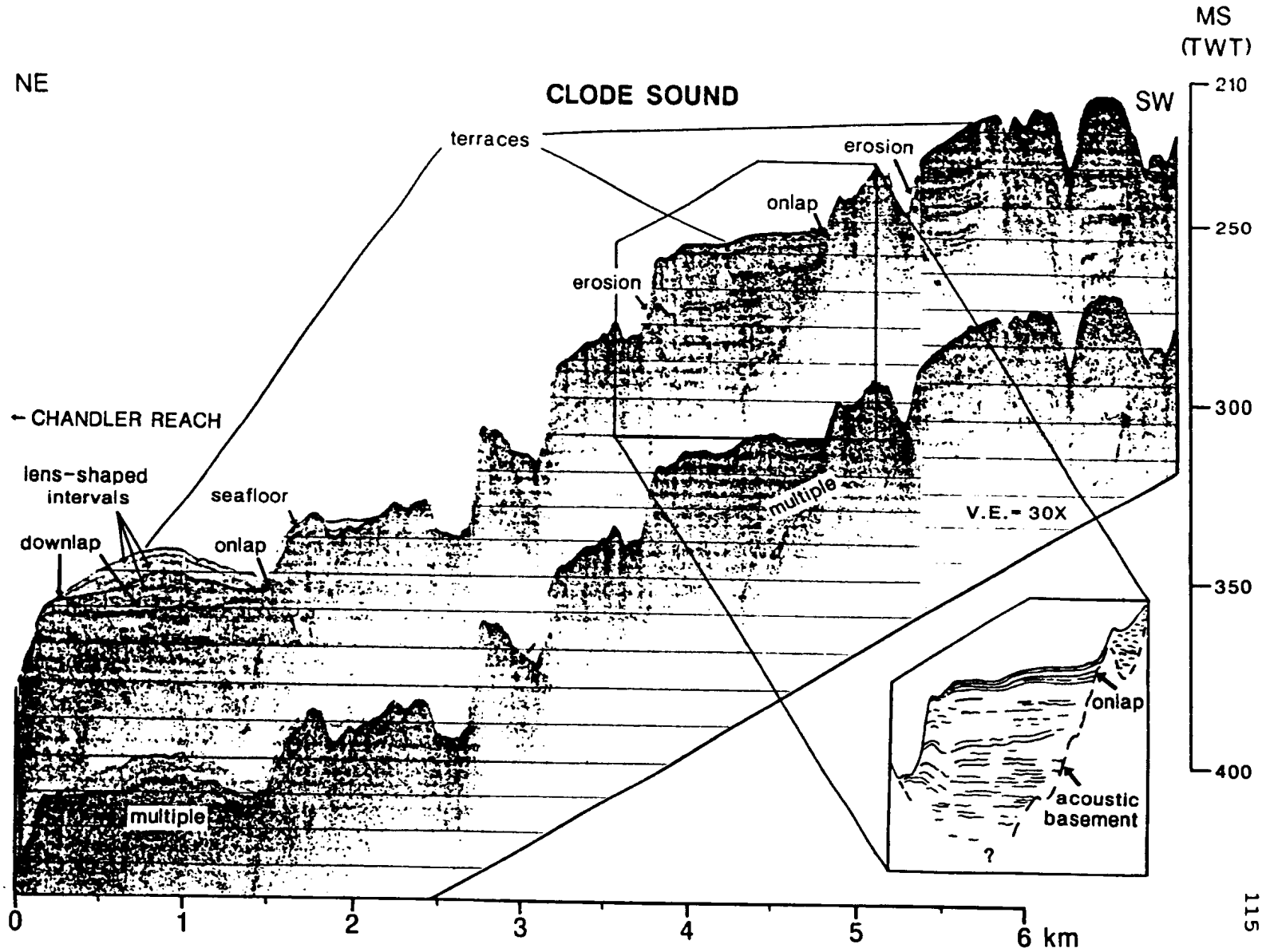
NE
CLODE SOUND
SW
MS
(TWT)
210
250
300
350
400
terraces
erosion
onlap
erosion
← CHANDLER REACH
lens-shaped
intervals
downlap
seafloor
onlap
multiple
V.E.= 30X
onlap
acoustic
basement
?
multiple
0
1
2
3
4
5
6 km

CHAPTER 4

CORE DATA

4.1 Introduction

On the basis of seismostratigraphic interpretation of the seismic profiles (Figs. 4.1-4.3), three core sites were chosen and three sediment cores were collected from the study area (Fig. 3.1). The intent was to sample as many seismic units as possible by coring in areas where the thickness of the uppermost units or entire seismic sequence is reduced. As a result, the intervals observed in the cores may not be fully representative of the entire seismic sequence present in the basin centers. This is particularly true for the uppermost sediments in core 87-030-001, where substantial erosion of seismic unit 3 has occurred in the coring region (Fig. 4.2).

Cores were sub-sampled for grain size and clay mineralogy analyses, as well as for preliminary palynological study (Section 2.3). The coarse fractions (>63 μm) of the grain size samples were briefly examined under a binocular microscope. It was noted that while the relative percentages of biogenic to lithic grains varied, the constituent grains almost always include quartz (quartzite), feldspars, various coloured sandstones and shales, micas and schists. The diversity of grain lithologies fits within the broad range of available source

Figure 4.1. 3.5 kHz profile through core site 86-026-011. Water depth at site is approximately 304 m. Seismic units 1 to 3 are discussed in Chapter 3. Dashed line denotes tentative seismic unit boundaries. V.E. = vertical exaggeration. Depth in milliseconds two-way-travel-time.

EASTERN BASIN
CORE SITE 86-026-011

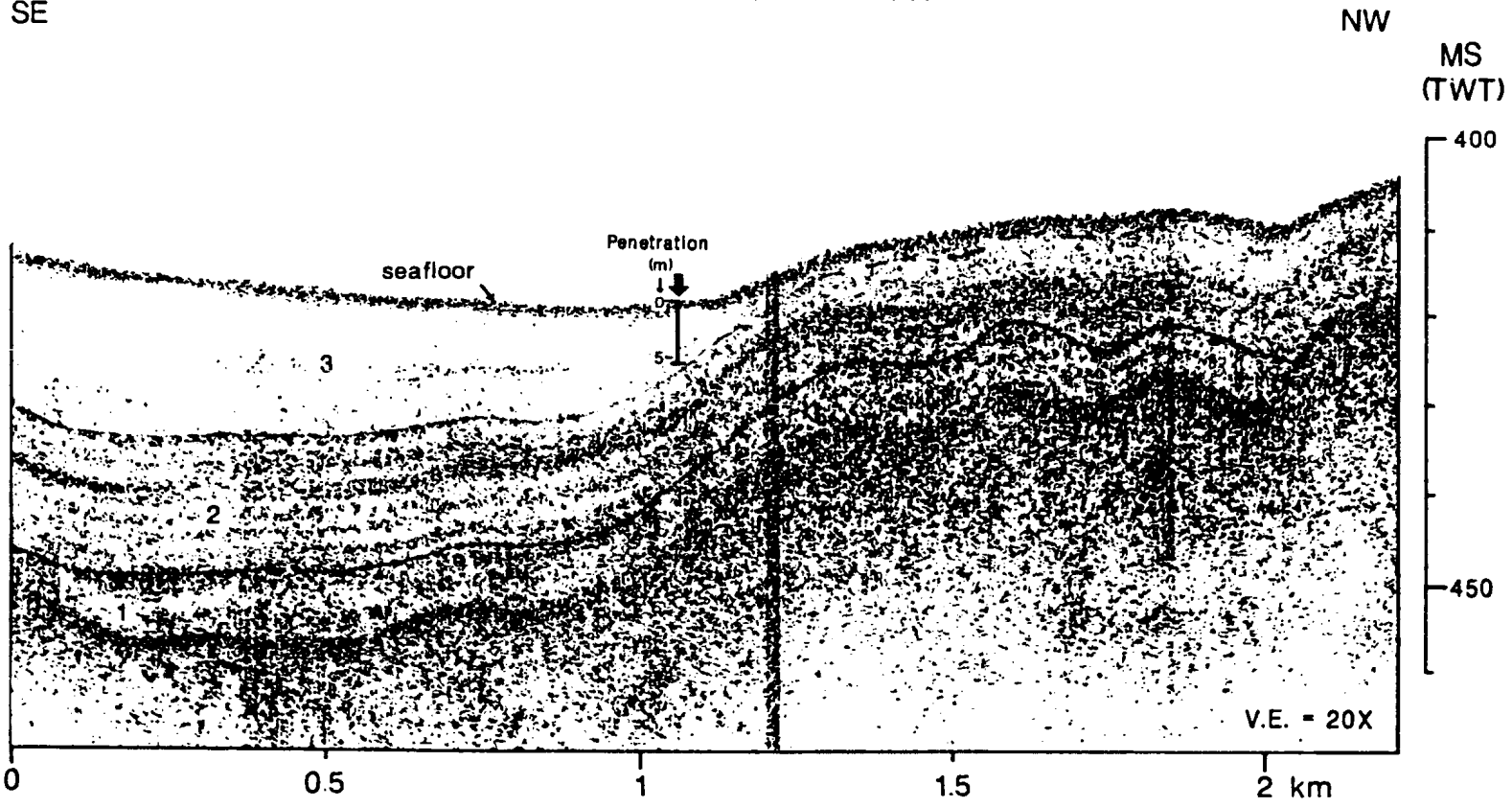

Figure 4.2. 3.5 kHz profile through core site 87-030-001. Water depth at site is approximately 325 m. Seismic units 1 to 3 are discussed in Chapter 3. V.E. = vertical exaggeration. Depth in milliseconds two-way-travel-time.

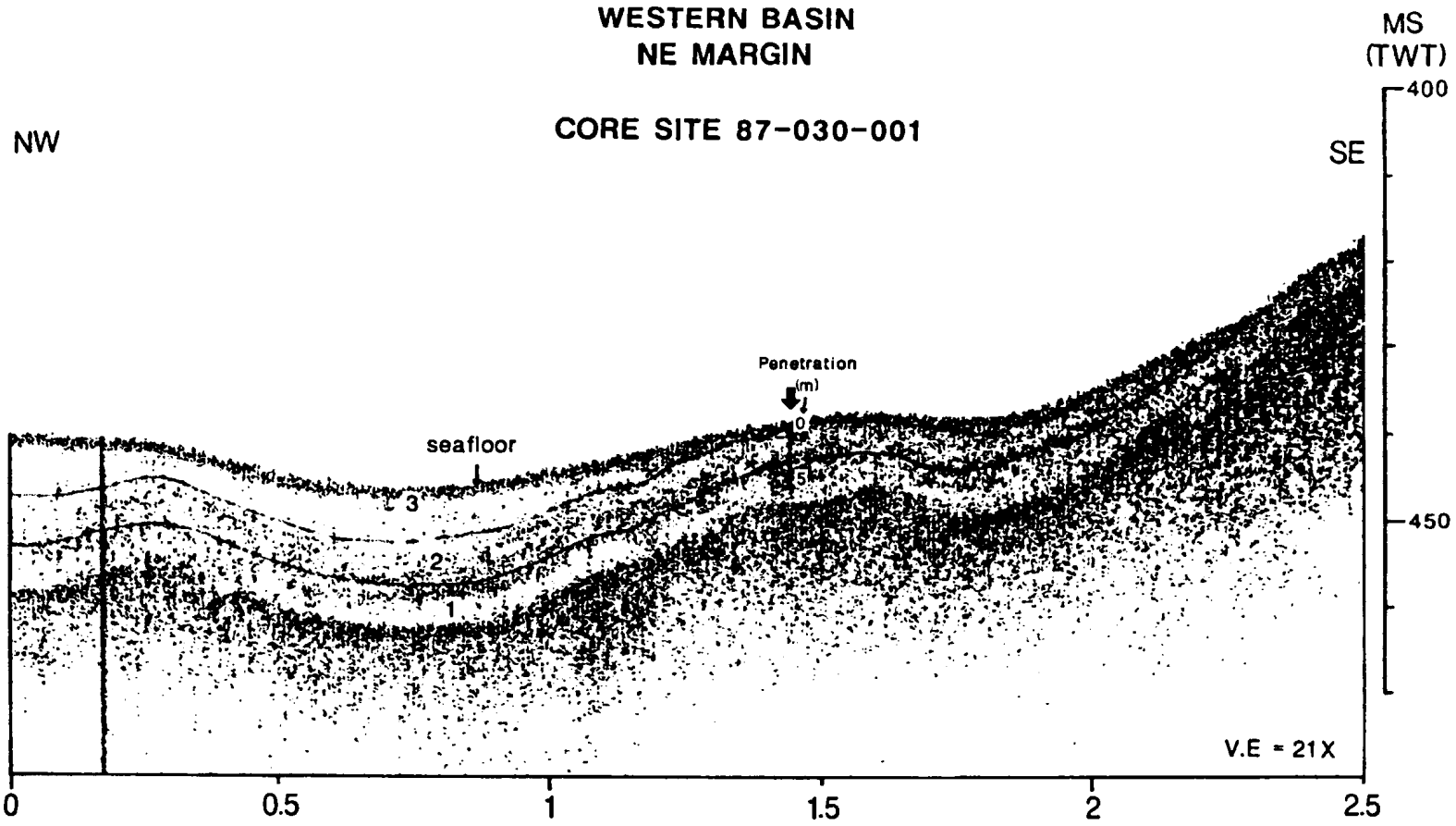
WESTERN BASIN
NE MARGIN
CORE SITE 87-030-001
NW
SE
MS
(TWT)
400
450
Penetration
(m)
0
5
seafloor
3
2
1
V.E = 21X
0
0.5
1
1.5
2
2.5

Figure 4.3. Huntec DTS profile through core site 87-033-020. Water depth at site is approximately 305 m. Seismic units A to D are discussed in Chapter 3. V.E. = Vertical exaggeration. Depth in milliseconds two-way-travel-time.

CHANDLER REACH
NE BASIN

E W

CORE SITE 87-033-020

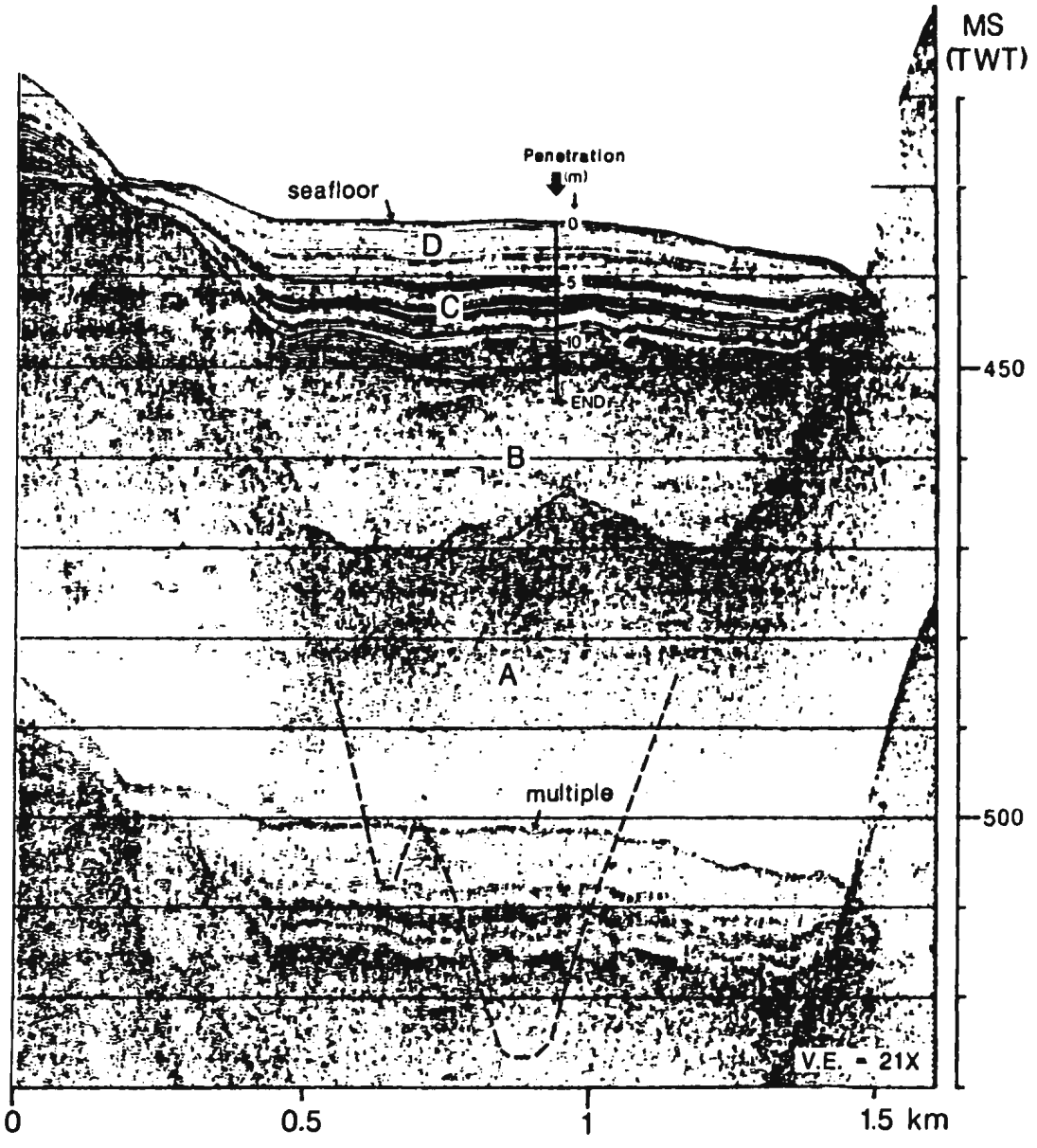

rock types and their widespread distribution (Section 1.2).

4.2 Lithofacies

Five lithofacies are identified on the basis of colour, sedimentary structures, grain size, clay mineralogy and palynology from the three cores (Fig. 4.4). Further support for the lithostratigraphic divisions within core 87-033-020 was provided by magnetic susceptibility data provided by Mr. F. Hall of the University of Rhode Island. Classification of colour was consistently carried out on moist sediment samples. The following facies descriptions are based upon initial core descriptions and x-radiographs. Subsequent sections discuss radiocarbon dates and clay mineralogic, grain size and biostratigraphic data. Section 4.10 attempts to summarize the data for each facies and provide interpretations.

Facies 1, at the top of each of the three cores, is comprised of a predominantly massive, olive-grey (5Y3/2) sandy, pebbly and shell bearing, silty mud. In cores 87-033-020 and 86-026-011 the colour gradually changes to greyish-olive (10Y4/2) at depth. Facies 1 within core 87-030-001 is only 15 cm thick, as opposed to greater than 5 m thicknesses in the other two cores. Sandy horizons of 1 to 3 cm thickness are common within this facies in cores 86-026-011 and 87-030-001, while the sand in facies 1 in core 87-033-020 is predominantly dispersed. In all cores,

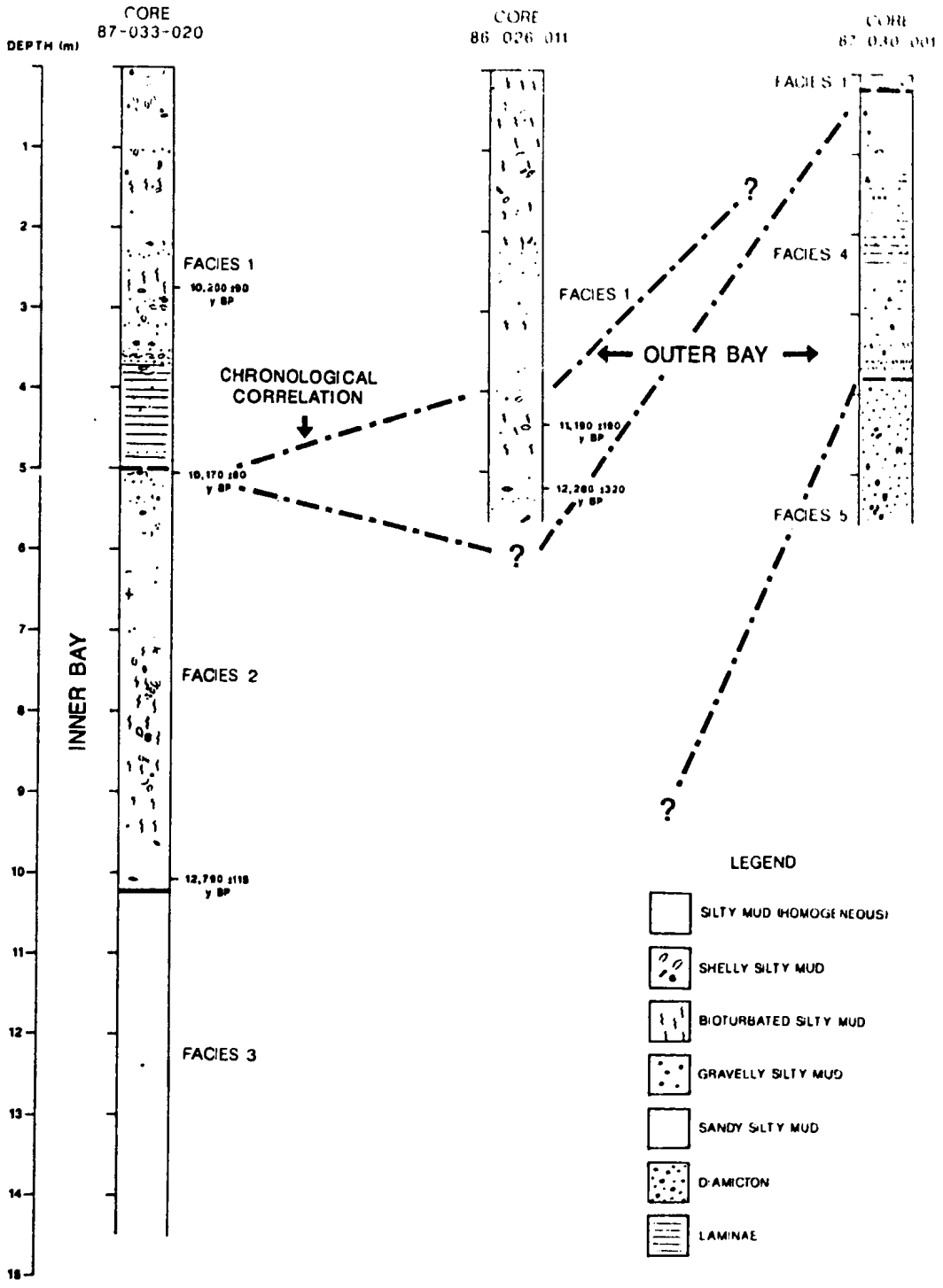

Figure 4.4. Lithofacies correlation and available radiocarbon age dates.

pebbles commonly occur within distinct, ungraded horizons, usually less than 10 cm thick. Bivalve mollusc and gastropod shells are common throughout the facies, occasionally concentrated within less than 5 cm thick intervals in core 87-033-020. Shells are largely intact, although many mollusc shells are disarticulated. Bioturbation is common within facies 1 and ranges from weak to moderate. A 1.3 m thick laminated interval occurs at the base of facies 1 in core 87-033-020 (Fig. 4.4), with faint, 3 to 4 millimetre (mm) thick colour banded laminations of lighter olive-grey (5Y5/2) silty mud every 2 to 3 cm within greyish-olive (10Y4/2) silty mud. The sediment comprising the laminations appears similar to that within the underlying facies 2 and may represent a transition between the two facies. The laminations are distinctly thinner and of a different colour than those within facies 4 (Fig. 4.4). Pebbly horizons occur over the laminated interval.

Facies 2 occurs over a 5 m interval within core 87-033-020 (Fig. 4.4). It is a predominantly massive, sandy, pebbly and shell bearing silty mud which varies in colour from pale greyish-olive (10Y5/2) at the top of the facies to light olive-grey (5Y5/1) at depth. Pebbles are most common within the upper 3 m of facies 2, often concentrated in horizons of 2 to 4 cm thickness or randomly dispersed within the sandy mud. A very coarse 25 cm thick interval, 10 cm from the top of facies 2, contains numerous pebbles, a 7 cm

long dropstone and mm scale laminations of grey (N4) sandy mud. Shells are abundant and consist mostly of bivalve molluscs (both as complete specimens and separated valves) and minor gastropods. X-rays indicate that most shells are unbroken. Wispy mycelia and pyritized burrows are also common. Some pinkish/pale red (10R5/2) bands and mottling are present in the lower 1.5 m of the observed interval of facies 2, together with a number of sandy laminations.

Facies 3 consists of a structureless and homogeneous pink/pale red (10R5/2) silty mud. A very few scattered pebbles and a 10 cm zone containing a few coarse sand grains are evident on x-radiographs. There are no shells or evidence of bioturbation. This facies comprises the lowermost 4.5 m of core 87-033-020.

Facies 4 is present only in core 87-030-001 and extends to a depth of 3.6 m, directly beneath the 15 cm thickness of facies 1. Facies 4 is comprised of two sub-facies, largely interlaminated on a mm to cm scale. Sub-facies 4A is a pale yellowish-brown (10YR5/2) to pale greyish-brown (5YR4/2) sandy pebbly mud. Sub-facies 4B is a light olive-grey (5Y5/2) sandy pebbly mud. Sub-facies 4A alone comprises the upper 60 cm of the observed 3.6 m of facies 4 and contains abundant pebbles and dropstones (one of which measures 6 x 3 cm). Within the laminated sequence, sub-facies 4A appears to have a higher abundance of pebbles than sub-facies 4B. The biogenic content of facies 4 is very low and is confined

to the uppermost metre. Only one complete shell, a bivalve mollusc, was found, but was too small to provide an AMS radiocarbon date. At the base of facies 4 is a 40 cm thick zone of transition into facies 5, consisting of mottled, greyish-red, sandy mud (sub-facies 4A) intermixed with dark grey, sandy-gravelly mud (facies 5). There are three 2 to 3 cm thick bands of facies 5 within this interval. Although the term "laminated" is used to describe much of facies 4, many of the intervals of sub-facies 4A or 4B actually exceed the 1 cm maximum thickness for laminae. For simplicity, and given an average thickness of less than 1 cm, no distinction is made. By comparison, the laminated sequence at the base of facies 1 (core 87-033-020) contains true laminations of 3 to 4 mm thickness.

Facies 5 consists of a stiff, dark grey (N3) sandy-gravelly mud. Pebbles of up to 5 cm maximum diameter are abundant. It contains no laminations, bioturbation or biogenic content. This sediment is termed a "diamicton" (Flint, 1971).

4.3 Correlation Between Lithofacies and Seismic Units

The cores are correlated with the seismic records, assuming an acoustic velocity of 1500 m/s (Figs. 4.1-4.3). Facies 1, uppermost within all three cores, is correlated with seismic units 3 and D in the outer and inner bay, respectively. In the inner bay, facies 2 is correlated with

seismic unit C. Facies 3 is correlated with seismic unit B. In the outer bay, facies 4 is correlated with seismic unit 2, and facies 5 is correlated with seismic unit 1. These correlations are intended to permit depositional histories interpreted from the lithofacies to be tentatively extended throughout the basins of the bay.

The penetration of core 87-030-001 (Fig. 4.2) is tentative, since a triggerweight core was not collected to confirm the completeness of the uppermost sediments. Judging by the level of mud on the outside of the barrel, the Benthos piston corer did not penetrate to the maximum possible extent and therefore collected a relatively complete sample.

4.4 Radiocarbon Dates

4.4.1 Dating of Seismic Units

Five AMS radiocarbon dates from two cores allow a partial chronostratigraphy to be developed (Table 4.1 and Fig. 4.4).

The date of 12,280 ± 320 y BP from 5.22 m in core 86-026-011 is 37 cm from the bottom of the core. 3.5 kHz data (Fig. 4.1 and profiles collected during core collection) indicate that the base of unit 3 occurs within 50 cm of the bottom of the core. The dated sample was therefore approximately 87 cm from the base of unit. Using a

Table 4.1: AMS radiocarbon dates on shell material.

Core #.	Depth (cm) from top.	Facies.	Age (y BP)	Laboratory Sample #.
86-026-011	441.5	1	11,110 ±190	Beta 21535
86-026-011	521.5	1	12,280 ±320	Beta 21536
87-033-020	275	1	10,200 ±90	TO 1732
87-033-020	506	1/2	10,170 ±80	TO 1733
87-033-020	1007	2	12,790 ±115	Beta 27227

Beta = Beta Analytic Inc. of Coral Gables, Florida, U.S.A.

TO = Isotrace Laboratory at the University of Toronto, Toronto, Canada.

sedimentation rate of 0.68 m/1000 years (ka) (Section 4.4.2), a maximum age of 13,500 y BP is suggested for the base of unit 3 at the core site. The base of unit D, at the same stratigraphic position from core 87-033-020 within Chandler Reach, is dated at 10,170 ± 80 y BP. The bases of the two correlated units are therefore diachronous.

The date of 10,170 ± 80 y BP at the base of unit D also provides the age of the top of unit C. Unit C is bracketed by this upper date of 10,170 ± 80 y BP and a date of 12,790 ± 115 y BP at its base. The top of unit B is also therefore dated at 12,790 ± 115 y BP.

4.4.2 Sedimentation Rates

Core 86-026-011

The two radiocarbon dates from near the base of core 86-026-011 allow calculation of a sedimentation rate for facies 1 (unit 3) near the middle of the Eastern Basin. There has, however, been some erosion of unit 3 at the core site (Fig. 4.1), so that caution is necessary in extrapolating sedimentation rates throughout the basin.

The date of 11,110 ± 190 y BP at 4.42 m depth allows calculation of a sedimentation rate to present of 0.40 m/ka. The lower date, at 5.22 m, of 12,280 ± 320 y BP provides a rate of 0.42 m/ka when calculating over the entire core. The sedimentation rate over the 0.8 m distance between these

two dates over 1,170 years is 0.68 m/ka. If sedimentation had occurred at this rate from 12,280 y BP to present, the dated shell would have been buried at a depth of 8.35 m, as opposed to 5.22 m, a difference of 3.1 m. The thickness of unit 3 in the middle of the Eastern Basin (Fig. 4.1) reaches 12.75 m (17 ms). This suggests that the sediments comprising facies 1 were not deposited as conformable cover across the basin and subsequently eroded, but were preferentially deposited within the basin center. The sedimentation rate of 0.68 m/ka from 12,280 to 11,110 y BP may be lower than the sedimentation rate in the middle of the basin, perhaps as a result of syn-depositional erosion. It is also possible that sedimentation rates increased after 11,110 y BP throughout the basin, being uniform everywhere, but that erosion has since removed sediments from the core site.

Core 87-033-020

The thickness of the seismic sequence at core site 87-033-020 is substantially less than that within the main basin of Chandler Reach (Figs. 4.3, 3.13).

A sedimentation rate for unit C (facies 2) of 1.9 m/ka is calculated for 5 m interval bracketed by the dates of 12,790 $\pm$ 115 y BP at the unit's base (10.08 m) and 10,170 $\pm$ 80 y BP near the contact with unit D at 5.06 m. Calculating a sedimentation rate for unit D (facies 1) within Chandler

Reach is complicated by the two similar dates, 2.31 m apart, within the cored interval. This can be explained if either the 2.31 m interval had an extremely high sedimentation rate, or if there has been post-depositional reworking. Bioturbation and shells are present between the two dates. The date of 10,170 ± 80 y BP at 5.06 m provides a sedimentation rate of 0.50 m/ka from the base of unit D to present. The rate indicated by the date of 10,200 ± 90 y BP at 2.75 m is 0.27 m/ka. In either case, sedimentation rates apply only to the NE basin, since the seismic sequence is thinner in comparison to the main basin in Chandler Reach.

4.5 Clay Mineralogy

The relative abundances of 10 clay and non-clay minerals have been calculated for the clay-sized fraction (<2 μm) of collected sediment samples. The results for each sample are normalized to 100% and plotted against depth in the three cores (Figs. 4.5, 4.6). Illite is the most abundant mineral, as is generally the case within surficial sediments of the North Atlantic (Biscaye, 1965). Although illite is dominant and tends to mask relative changes in the remaining minerals, some trends can be distinguished. The variability of the surrounding geology (Section 1.2) and the lack of terrestrial clay mineral data precludes a detailed discussion of sources for the clays. However, variations which are evident downcore help to differentiate the facies.

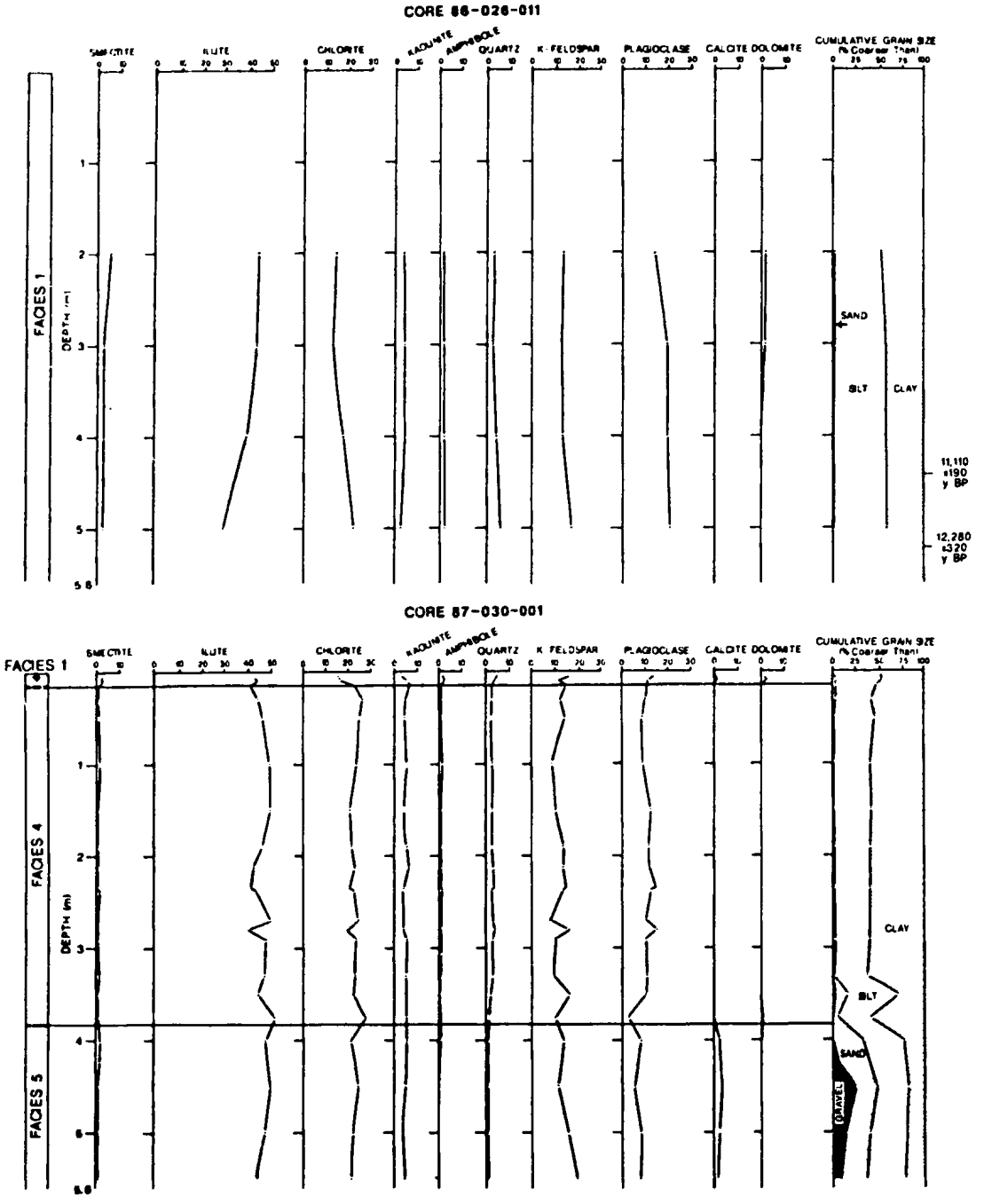

Figure 4.5. Relative abundances of clay and non-clay minerals within the clay-sized fraction, as well as cumulative grain size data, plotted against depth in cores 86-026-011 and 87-030-001. Data for each sample normalized to 100%.

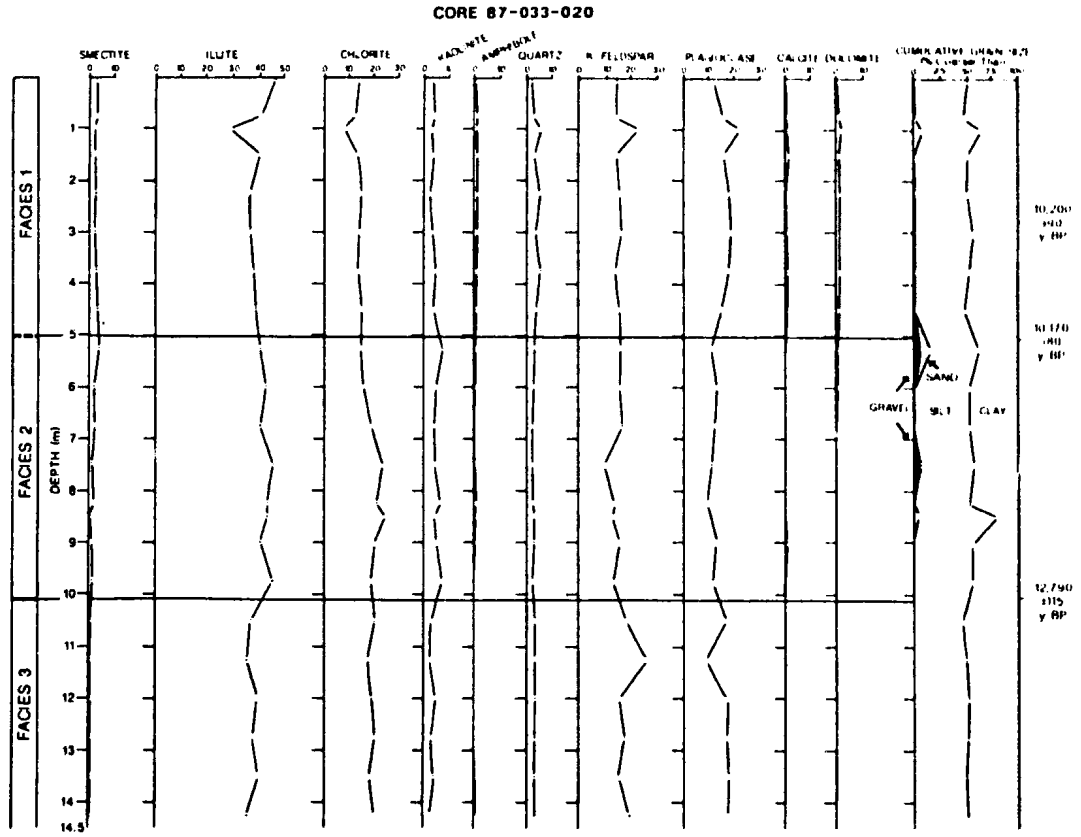

Figure 4.6. Relative abundances of clay and non-clay minerals within the clay-sized fraction, as well as cumulative grain size data, plotted against depth in core 87-033-020. Data for each sample normalized to 100%.

The mean relative abundances of clay-sized minerals for each facies are displayed in table 4.2. Facies 1 is presented separately for each core location (Fig. 2.1). Potential source rocks may have varied between sites, along with sediment transport mechanisms and distances travelled by grains. In general, caution is necessary when comparing relative abundances between facies from different cores.

Facies 1 in all three cores contains the highest relative abundances of smectite, amphibole and quartz of the five facies. Values for chlorite are at a minimum. Calcite and dolomite, which are rare in other facies, are often present.

Facies 2 displays a down-core decrease in the abundance of smectite and a corresponding increase in chlorite. Kaolinite is slightly more common within facies 2 than within facies 1 or 3. Plagioclase and K-feldspar are less abundant within facies 2 than within facies 3 and, to a lesser degree, facies 1.

Facies 3 contains small amounts of smectite but relatively abundant chlorite. Quartz, plagioclase and K-feldspar are higher in abundance when compared to levels in facies 2.

Facies 4 is host to low levels of smectite and high amounts of chlorite in comparison to facies 1. Chlorite abundance is the highest of all the facies. Amphibole, quartz, plagioclase and K-feldspar are all decreased in

Table 4.2: Mean relative percentages of minerals within the clay-sized (<2μm) fraction for individual lithofacies.

LITHOFACIES	CORE	$\bar{X}_{SME}$	$\bar{X}_{ILL}$	$\bar{X}_{CHL}$	$\bar{X}_{KAO}$	$\bar{X}_{AMP}$	$\bar{X}_{QUA}$	$\bar{X}_{FLD}$	$\bar{X}_{PLG}$	$\bar{X}_{CAL}$	$\bar{X}_{DOL}$
1	86-026	3.2	38.6	16.4	3.4	1.6	3.7	13.7	18.5	0.2	0.9
1	87-033	3.1	38.6	13.5	3.8	1.3	4.2	15.9	17.5	0.7	1.5
2	87-033	2.1	42.6	19.9	5.5	0.6	2.9	14.0	12.1	0.2	0.2
3	87-033	0.7	37.4	19.1	3.0	0.6	3.3	18.8	17.1	0.1	0.0
1	87-030	2.4	42.8	16.2	4.5	1.6	3.8	13.8	12.6	0.7	1.8
4	87-030	0.8	45.2	23.1	4.9	0.5	2.5	12.2	10.8	0.0	0.1
5	87-030	0.8	46.8	22.3	4.4	0.1	0.9	15.2	7.4	2.2	0.0

comparison with facies 1.

Facies 5 has similar abundances to facies 4, with the exception of a further decrease in quartz, the existence of calcite, an increase in K-feldspar and a decrease in plagioclase.

The relative decline in the amount of smectite (never >5%) below facies 1 and upper facies 2 suggests that this mineral was uncommon within the primary source rocks for underlying facies. Smectite within facies 1 and 2 may have originated from different terrestrial sources. Altered volcaniclastic rocks of the Connecting Point Group are a possible source of smectite (Dec et al., 1989), although low grade metamorphism may have produced alteration to illite or chlorite (Folk, 1974). It is more likely, however, that the smectite increase originates from ocean current (Labrador Current) transport of sediment from known Tertiary sources to the north; a theory proposed by Piper and Slatt (1977) to explain similar trends observed farther offshore. Calcite and dolomite, common within facies 1, may have originated from very limited terrestrial sources (Adeytown or Harcourt Groups; Section 1.2) but likely reflect ocean current transport of clay-sized minerals from sources outside the study area. The presence of calcite within facies 5 is intriguing, again given limited potential terrestrial sources. In this case, another possible source might be biogenic debris within marine sediments incorporated into

the diamicton. The increase in chlorite which occurs down-core likely reflects a source within the low grade metamorphosed rocks of the Avalon and Gander Zones which surround the bay. Chlorite is an easily weathered silicate which can be concentrated by glacial erosion (Jackson et al., 1948). Facies 2 has lower abundances of quartz, plagioclase and K-feldspar than either facies 1 or 3 in core 87-033-020, likely reflecting a reduced influence of granitic source rocks.

4.6 Grain Size Data

Plots of cumulative grain size against depth for each of the three cores are displayed in figures 4.5 and 4.6. Facies 1, 2 and 3 consist primarily of a nearly even mixture of silt and clay, with minor amounts of sand and occasionally gravel. Facies 4 has a higher clay than silt content, again with intervals containing minor sand and gravel. Facies 5 is distinctly coarser. On a ternary plot (Fig. 4.7), samples from facies 1,2,3 and 4 generally plot close to the silt/clay axis, whereas samples from facies 5 plot towards the sand/gravel apex. Samples from facies 1,2 and 4 that plot away from the silt/clay axis are from coarser horizons which are common to all three facies.

Individual cumulative frequency curves are presented for each facies (Figs. 4.8-4.10). The cumulative weight percents (% coarser than) are plotted on a probability

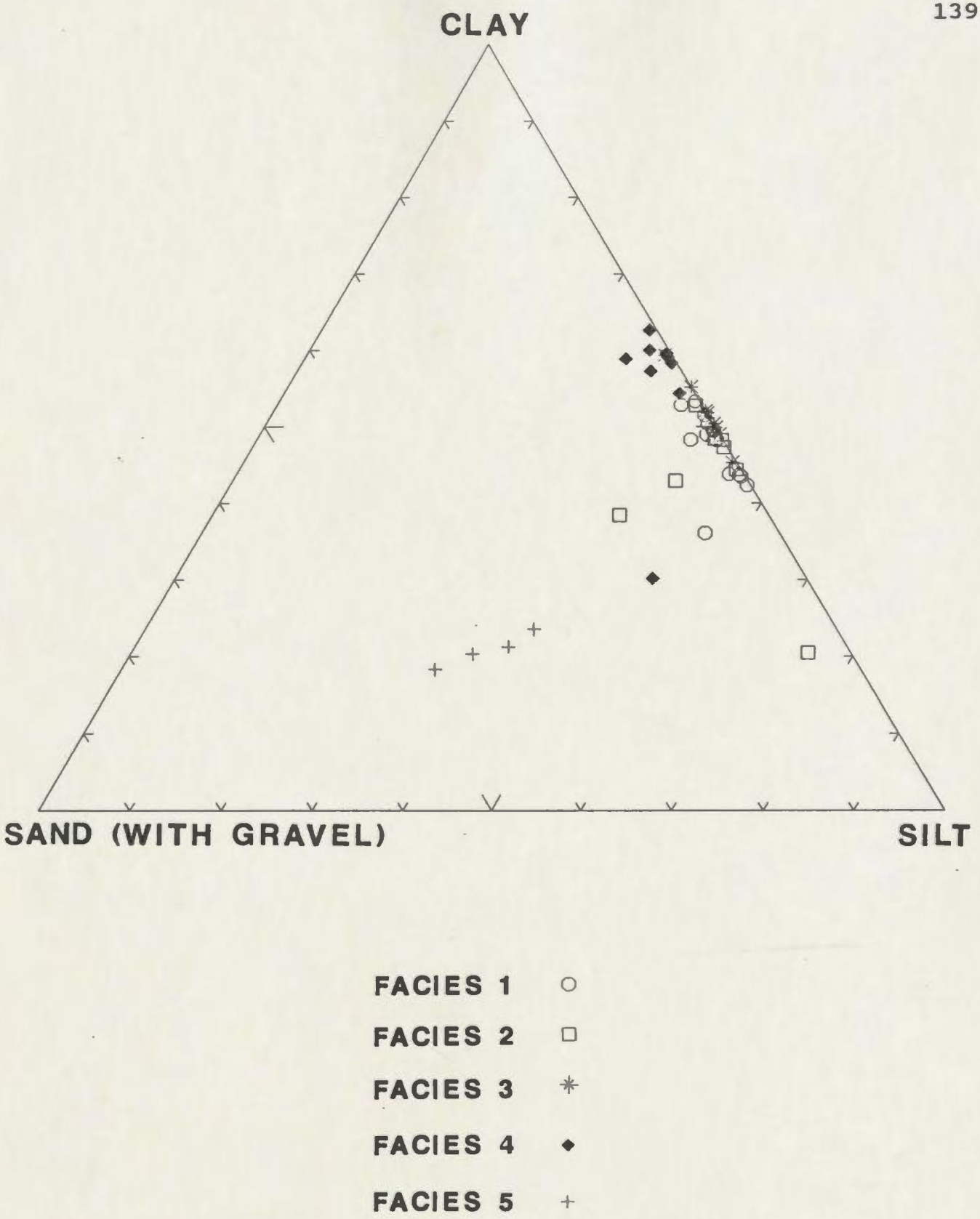

Figure 4.7. Ternary diagram (Shepard, 1954) displaying all samples from the five lithofacies described. Gravel has been included with the sand fraction to incorporate all data.

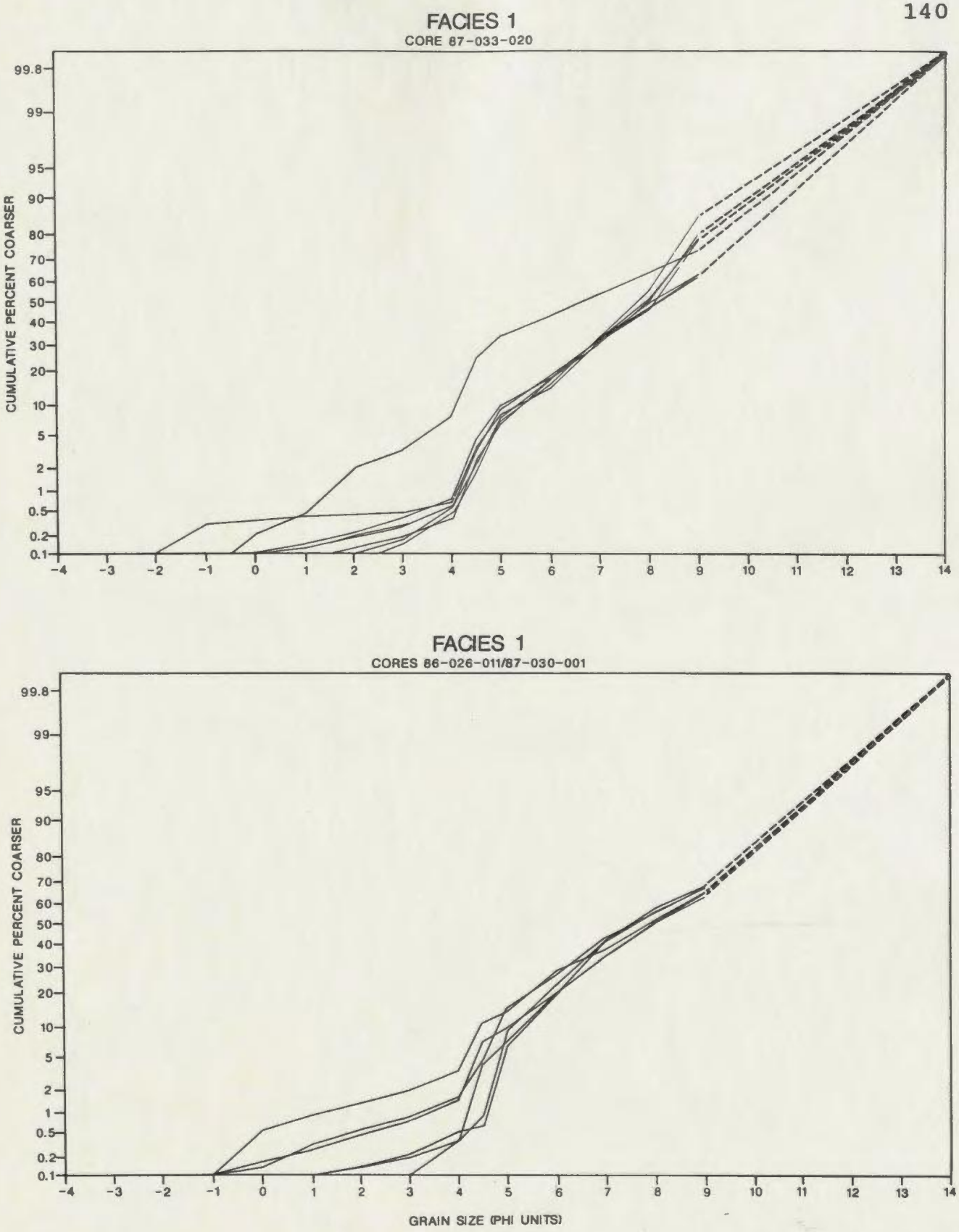

Figure 4.8. Cumulative grain size curves, plotted on probability scale ordinate, for facies 1 in inner and outer Bonavista Bay. Data are extrapolated from 9Φ to an assumed minimum grain size of 14Φ.

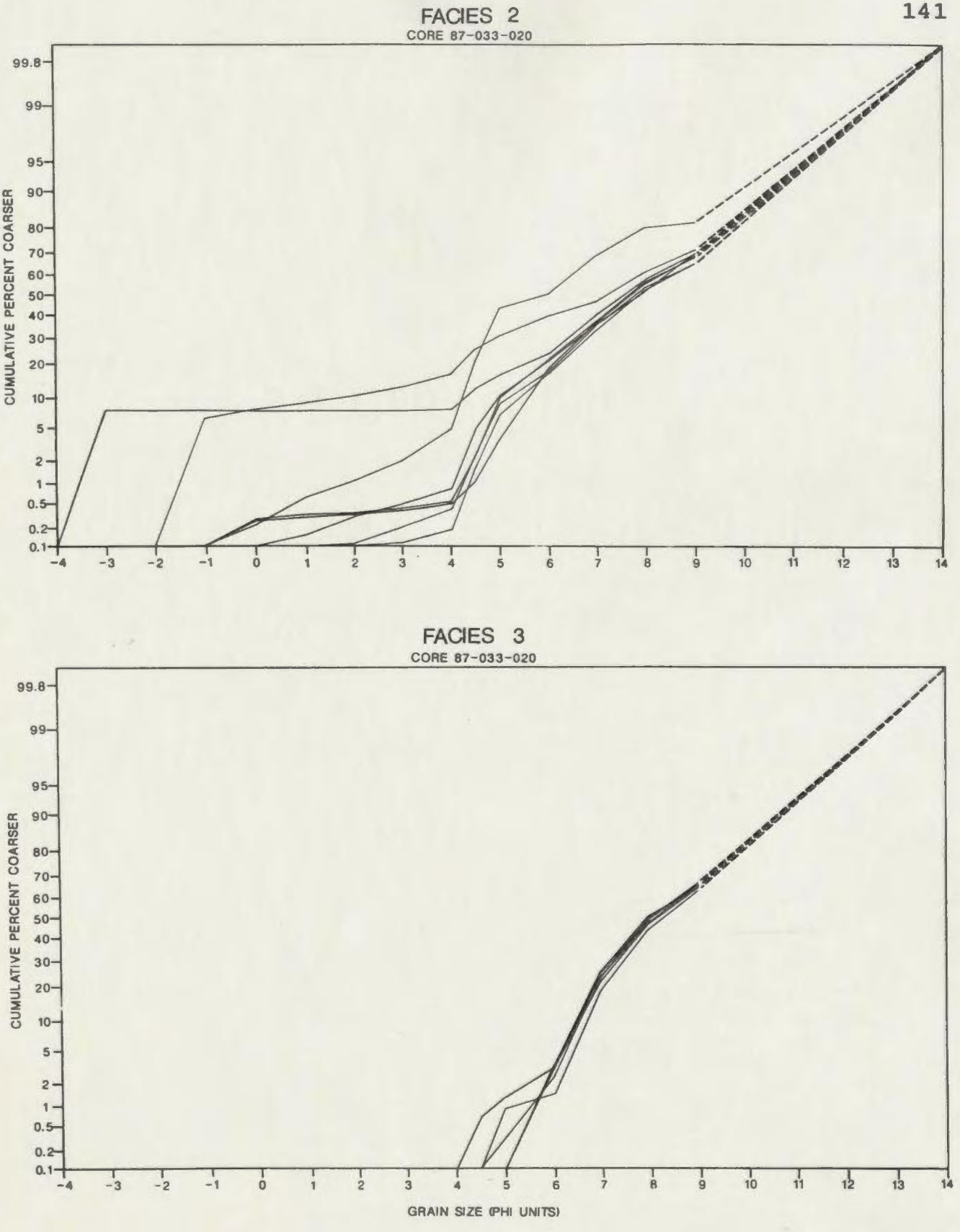

Figure 4.9. Cumulative grain size curves, plotted on probability scale ordinate, for facies 2 and 3. Data are extrapolated from 9Φ to an assumed minimum grain size of 14Φ.

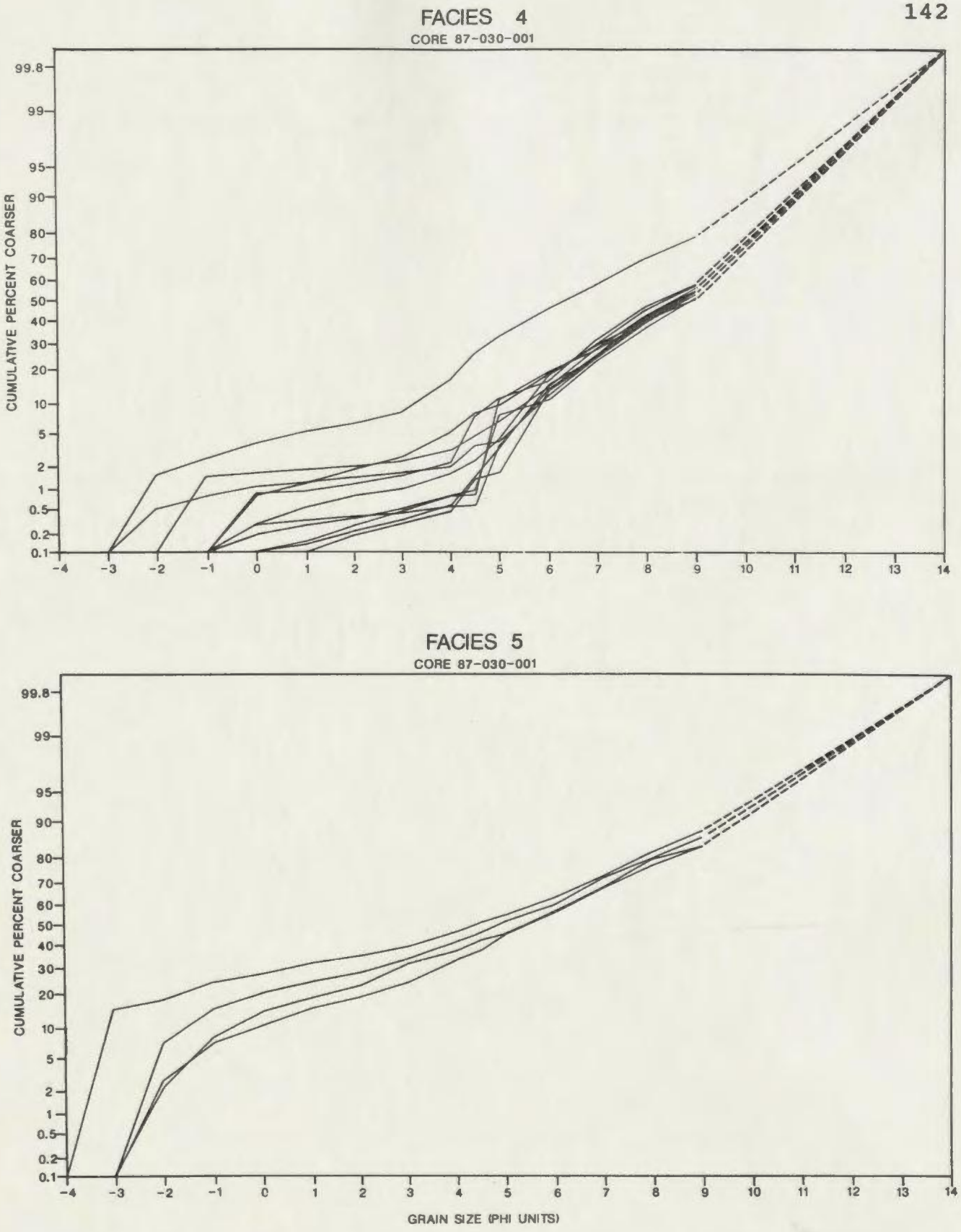

Figure 4.10. Cumulative grain size curves, plotted on probability scale ordinate, for facies 4 and 5. Data are extrapolated from 9Φ to an assumed minimum grain size of 14Φ.

scale. Plots of this type produce a straight line for a sample with perfect (log) normal (Gaussian) grain size distribution. A well-sorted sample produces a steeper line than one which is poorly-sorted. A plot which contains two or more distinct segments can be interpreted to indicate the presence of multiple grain size populations (i.e.: Visher, 1969; Gipp, 1989).

Individual plots were analyzed to produce statistical measures of mean grain size, median grain size, sorting, skewness and kurtosis for each sample (Table 4.3), using the method of Folk (1974):

The mean grain size, or graphic mean (M_Z) is averaged from three percentiles;

$$M_Z = \frac{\Phi_{16} + \Phi_{50} + \Phi_{84}}{3}$$

The median grain size corresponds with the grain size in phi units (Φ) at the mid-point of the grain size distribution, or the 50th percentile (Φ_{50}).

The degree of sorting is inferred from the value of the inclusive graphic standard deviation (σ_1);

$$\sigma_1 = \frac{\Phi_{84} - \Phi_{16}}{4} + \frac{\Phi_{95} - \Phi_5}{6.6}$$

A value of σ_1 within the range 0.35-0.5Φ indicates a well-sorted sample; 0.5-0.71Φ = moderately well-sorted; 0.71-1.0Φ = moderately-sorted; 1.0-2.0Φ = poorly-sorted; 2.0-4.0Φ = very poorly-sorted and >4.0Φ = extremely poorly-sorted.

Table 4.3: Statistical measures of grain size data.

FACIES 1

Core 87-033-020 (Inner bay)

SAMPLE DEPTH (cm)	MEDIAN GR. SIZE (Φ)	MEAN GR. SIZE (Φ)	SORTING σ_I (Φ)	SKEWNESS Sk_I	KURTOSIS K_G
5	7.95	7.77	1.77	-0.10	1.14
75	8.20	8.08	2.13	-0.06	0.89
101	6.55	6.88	2.54	0.19	0.70
150	8.05	8.07	2.06	0.01	0.92
225	8.15	8.08	2.07	-0.03	0.89
300	7.75	7.90	1.85	0.04	1.11
375	7.90	7.73	1.89	-0.08	1.12
450	8.15	7.95	1.80	-0.14	1.17
Core 86-026-011 (Outer bay)					
198	8.00	7.97	2.10	-0.01	0.85
298	7.50	7.53	2.25	0.07	0.77
398	7.60	7.82	2.03	0.15	0.85
498	7.50	7.72	2.10	0.16	0.82
Core 87-030-001 (Outer bay)					
5	8.00	7.97	2.19	-0.03	0.89
10	7.85	7.75	2.34	-0.04	0.79

FACIES 2

Core 87-033-020

SAMPLE DEPTH (cm)	MEDIAN GR. SIZE (Φ)	MEAN GR. SIZE (Φ)	SORTING σ_I (Φ)	SKEWNESS Sk_I	KURTOSIS K_G
525	7.25	7.02	3.31	-0.24	1.07
600	7.90	8.00	2.04	0.06	0.89
675	7.80	7.95	2.09	0.09	0.89
750	7.60	7.52	3.43	-0.27	1.85
825	7.85	7.80	2.10	-0.02	0.92
848	6.00	6.55	2.08	0.50	0.80
901	7.70	7.87	1.95	0.15	0.86
975	7.70	7.75	2.10	0.07	0.85

FACIES 3

Core 87-033-020

SAMPLE DEPTH (cm)	MEDIAN GR. SIZE (Φ)	MEAN GR. SIZE (Φ)	SORTING σ_I (Φ)	SKEWNESS Sk_I	KURTOSIS K_G
1050	8.30	8.48	1.57	0.20	0.89
1125	8.15	8.33	1.61	0.21	0.87
1200	7.95	8.30	1.65	0.32	1.04
1275	8.00	8.28	1.61	0.27	0.84
1350	8.15	8.33	1.59	0.20	0.91
1425	8.00	8.27	1.60	0.27	0.91

FACIES 4

Core 87-030-001

SAMPLE DEPTH (cm)	MEDIAN GR. SIZE (Φ)	MEAN GR. SIZE (Φ)	SORTING σ_I (Φ)	SKEWNESS Sk_I	KURTOSIS K_G
15	8.20	8.18	2.11	-0.08	0.86
30	8.50	8.37	2.12	-0.11	0.95
50	8.40	8.22	2.08	-0.08	0.82
100	8.55	8.37	2.05	-0.09	0.93
150	8.60	8.45	2.01	-0.09	0.90
190	8.60	8.43	1.97	-0.07	0.87
236	8.70	8.28	2.24	-0.20	0.86
290	8.75	8.53	2.03	-0.14	0.89
330	8.90	8.63	2.07	-0.19	0.98
350	6.30	6.57	2.92	0.03	0.99
375	8.90	8.42	2.40	-0.29	0.95

FACIES 5

Core 87-030-001

SAMPLE DEPTH (cm)	MEDIAN GR. SIZE (Φ)	MEAN GR. SIZE (Φ)	SORTING σ_I (Φ)	SKEWNESS Sk_I	KURTOSIS K_G
400	5.40	5.27	3.78	-0.09	1.04
450	4.35	3.42	4.78	-0.19	0.68
500	4.90	4.25	4.24	-0.17	0.80
550	5.40	4.97	3.94	-0.15	0.90

Skewness (Sk_I) calculations provide an indication of the degree of symmetry of a plot about the median;

$$Sk_I = \frac{\Phi_{84} + \Phi_{16} - 2\Phi_{50}}{2x(\Phi_{84} - \Phi_{16})} + \frac{\Phi_{95} + \Phi_{5} - 2\Phi_{50}}{2x(\Phi_{95} - \Phi_{5})}$$

A positive skewness value indicates that the mean grain size of a curve lies to the right (finer-grained) side of the median and that there is an excess of fine-grained material. A negative skewness value indicates an excess of coarse material. Sk_I values of 0.00 to ($\pm$)0.10 are near symmetrical; ($\pm$)0.10-0.30 = skewed; ($\pm$)0.30-1.00 = strongly skewed.

Kurtosis (K_G) provides an indication of the sorting within the central 50% of the sample (between Φ_{25} and Φ_{75}) as compared to sorting within the "tail" regions (extending to Φ_{95} and Φ_{5}). This is equivalent to the "peakedness"of the grain size distribution;

$$K_G = \frac{\Phi_{95} - \Phi_{5}}{2.44x(\Phi_{75} - \Phi_{25})}$$

A value of 1.00 indicates an even degree of sorting, >1 indicates poorer sorting in the tails (i.e.: a peaked distribution), <1 indicates poorer sorting within the cental interval.

Since the statistical calculations only incorporate measures from above Φ_5, the entire sample may not always be characterized. For facies 1,2 and 4, the cumulative frequency curves generally contain at least two segments (Figs. 4.8-4.10). For most samples from these facies, the

largest segment extends from 9Φ to approximately 4.5Φ, and ends near the 5th percentile (Φ_5). The statistical calculations therefore apply solely to this finer grain size population, and do not reflect a coarser grain size population which may be present beneath Φ_5. Breaks which occur near 4Φ in the curves are likely the result of combining pipette analysis data with sieve data.

The massive, unstructured zones of facies 1 have a mean grain size of 7.8Φ in both the inner and outer bay. A poorly-sorted to very poorly-sorted fine-grained population comprises over 90% of the sample weight. The degree of sorting decreases from inner to outer bay. The flatter slope of the coarse population (>4Φ) indicates an even lower degree of sorting than in the fine population (Fig. 4.8). Skewness occurs on both sides of the median. Most samples have K_G values <1, indicating that the grain size distribution is not increasingly sorted or peaked within the central 50%.

The mean grain size of facies 2, at 7.6Φ, is very similar to facies 1, as is the poor to very poor degree of sorting. Above average values of σ_I for samples at 525 and 750 cm are a result of the coarse population exceeding 5 percent by weight and being included in the calculation of σ_I. While these two samples display negative skewness, the majority of the remaining samples are positively skewed towards an excess of fine-grained sediments. The values of

K_G >1 for these two samples result from the central 50% of the distribution appearing peaked when compared to the poorly-sorted coarse population. K_G is <1 for all other samples in facies 2. Visual examination of facies 2 curves (Fig. 4.9) indicates that with the exception of three samples plotting to the upper right, the grain size distributions are very much like those of facies 1. The three exceptions are all samples from coarse-grained horizons.

Facies 3 has a mean grain size of 8.3ϕ. Although poorly-sorted, it has the highest degree of sorting of all the facies. There is no coarse population evident, either within the samples analyzed (Fig. 4.9) or within x-radiographs of facies 3. All samples are finely skewed. With one exception, values of K_G are <1.

Facies 4 is unique in that it consists of two interlaminated sub-facies. Some samples for grain size analysis were collected from only one sub-facies, while most contain both. When viewing the grain size data, the two facies are not distinctly different. The sample which plots separately from others in facies 4 (Fig. 4.10) is from the transitional zone with facies 5. The mean grain size of facies 4 is close to that of facies 3 at 8.2ϕ. The majority of samples are very poorly-sorted and display negative (coarse) skewness. All samples have values of K_G <1. Curves from facies 4 (Fig. 4.10) display distinct

populations coarser than 4ϕ which are limited to 5% or less of the sample.

The cumulative frequency curves and statistical measures for facies 5 are distinctly different than those of facies 1-4. The mean grain size is 4.5ϕ. Sorting is very poor to extremely poor, as is visually suggested by the low slope of the curves (Fig 4.10). Only one grain size population is evident. All samples have negative skewness. Values of K_G are mostly <1.

4.7 Magnetic Susceptibility

A plot of the uncorrected magnetic susceptibility (MS) of sediments in core 87-033-020, prepared by F. Hall of the University of Rhode Island, supports the differentiation of facies 1,2 and 3 (Fig. 4.11). Variations in MS are linked to the amount of magnetic material, the mineralogy of constituent grains and grain size of the sediments (Andrews and Jennings, 1986). The present study does not attempt to identify the magnetic minerals which are present within the core, given that there is a lack of data concerning terrestrial sources. The grain size distribution does not vary greatly between the three facies present, with the exception of coarser horizons. It is conceivable that the large decrease in susceptibility in facies 1 is due to a decrease in terrestrial sedimentary input, although little else can be inferred.

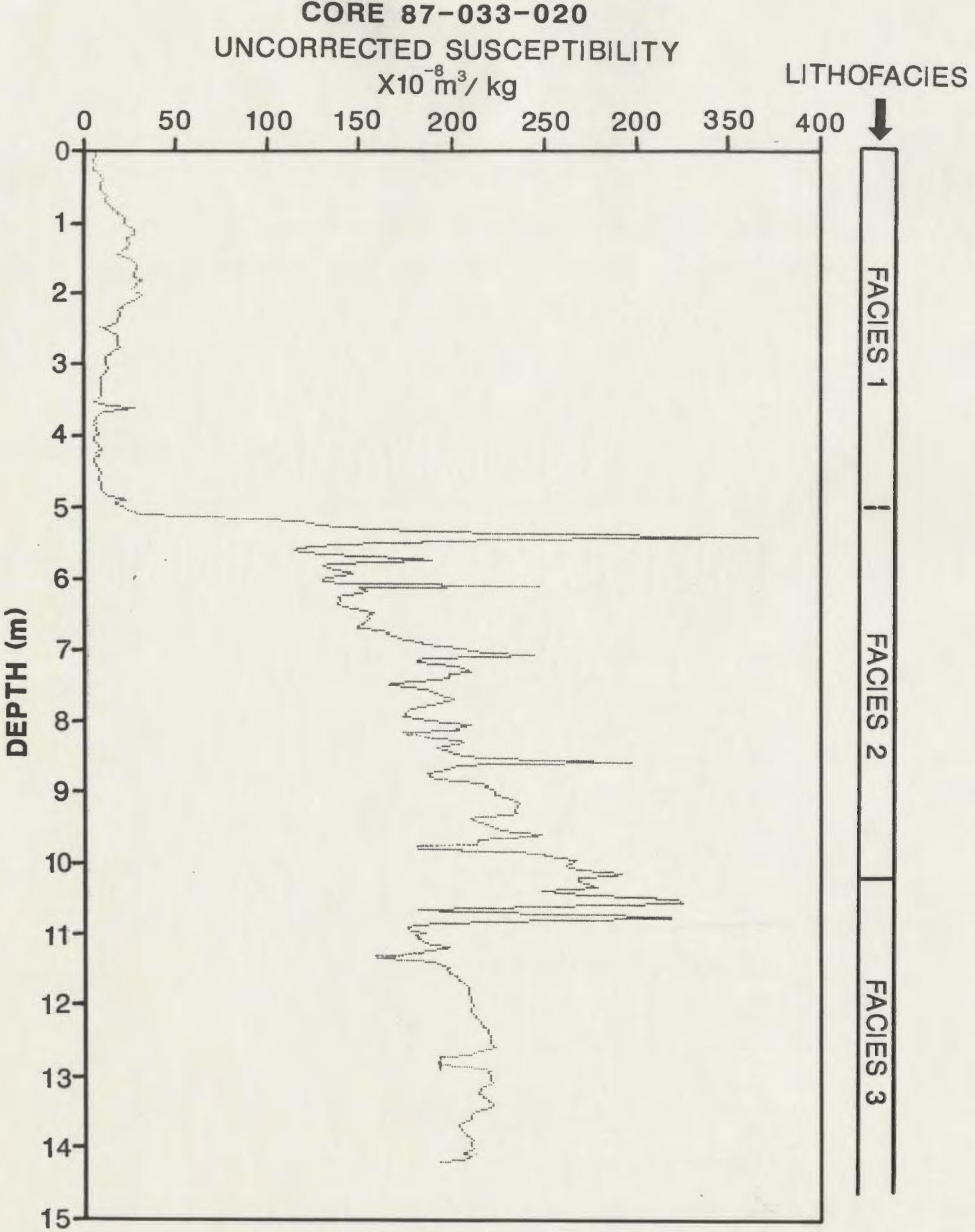

Figure 4.11. Uncorrected magnetic susceptibility of sediments within core 87-033-020 plotted against depth in core.

4.8 Biostratigraphy

The relative abundances of pollen and spores, dinoflagellates and acritarchs to the standard lycopodium grains are presented in figure 4.12. Pollen grains and spores display an overall decrease in abundance from the top to bottom of facies 1 (i.e.: near present to early Holocene/ Late Wisconsinan). A low abundance at the base of core 86-026-011 supports the assumption made in section 4.4.1 that the core penetrated to near the base of facies 1/unit 3. Apart from facies 1, the uppermost 1 m of facies 4 is the only other interval where pollen and spores are abundant. Low pollen abundances within core 87-030-001 are probably linked to the greater distance from shore of the core site; an assumption supported by the low abundances within facies 1 at the top of the core.

Dinoflagellate abundances decrease from top to bottom of facies 1; a trend that continues within facies 2. Values within facies 3 are very low. Dinoflagellates are abundant within the top 1 m of facies 4 but decrease in abundance downcore. One sample near the top of facies 5 provided a small peak in abundance.

These biostratigraphic data indicate environmental conditions during sediment deposition. Palynological input would vary with the amount of terrestrial vegetation present and the ability of palynomorphs to reach the core site. Dinoflagellates within the sediment would indicate the

Figure 4.12. Relative abundances of pollen grains and spores, dinoflagellates and acritarchs to lycopodium grains, plotted against depth in core.

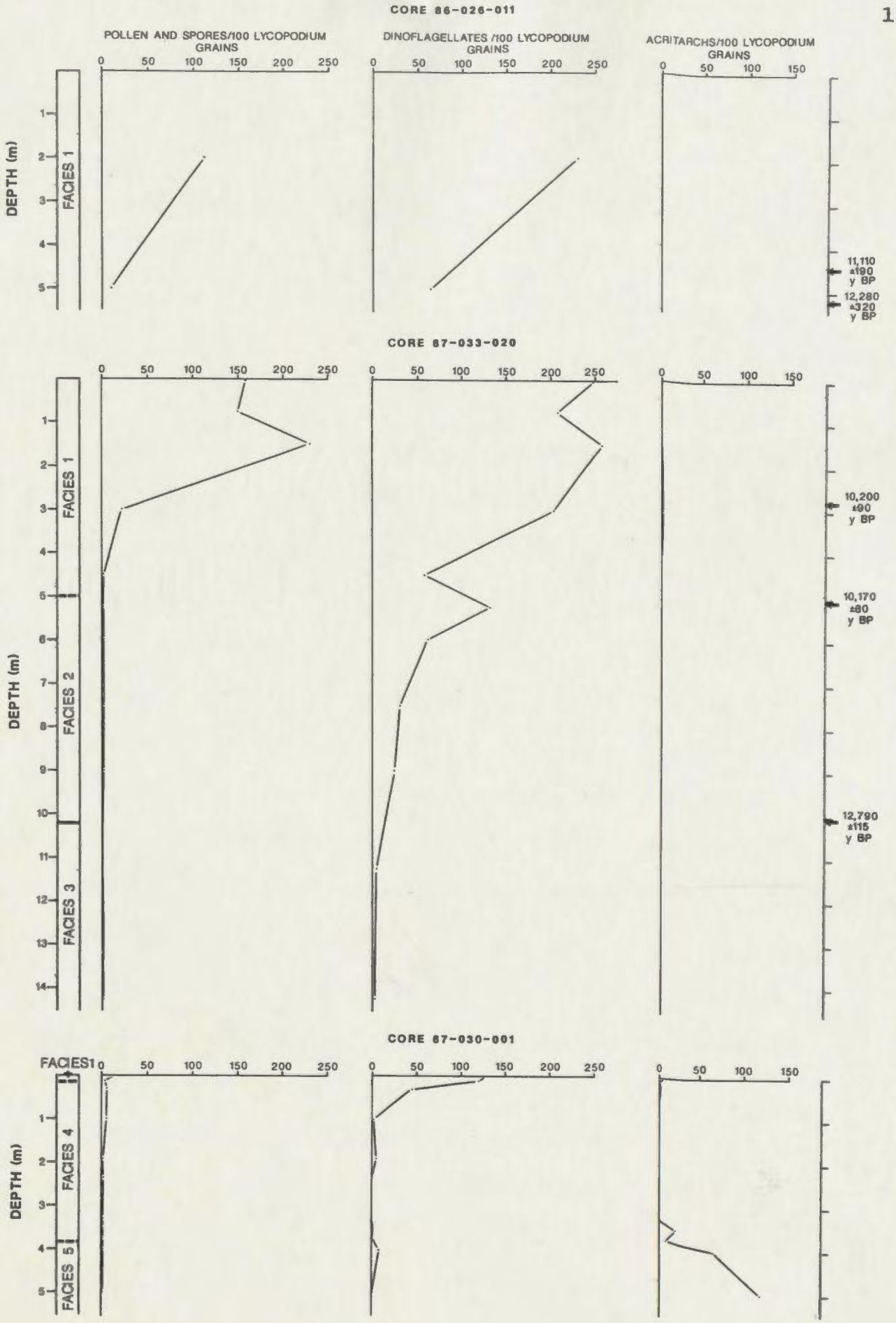
CORE 86-026-011
POLLEN AND SPORES/100 LYCOPODIUM GRAINS
DINOFLAGELLATES /100 LYCOPODIUM GRAINS
ACRITARCHS/100 LYCOPODIUM GRAINS
0 50 100 150 200 250
0 50 100 150
DEPTH (m)
FACIES 1
11,110 ±190 y BP
12,280 ±320 y BP
CORE 87-033-020
FACIES 2
FACIES 3
10,200 ±90 y BP
10,170 ±80 y BP
12,790 ±115 y BP
CORE 87-030-001
FACIES1
FACIES 4
FACIES 5

presence of a marine environment of the core site (Harland, 1983), as opposed, perhaps, to subglacial (grounded ice) conditions.

There are three distinct variations in abundances of pollen/spores and dinoflagellates: i) A peak in pollen and spores, and to a lesser extent dinoflagellates, occurs at 1.5 m depth within facies 1 in core 87-033-020. The age of this level is between 3000 and 5600 y BP, using a sedimentation rate of either 0.50 m/ka or 0.27 m/ka (Section 4.4.2). These peaks may correspond with a vegetational and temperature peak which occurred between 5300 and 3200 y BP on the Avalon Peninsula (Macpherson, 1982). ii) The rise in dinoflagellate abundance at the top of facies 2 and the subsequent decline at the base of facies 1 represents a fluctuation in the trend towards higher dinoflagellate abundances at the top of core 87-033-020. This fluctuation occurred at approximately 10,000 y BP. iii) The small peak in dinoflagellate abundance at the top of facies 5 is unique within facies 5 and the base of facies 4.

In addition to pollen, spores and dinoflagellates, acritarchs were observed within a number of slides. Acritarchs are microfossils of unknown affinity which range from PreCambrian to Cenozoic age and have similar wall compositions to spores and cysts (Parsons, 1987). Acritarchs within facies 5 and its transition interval with facies 4 were examined by Grace Parsons of the University of

Toronto, the author of a 1987 M.Sc thesis on acritarchs of middle Cambrian to lower Ordovician age from Random Island, Trinity Bay (Fig. 1.2). Three particular acritarchs observed within the facies 5 diamicton have age ranges from upper Cambrian to lower Ordovician (Tremadocian): i) Ooidium Rossicum (Timofeev, 1957), ii) Veryhachium Dumontii (Deunff, 1954; Vaguestaine, 1973) and, iii) an example of the genus Saharidia (Combaz, 1967) (species uncertain). All three are present within assemblages recognized on Random Island (Parsons, 1987). The Cambro-Ordovician rocks of Random Island (Fig. 1.2) are the only known potential terrestrial source for these microfossils. Hofmann et al. (1979) examined rocks of the Connecting Point and Musgravetown Groups for acritarchs but found very low abundances and none of the above species. In any case, these rocks are older than the indicated age range for the acritarchs within facies 5.

Potential sources, other than Random Island, for the acritarchs are: i) The oval bedrock outcrop of Cambrian sediments which Haworth et al. (1985) interpreted as extending 50 km NE of the Bonavista Peninsula (Section 1.2). Assuming their interpretation is correct, the outcrop extends within 5 km S-SE of core site 87-030-001, and would be a likely source. ii) Reworking of surficial sediments which contained Cambro-Ordovician rocks. The high abundance of acritarchs argues against this, since the source is small

and some dilution of sediments would be expected during multiple reworkings. iii) Cambro-Ordovician rocks of the Gander Zone which might contain acritarchs. This cannot be discounted since no micropalaeontological work has been done on these rocks. However, acritarch samples from facies 5 are not generally deformed and do not display the effects of metamorphism which might be expected from rocks of the Gander Zone.

4.9 Thin-Sections

The laminated sequence of facies 4 was examined in six thin-sections (Fig. 4.13) using a transmitted light microscope. Sample locations ranged from the top to near the bottom of the interval. Laminations of light olive-grey sub-facies 4B and pale greyish-brown sub-facies 4A, 2-7 mm thick, are present within the thin-sections.

Light olive-grey laminations of sub-facies 4B fine upwards from sharp basal contacts (Fig. 4.13; slide 2, 137.5 cm). There is no evidence of erosion of underlying brown (sub-facies 4A) laminations. The graded interval is generally thin (<1 mm). Although coarse silt to fine sand is present within a finer matrix (silty clay, from grain size data), outsized clasts (greater than 0.5 mm) are rare. Minor amounts of organic mottling are present. At the top of the olive-grey laminations of sub-facies 4B, a gradual transition occurs to pale greyish-brown laminations of sub-

Figure 4.13. Photographs of thin-sections prepared from facies 4. Note the poorly sorted coarse fraction within sub-facies 4A (darker laminations). Graded base of sub-facies 4B most evident within the middle of slide 2. Elongated burrow present in the middle of slide 3. Scale bar is 1 cm long.

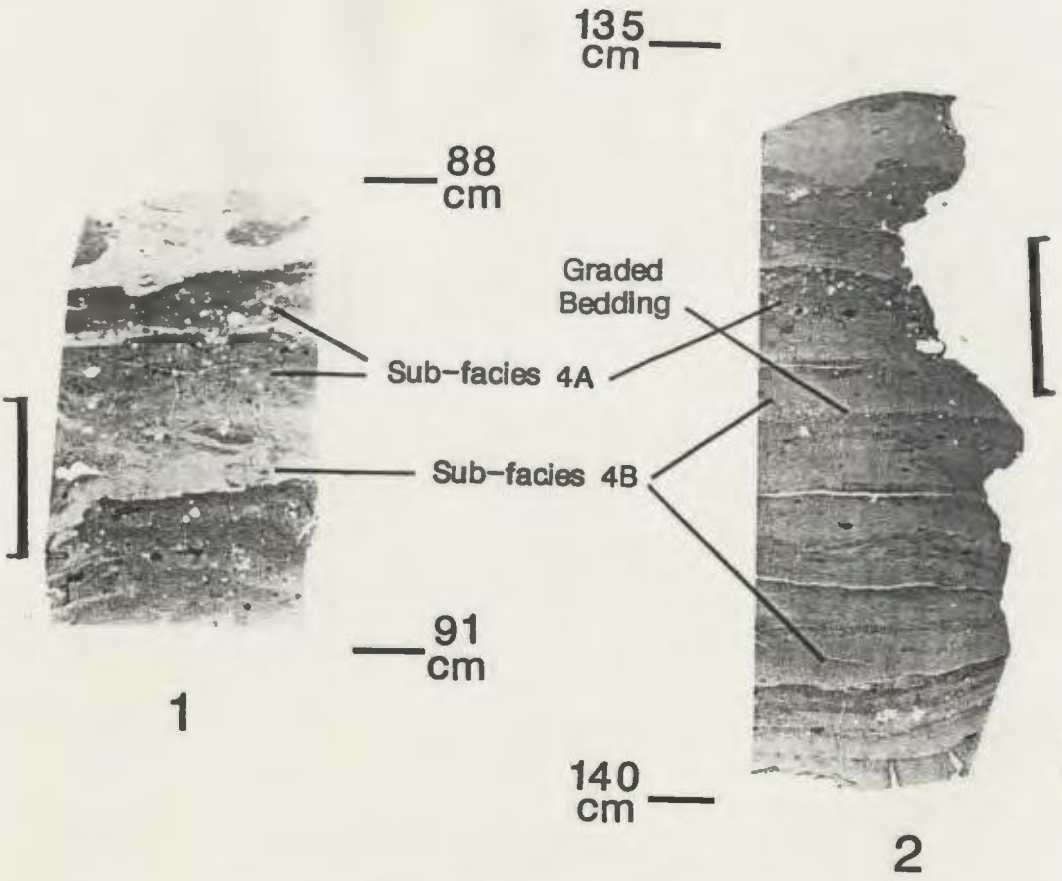

CORE 87-030-001
LITHOFACIES 4

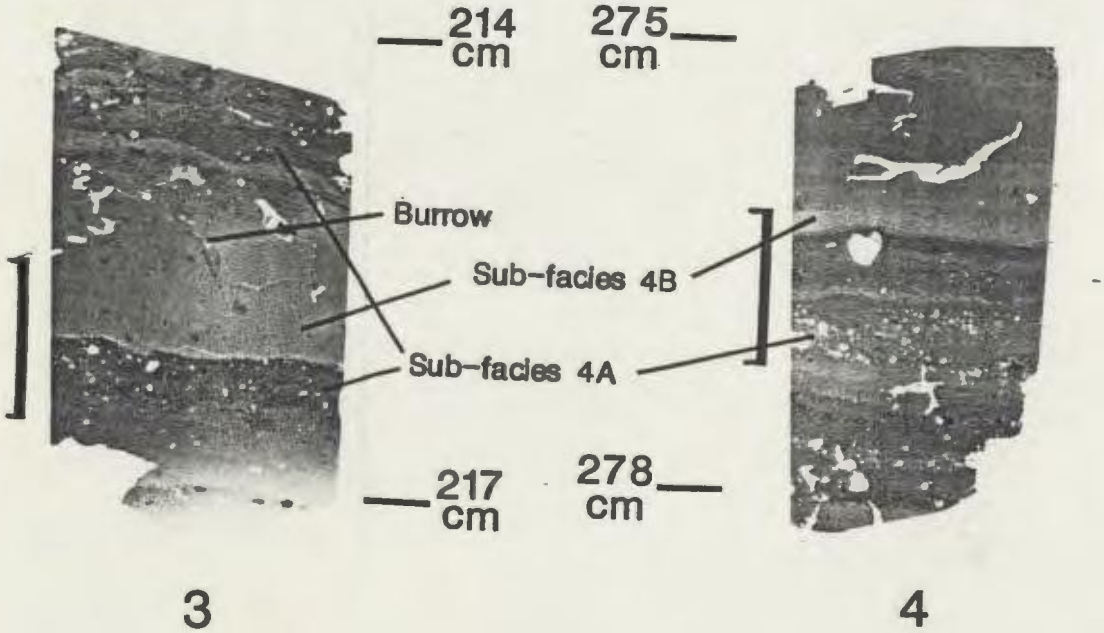

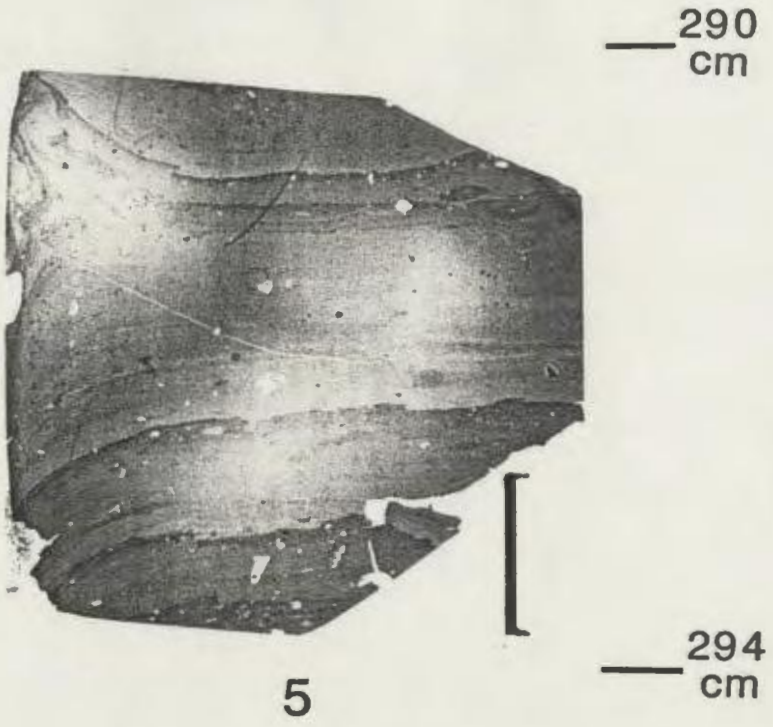

5

CORE 87-030-001
LITHOFACIES 4

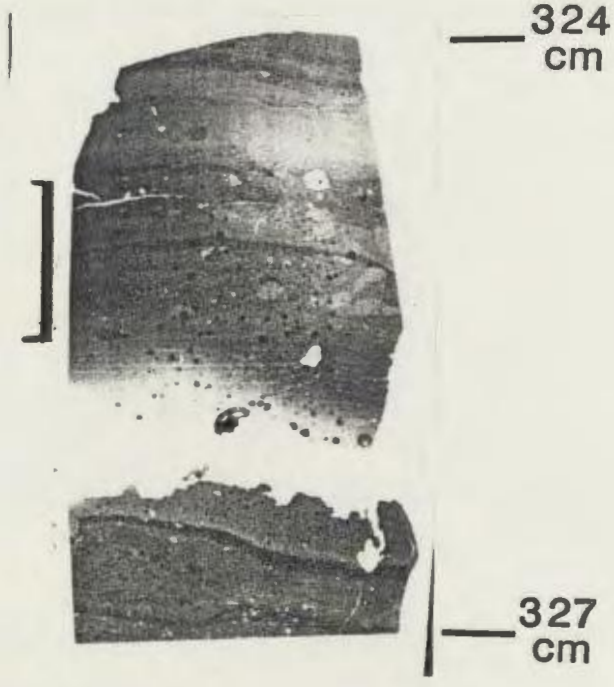

6

facies 4A (Fig. 4.13). Corresponding with the colour changeis an increase in the abundance of outsized clasts. Sub-facies 4A contains a distinct, very poorly-sorted coarse population within a fine matrix. Organic mottling is common. Bioturbation, in the form of occasional burrow-like features (Fig. 4.13; slide 3, 215.5 cm) and disruptions in stratification, is present within the transition between the sub-facies and within sub-facies 4A. However, none is displayed on x-radiographs of facies 4.

The olive-grey laminations of sub-facies 4B have the appearance of small scale, fine-grained turbidites, perhaps corresponding with the E2 and E3 divisions of Piper (1978). The increase in organic mottling and bioturbation within sub-facies 4A suggests a reduced rate of sedimentation in comparison to sub-facies 4B. The reversion to greyish-brown sediments (4A) after each lamination of 4B suggests differing sources for the sub-facies.

4.10 Summary and Interpretations

Facies 1 is an olive-grey to greyish-olive sandy, pebbly and shelly mud which occurs at the top of all three cores and is correlated with seismic units 3 and D in the outer and inner bay respectively. Radiocarbon dates indicate that facies 1 is primarily of Holocene age, but was initially deposited within the outer bay as early as 13,500 y BP. Sedimentation rates may have been greatest in mid-

basin in the outer bay. The bioturbated, poorly-sorted, fine-grained population which comprises most of facies 1 is interpreted to represent hemipelagic sedimentation. The coarse-grained population may represent ice-rafted dropstones, given the very large size of a number of clasts within the facies and the abundance of pebbly horizons seen in x-radiographs (Leeder, 1982). The clay mineralogy suggests conditions similar to the present day, particularly at the top of the cores. The higher levels of smectite, calcite and dolomite in comparison with underlying facies may result from ocean current transport of clay-sized minerals from sources outside the study area, perhaps related to the Labrador Current (i.e.: Piper and Slatt, 1977) . The decrease in dinoflagellate abundance at the base of facies 1 (at ~10,000 y BP) within core 87-033-020 may represent an environmental fluctuation in the overall trend towards increased biological abundances at the top of facies 1.

Facies 2 is a greyish-olive to olive-grey, sandy, pebbly and shelly silty mud which is correlated with seismic unit C within Chandler Reach in the inner bay. The top of the unit is dated at 10,170 $\pm$ 80 y BP and the base is dated at 12,790 $\pm$ 115 y BP, indicating that deposition occurred synchronously with the base of unit 3 (facies 1) in the outer bay. A sedimentation rate of 1.9 m/ka for unit C is approximately three times greater than the rate of 0.68 m/ka

at the base of unit 3 in core 86-026-011. The degree of bioturbation and grain size distributions within facies 2 are similar to those observed within facies 1, with the exception of several coarse horizons. The fine grain size population of facies 2 is interpreted as hemipelagic, although with a distinct terrigenous component. The coarse fraction includes large dropstones, indicative of an ice-rafted origin (Leeder, 1982). The absence of pollen grains within facies 2 suggests that little vegetation existed at the sediment source(s). The gradual rise in dinoflagellate abundances indicates development of increasingly open marine conditions over the period of deposition of facies 2. Chlorite abundance in the clay mineralogy suggests greater input from the regional geology than within facies 1. The decrease in abundances of plagioclase and K-feldspar suggest a lesser influence from granitic sources than within facies 1 or 3. Thin laminae of facies 2, which occur at the base of facies 1, may have originated from periodic pulses of terrigenous sediment during the transition between facies.

Facies 3 is a structureless and homogeneous pink/pale red silty mud which is correlated with seismic unit B in the inner bay. The top of unit B is dated at 12,790 $\pm$ 115 y BP. The facies consists of a poorly-sorted fine-grained population and displays no evidence of bioturbation. Abundances of pollen, spores and dinoflagellates are very low. Facies 3 is interpreted as a rapidly deposited

glaciomarine sequence, with sedimentation rates too high for bioturbation and with minimal input of a coarse grain size population. The high relative abundances of chlorite, quartz, plagioclase and K-feldspar within the <2μm fraction suggest that source rocks were the meta-sediments and granitic intrusions of the region. The lack of rain-out debris suggests that there was no floating ice cover during deposition of facies 3, although a lack of dinoflagellates suggests that open marine conditions did not prevail. The pinkish mottling within the lower 1.5 m of facies 2 likely represents a transition from deposition of facies 3 sediments.

Facies 4 consists predominantly of interlaminated sub-facies 4A and 4B and is correlated with seismic unit 2 in the outer bay. Both sub-facies have very poorly-sorted fine grain size populations and minor coarse populations. The sharp basal contacts and fining upwards sequences and overlying ungraded mud of sub-facies 4B likely correspond with the E2 and E3 turbidite divisions of Piper (1978). Organic mottling and bioturbation are most common within sub-facies 4A, supporting a hemipelagic environment. Based largely on the thin-section observations of individual laminae and boundary relationships between the sub-facies, facies 4 is interpreted to consist of a hemipelagic sequence, sub-facies 4A, which was repetitively interrupted by fine-grained, distal turbidites of sub-facies 4B. The

population of outsized clasts within sub-facies 4A was likely ice-rafted (i.e; Von Huene et al., 1973). The high chlorite abundances in the <2μm fraction suggest regional terrestrial input. The different colours of the sub-facies likely reflect differing sources. The sole presence of sub-facies 4A within the uppermost 0.6 m of facies 4 suggests that turbiditic flows had ceased, leaving only hemipelagic sedimentation. Abundant pebbles and dropstones indicate that ice-rafting was an ongoing process. Increased abundances of pollen, spores and dinoflagellates within the upper metre may correspond with increases in terrestrial vegetation and development of marine conditions not unlike those of facies 1.

Facies 5 is a stiff, dark grey, sandy gravelly mud which is correlated with unit 1 in the outer bay. It is extremely poorly-sorted, displays no structures or bioturbation and is essentially barren of pollen and spores. Facies 5 is a diamicton, which was probably deposited beneath floating ice cover, since the presence of circulating waters is indicated by the dinoflagellates at the top of facies 5 (Harland, 1983). Three thin intervals of facies 5 occur within the transition to facies 4, separated by fine-grained sediments. Presumably these were deposited by floating ice, since ice grounding would have eroded the fine material. Sediment transport from the south or SW to core site 87-030-001 is indicated by the

correlation of acritarchs within facies 5 with those observed on Random Island (Parsons, 1987). The acritarchs may also have originated from Cambrian sediments forming part of the pre-Quaternary geology to the south of the core site (Haworth et al., 1985).

CHAPTER 5

SEDIMENTOLOGICAL INTERPRETATION OF SEISMIC UNITS

5.1 Isopach Maps

Figures 5.1-5.6 are isopach maps for the study area and include: i) total thickness of sediment overlying acoustic basement, ii) glacial and proglacial sediment, comprised of seismic units 1 and 2 in the outer bay and units A-C in the inner bay, and iii) post-glacial sediments, mapped from units 3 and D in the outer and inner bay respectively. Within the outer bay, poor resolution of unit 1 on the basin margins does not allow separate mapping of units 1 and 2.

Comparison of figures 5.1-5.6 with the bathymetric map of Bonavista Bay (Fig. 1.4) illustrates that the majority of sediments have infilled pre-existing basins defined by the topography of acoustic basement (i.e.: Figs. 3.5, 3.12). The increased thickness of units within the middle of the basins is the result of either basin infilling, as indicated by onlapping reflections in units 1 and 2, or post-depositional erosion, such as is evident for units 3/D and occasionally unit 2.

Much of the linearity of contours mapped in figures 5.1-5.6 originates from the draping of seismic units over interpreted acoustic basement ridges (Section 3.2). Figure 3.5 illustrates that variations in unit thickness over such features occur in both lower and upper units.

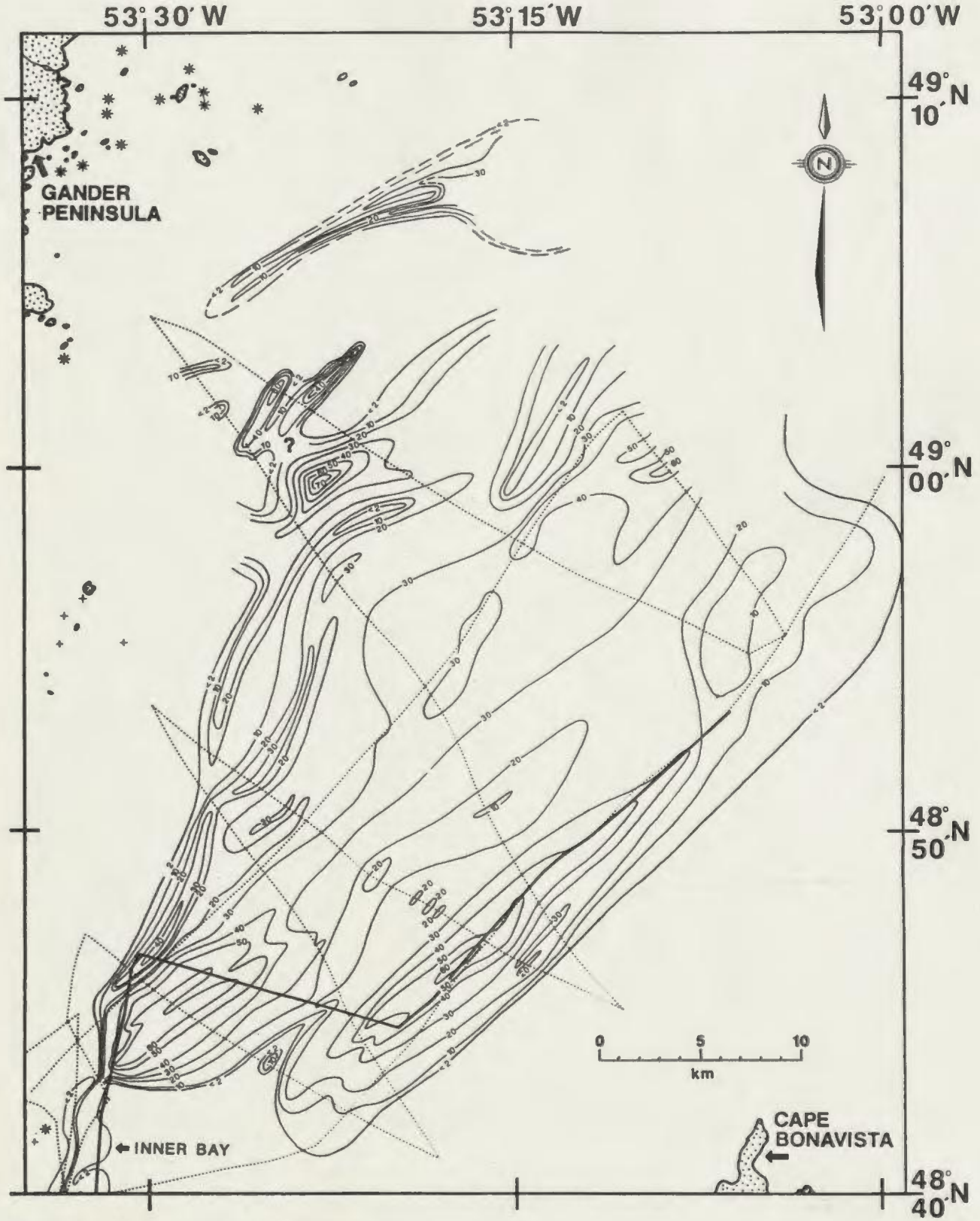

Figure 5.1. Total sediment thickness above acoustic basement within the outer bay. Contours in milliseconds two-way-travel-time. Dashed contour to the north denotes area of uncertain correlation.

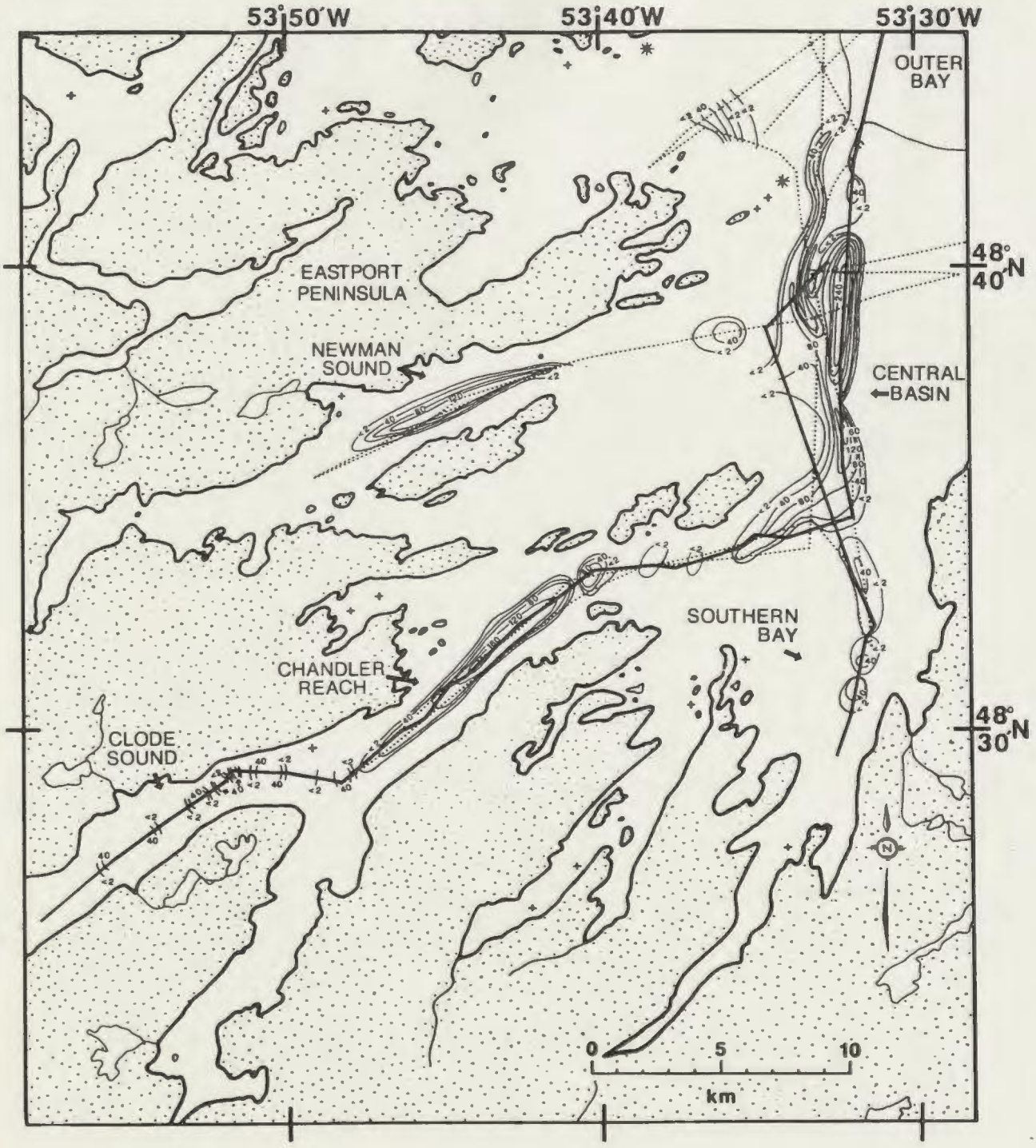

Figure 5.2. Total sediment thickness above acoustic basement within the inner bay. Contours in milliseconds two-way-travel-time. The nature of contours within Clode Sound are uncertain.

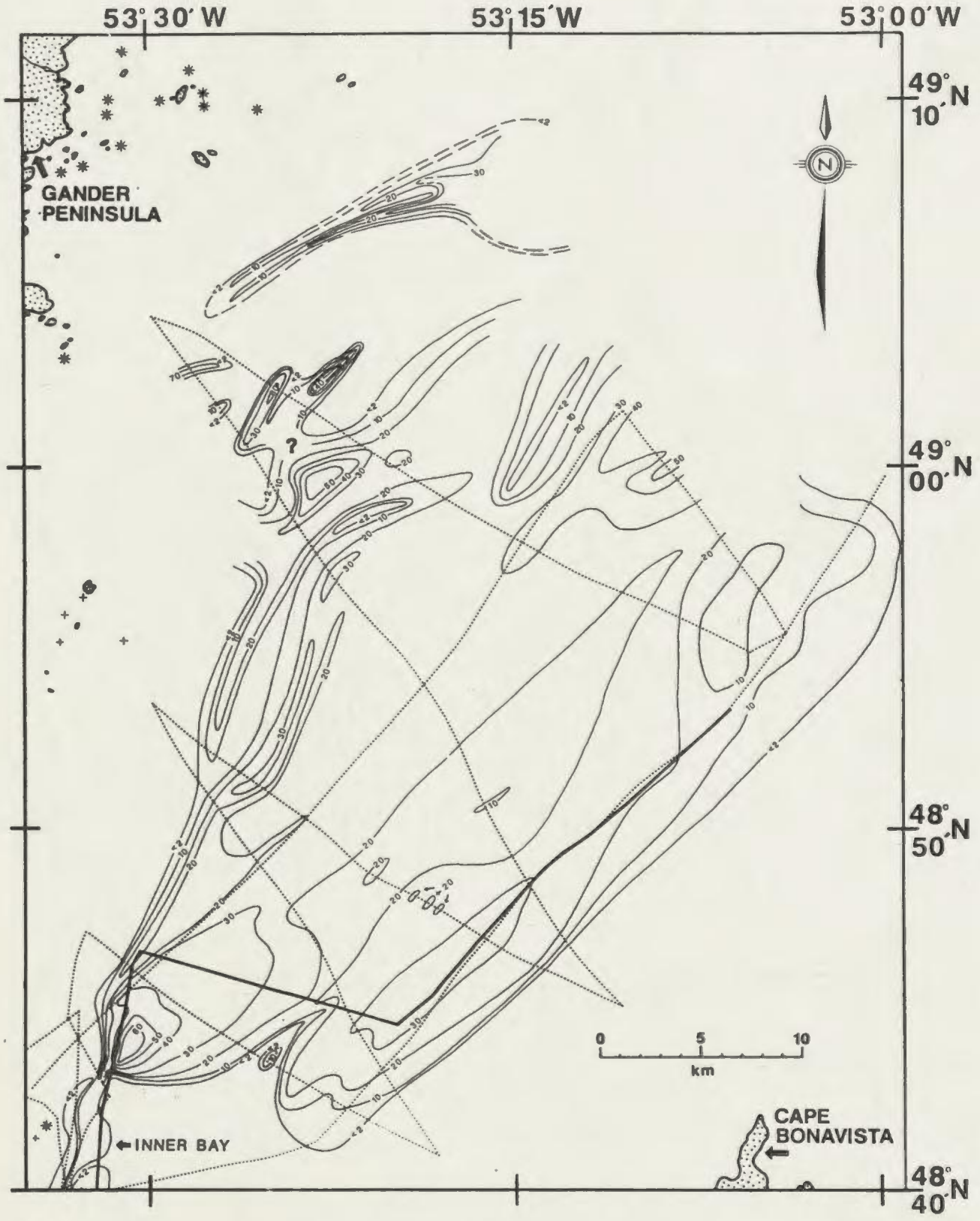

Figure 5.3. Glacial and proglacial sediment thickness within the outer bay (seismic units 1 and 2). Contours in milliseconds two-way-travel-time. Dashed contour to the north denotes area of uncertain correlation.

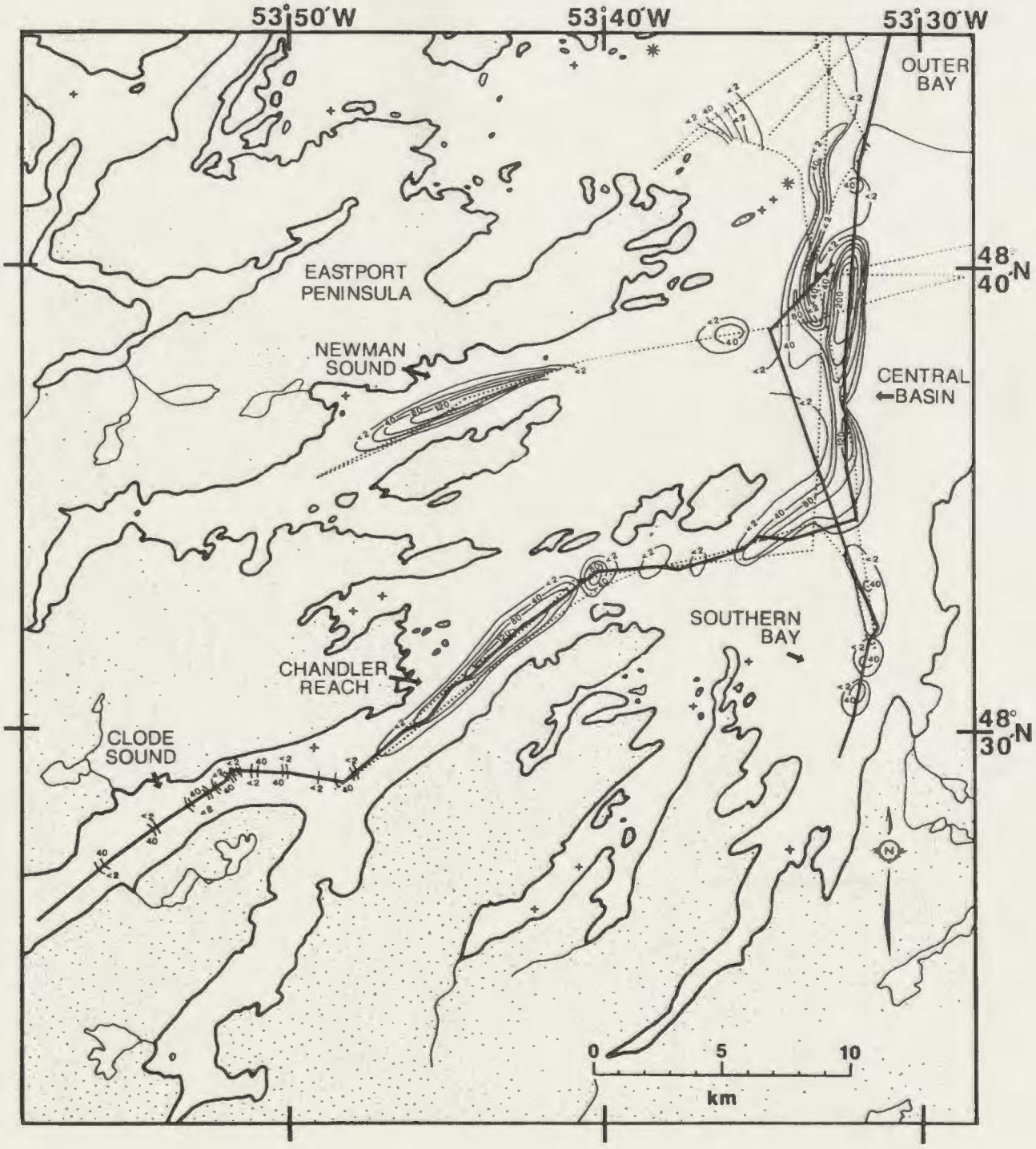

Figure 5.4. Glacial and proglacial sediment thickness within the inner bay (seismic units A to C). Contours in milliseconds two-way-travel-time. The nature of contours within Clode Sound are uncertain.

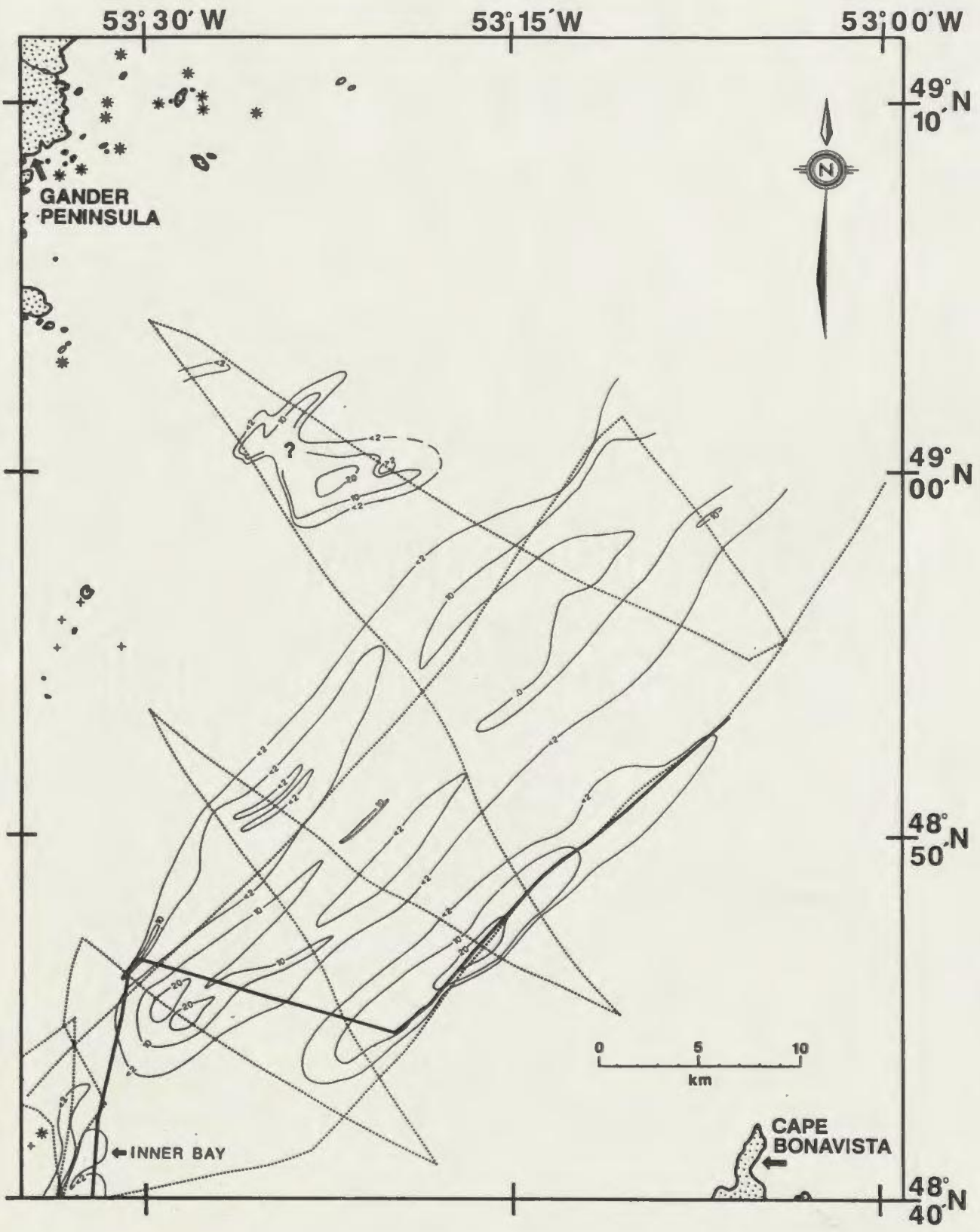

Figure 5.5. Post-glacial sediment thickness within the outer bay (seismic unit 3). Contours in milliseconds two-way-travel-time.

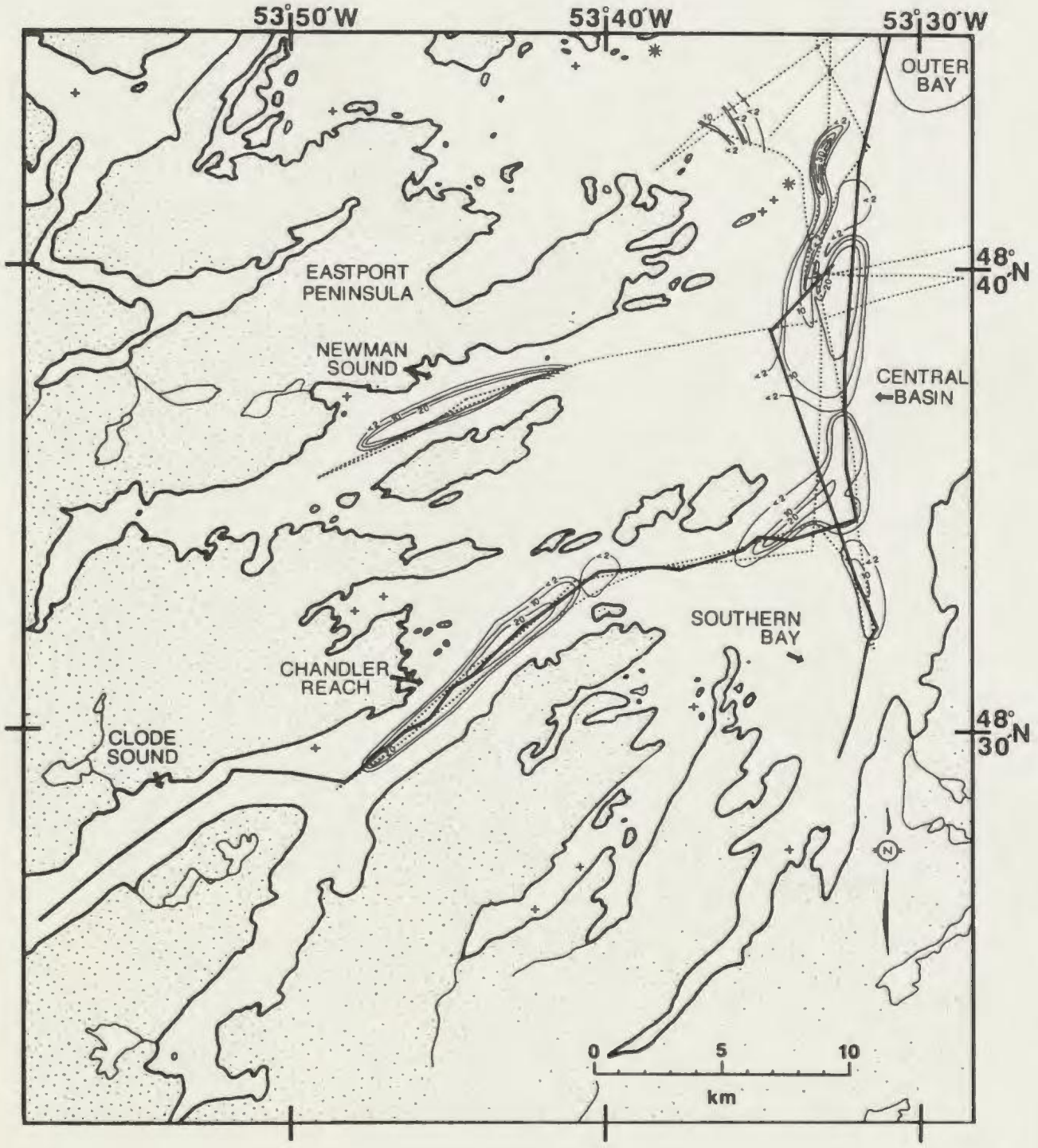

Figure 5.6. Post-glacial sediment thickness within the inner bay (seismic unit D). Contours in milliseconds two-way-travel-time.

5.2 Interpretation of Seismic Units

The sedimentological interpretations of the lithofacies within the cores are extrapolated to the correlated seismic units throughout the bay (i.e.: Barrie and Piper, 1982; King and Fader, 1986; McLaren, 1988; Gipp, 1989) and three generalized depositional environments are recognized; i) glacial sediments, deposited either from ice contact or from direct rain-out beneath floating ice, ii) proglacial sediments, deposited with substantial outwash and perhaps ice-rafted sediment input and iii) post-glacial sediments.

5.2.1 Glacial Sediments

Units 1 and A are interpreted to represent glacial sediments. While unit 1 has been correlated with the diamicton at the base of core 87-030-001, unit A has not been sampled by coring, and is interpreted only on the basis of its acoustic character, morphology and stratigraphic position. Seismic unit 1 forms a thin basal sequence throughout the Eastern and Western Basins. It includes a number of distinct acoustic facies which are interpreted separately:

i) The sequence observed on 3.5 kHz data is interpreted as a diamicton deposited by sediment rain-out beneath floating ice cover. The presence of internal, continuous reflections suggests that deposition was occurring relatively uniformly throughout most of the basins of the

outer bay, while the occasionally ponded morphology implies that the ice cover may only have been buoyant over the basins and was pinned around the basin flanks. The lens-shaped zones within unit 1 which contain continuous reflections are interpreted as channels incised in the diamicton which were infilled with glaciomarine sediments (Figs. 3.7, 3.9). The acoustically incoherent zones which interfinger with weakly stratified sediments of unit 1 (Fig. 3.7) may represent small scale debris flow tills, where deposition probably occurred near the grounding line of an ice sheet (i.e.: Powell, 1984).

ii) The lens-shaped mounds which occur at the base of the upper sequence (as discussed above) on the basin margins are interpreted as ice recessional moraines, based on their morphology and acoustic character (Fig. 3.7) (i.e.: King and Fader, 1986). Their limited distribution and apparent lack of continuity suggest that they are not representative of large-scale continuous moraine development. Their position suggests that they are discontinuous lateral moraines formed during a grounding line pause on the margins of the basins.

iii) The base of unit 1, which is only observed in airgun profiles, has greater lateral extent than the upper, ponded interval (Fig. 3.5). This lowermost sequence is interpreted as a basal till because of its presence beneath the moraines, its continuity on basin margins and, to a lesser extent, the inability of the Huntec and 3.5 kHz

systems to penetrate it (i.e.: Bell et al., 1987).

Unit 1 in the SW region of the Western Basin is acoustically distinct from elsewhere in the outer bay. The interlayered series of acoustically incoherent and stratified zones (Fig. 3.10) is interpreted to have arisen from sediments deposited proximal to the grounding line of an ice sheet. The acoustically incoherent zones are interpreted as diamicton of unit 1. Their apparent lenticular shape indicates deposition from either sediment gravity flows or direct ice contact (King et al., 1991; King and Fader, 1986). Stratified zones with high intensity internal reflections are interpreted to be the product of subaqueous glaciomarine deposition (King and Fader, 1986; King et al., 1987). A number of acoustically incoherent lens-shaped bodies and surrounding stratified sediment appear similar to till tongues described by King and Fader (1986) on the Scotian Shelf and by King et al. (1987) on the Norwegian Shelf, which were interpreted to represent deposition during small scale oscillations of an ice grounding line.

Seismic unit A is interpreted, on the basis of acoustic character and its gradational transition to an overlying glaciomarine sequence (unit B), to have been directly deposited beneath ice cover. The ponded morphology and the presence of continuous airgun and occasional 3.5 kHz reflections suggests subaqueous deposition from sediment

rain-out as opposed to deposition from grounded ice (King et al., 1991) (ie: diamicton versus till). This unit is probably diachronous between the basins of the inner bay, reflecting time transgressive ice retreat.

The appearance of infilled channels within unit A in Newman Sound indicates that some sediment reworking occurred during deposition, perhaps related to outwash from a proximal ice grounding line (i.e.: Hoskin and Burrell, 1972; Carlson et al., 1989). Convergent reflections within unit A may have resulted from sediment gravity flows associated with the steep margins of the basins (Fig. 3.15). The contact between units A and B is gradational and may reflect gradual retreat of a floating ice cover. Within the smaller, secondary basins of the inner bay (i.e.: NW margin of Central Basin; in Southern Bay; mouth of Chandler Reach), unit A contains less coherent reflections on the airgun data and does not display well developed internal structure. Deposition of unit A within these basins may have occurred primarily beneath grounded ice (King and Fader, 1986).

5.2.2 Proglacial Sediments

Core data indicate that units 2, B and C are all comprised of proglacial sediments. Although depositional environments differed, each unit received substantial sediment input from glacial outwash and, except for unit B, ice-rafting.

Seismic unit 2 has been correlated in core 87-030-001 with a predominantly interlaminated sequence of turbidites and hemipelagic/ice-rafted sediment. On the seismic data, convergent and onlapping reflections on the basin margins suggest that the draping basin-fill morphology of unit 2 largely developed from preferential deposition within the basins (Barrie and Piper, 1982). A lack of sediment outside the basins and their immediate margins (Fig. 5.3) implies that a source for the turbidites, probably an ice margin, was situated close to the basins. Syn-depositional ocean currents may have also restricted the distribution of hemipelagic sedimentation to within the basins (i.e.: Orheim and Elverhoi, 1981).

Turbidites flowing in mid-basin likely originated from the SW, given previous interpretations of southwesterly ice retreat (i.e.: Jenness, 1963) and evidence of a southwestern ice margin discussed in the previous section (5.2.1). The presence of continuous coherent and parallel reflections extending on the western margin of the Western Basin suggests a second source may also have existed on the west side of Bonavista Bay. The decrease in intensity and continuity of reflections within unit 2 from the center of the basin to the margin probably reflects a concentration of sediment flow within the basin centers during individual events. Converging reflections and occasional offlap imply that flows extending onto the margins were of reduced

thickness. Onlapping reflections indicate that some flows occurred only within mid-basin. The small scale of turbiditic sequences seen in core 87-030-001 may therefore be linked to the basin marginal location of the core site. The transition to a more acoustically incoherent unit on the margins probably reflects the inability of seismic systems to resolve individual events thinner than 10-20 ms.

Seismic unit B in Chandler Reach (core 87-033-020) is a homogeneous, fine-grained glaciomarine sequence which was rapidly deposited from terrestrial outwash. The lack of ice-rafted sediment suggests that deposition occurred during ice free conditions. From the consistency of acoustic character and the ponded morphology of unit B, it is interpreted that a similar depositional environment existed for this unit within all the basins of the inner bay. Continuous reflections within unit B which converge and downlap at the inner ends of Chandler Reach and Newman Sound (Fig. 3.13) may reflect outwash sedimentation from an ice margin receding landward during the transition from an ice shelf environment of unit A to open water conditions (i.e.: Seramur and Powell, 1987). Deposition of unit B was probably diachronous between the basins, arising from differences in the timing of ice retreat within the study area.

Seismic unit C is a proglacial sequence containing substantial amounts of terrestrial and ice-rafted sediment.

The increase in biogenic activity and ice-rafted sediment, subsequent to deposition of unit B in Chandler Reach (core 87-033-020), marks a transition to hemipelagic sedimentation. Sediment input from glacial outwash was high, as indicated by a sedimentation rate of 1.9 m/ka. This is three to four times higher than sedimentation rates calculated for post-glacial units 3 and D (Section 4.4.2). While the transition from units B to C may have been diachronous between basins, the influx of ice-rafted sediment likely began at a similar time, through the presence of floating ice throughout the bay. A change in sediment source from units B to C, such as evidenced in Chandler Reach, may not have occurred everywhere.

Seismic unit C has a variable morphology within the basins of the inner bay; being occasionally ponded in Chandler Reach and Newman Sound, but displaying a draping basin-fill morphology in the Central Basin. The change to a draping basin-fill morphology for unit C above unit B probably reflects the transition to hemipelagic sedimentation and a greater degree of suspension fallout (Barrie and Piper, 1982). The erosion of the uppermost reflections of unit C within Newman Sound, beneath unit D (Fig. 3.16), may have originated from ocean current activity at the transition between glacial and post-glacial sedimentation. Erosion of upper reflections in unit C has also occurred over the acoustic basement rise within the

Central Basin, although apparently subsequent to the deposition and erosion of unit D (Figure 3.18).

The seismic sequences within the innermost basins of Southern Bay and in Clode Sound which do not correlate with units A-D are interpreted to be glacial and proglacial sediments. This interpretation is made only on the basis of their acoustic character and morphology (i.e.: King et al., 1991).

The two innermost basins in Southern Bay contain interfingering acoustically incoherent and stratified zones which are interpreted to represent glaciomarine and diamict sedimentation proximal to a retreating ice margin. These sediments overlie an acoustically incoherent unit which is interpreted as a diamicton deposited from either floating or grounded ice.

The origin of a series of terraces which occur at gradually diminishing depths in Clode Sound is difficult to interpret. The ability of the Huntec DTS data to display the internal acoustic stratification of the sequence supports an interpretation as proglacial sediments, as opposed to a diamicton or basal till (King and Fader, 1986). Only a thin (5 ms) veneer at the seaward edge of the terraces is similar to the acoustic character of Holocene unit D in neighbouring Chandler Reach. If the terraced sediments were deposited during the retreat of glacial ice, it might be expected that sedimentation would occur within

all acoustic basement depressions, instead of overfilling some and leaving others empty. It is possible, however, that localized syn-depositional currents were responsible for the irregular sediment distribution. The erosional downcutting of up to 30 ms depth, which is evident at the edges of some terraces, is also of uncertain origin. It may have been caused by post-depositional current activity, although it is debatable whether proglacial sediments could be so strongly eroded by currents, especially if the sediments contain a gravel component (G. Fader, pers. communication, 1990). Alternatively, the erosion may have been ice related. While erosion to depths of over 20 m argues against isolated iceberg scouring (Lewis and Parrott, 1987), a late stage readvance of ice into Clode Sound may have been responsible. Complicating this interpretation is the localized nature of the erosion, the lack of disruption of reflections internally evident within the terraces, and lack of overlying or infilling sediments in unconformable contact with the terraced sediments.

Seismic sequences similar to those within Clode Sound have been described from Glacier Bay, Alaska (i.e.: entrance to Muir Inlet) (Powell, 1983). Wedges of sediment which are not contained within bedrock basins were interpreted by Powell (1983) as ice contact outwash deposits overlying morainal banks.

5.2.3 Post-glacial Sediments

Seismic units 3 and D are comprised of post-glacial hemipelagic sediments which have received variable amounts of coarse, ice-rafted sediment. In the outer bay, unit 3 has experienced gradual erosion outside the basin centers. Sediment of up to 20 ms thickness may have been eroded if deposition was uniform across the basins. Some erosion has also occurred in deeper areas of the basins, as opposed to on the margins (i.e.: Figs. 3.10; 3.6, 4.2 km along track; 3.8, 6 km along track). Within the inner bay, erosion of unit D is most evident over the bedrock high within the Central Basin (Fig. 3.18; 1.75 km along track), but also occasionally occurs on the margins of the various basins (i.e.: Figs. 3.14, 3.21) downslope of the point where the unit pinches out. In general, the distribution of (resolvable) post-glacial sediments has been limited to within the basins of Bonavista Bay by post-depositional (and perhaps syn-depositional) erosional currents. The base of units 3 and D is diachronous between the outer and inner bay, reflecting the gradual retreat of the last glacial environment from Bonavista Bay.

CHAPTER 6

GLACIAL HISTORY

6.1 Existing Models

Previous studies of the Wisconsinan glacial and sedimentary history of the eastern Canadian continental margin (Sections 1.4.1, 1.4.2) have provided a number of possible models for the study area. The Quaternary sedimentary history of the region is expressed through two opposing theories of minimalist/ maximalist Late Wisconsinan glacial exten (i.e.: Ives, 1978: Denton and Hughes, 1981a). If the minimalist models are correct, then the last grounded ice in outer Bonavista Bay was an Early to Middle Wisconsinan ice sheet which extended onto the continental shelf of Eastern Canada (Grant and King, 1984; King and Fader, 1986; Vincent and Prest, 1987; Dredge and Thorleifson, 1987). If grounded and eroding Late Wisconsinan ice extended onto the shelf beyond the mouth of Bonavista Bay, then the majority of the Quaternary sediments within the study area would likely have been derived during the last (Late Wisconsinan) deglaciation.

Previous studies can be categorized into the following four models:

Model 1:

Late Wisconsinan ice from a central Newfoundland ice cap extended only into the southern region of Bonavista Bay.

The ice front at glacial maximum trended NW-SE and either terminated at the dividing sill between inner and outer bay (Fig. 3.1) (Grant, 1977; Rogerson, 1982) or perhaps 10-20 km inland (to the SW) (Ives, 1978; Quinlan and Beaumont, 1982). A separate Late Wisconsinan ice cap may have existed upon the Bonavista Peninsula (Brookes, 1989).

Model 2:

A grounded ice sheet developed during the Early Wisconsinan which extended to the edge of the continental shelf (King and Fader, 1986). By 46,000 y BP the ice sheet had deposited a basal till and become buoyant in deep basins. From 46,000-32,000 y BP the position of the grounding line of the ice sheet oscillated, and till tongues were deposited on the outer shelf. From 32,000-16,000 y BP the ice retreated to the present coastline. The Late Wisconsinan may have seen a minor ice re-advance. This scenario is not unlike model 1, since the majority of sediments in the outer bay would have been deposited by ice retreating during the Middle Wisconsinan to early Late Wisconsinan. The chronology of King and Fader (1986) has been called into question by a number of subsequent workers (i.e.: King and Fader, 1988; Gipp and Piper, 1989)

Model 3:

During the Late Wisconsinan a grounded ice sheet extended beyond the study area to the outer continental shelf (Flint, 1971; Mayewski et al., 1981; Denton and

Hughes, 1981a). Pre-existing Quaternary sediments would have been eroded by a grounded ice advance, so that the entire seismic sequence within the study area would represent the Late Wisconsinan ice retreat. This model is supported by recent studies on the Northeast Newfoundland Shelf (east-northeast of the study area) which indicate the presence of retreating glacial ice during the Late Wisconsinan (G. Fader, pers. communication, 1990).

Model 4:

Ice from the Newfoundland Ice Cap flowed preferentially into Bonavista Bay from the SW and was more active and extensive within the bay than on the neighbouring peninsulas. Grounded ice, channelized in the bay, may have originated during the Late Wisconsinan glaciation or existed throughout the Wisconsinan. On the Bonavista Peninsula, a separate Late Wisconsinan ice cap extended at least to the present coast, although a small nunatak was present at the NE tip of the peninsula. The Gander Peninsula was host to a subsidiary ice cap of the main Newfoundland Ice Cap (Brookes, 1989).

6.2 Interpreted Glacial History

In airgun data from the outer bay, the diamicton of unit 1 directly overlies the acoustic basement, which is interpreted to be of Palaeozoic age throughout the study area. It is inferred from this that the base of unit 1 was

initially deposited during the last occupation of the region by grounded and eroding ice. The continuity of unit 1 and a lack of underlying glacial or interglacial sediments within the study area suggests that grounded ice extended throughout and beyond Bonavista Bay. While no chronological control on this glaciation is available from either the diamicton or the overlying unit 2, some evidence is provided by the sedimentary record from diamicton to Holocene sediments displayed in core 87-030-001. Core data from the interlaminated sequence of unit 2, including grain size data, clay mineralogy, lamination thickness and biological content, display very little change from the base of the unit to the top. This suggests that very little variation in depositional environment occurred over the period of deposition of unit 2, apart from the repetitive alternation between turbiditic and hemipelagic/ice-rafted sedimentation. The low biological content of unit 2 presumably resulted from either high rates of deposition, low salinities and/or temperatures, since there is no evidence of high energy conditions (i.e.: wave reworking) within core 87-030-001. The uppermost, unlaminated interval within unit 2 was deposited after the flow of turbidity currents ceased, and displays a gradual increase in biological activity prior to the establishment of a post-glacial sedimentary environment (unit 3).

If either of Models 1 or 2 is correct, then the

diamicton (unit 1) must have been deposited in the outer bay during either an Early or Middle Wisconsinan (de)glaciation. Deposition of unit 2 would therefore have occurred during the Middle Wisconsinan and throughout the Late Wisconsinan. Even if ice persisted in the region during the Middle Wisconsinan, retreating to a position inland of the present coast prior to a small scale Late Wisconsinan re-advance, it is probable that a normal marine environment would have existed within the outer bay at some point during the deposition of unit 2. However, the absence of any interval of abundant biological activity within the unit argues that no such conditions were established, prior to the transition to unit 3. There is no seismic or sedimentological evidence for erosion of unit 2 at core site 87-030-001 (Fig. 4.2) which might have removed any normal marine sediments. It is therefore interpreted that unit 2 represents only Late Wisconsinan sediments and that the diamicton of unit 1 was also deposited during the Late Wisconsinan by grounded ice which extended beyond the NE limits of the present study. This interpretation argues against models 1 and 2, which are therefore discarded for the study area. Models 3 and 4 are discussed below.

6.2.1 Deglaciation of Bonavista Bay

The absence of any continuous lateral or end moraine development within the study area suggests that a grounded

Late Wisconsinan ice sheet within Bonavista Bay extended NE beyond the study area and farther east and west than the extent of the primary survey (Fig. 6.1). Reworked acritarchs (Section 4.8) and glacial striae (Section 1.3) suggest that the ice sheet advanced from SW to NE, eroding Cambro-Ordovician sediments from outcrops near the base of the Bonavista Peninsula and/or from the offshore bedrock geology. The clay mineralogy also indicates that sediment input originated from the SW.

The scarcity of lift-off moraines, till tongues and prograding glaciomarine sediments, which are generally associated with a gradually retreating grounding line (King and Fader, 1986), suggests that lift-off of the ice sheet and development of an ice shelf occurred rapidly and almost concurrently over the basins of the outer bay. Retreat of the grounding line likely slowed or paused at a position near the SW end of the outer basins and on the western margin of the Western Basin. During this time the isolated moraines within unit 1 were deposited (Fig. 6.2). The remainder of unit 1 was deposited throughout the outer basins beneath a floating ice shelf, as indicated by its occasionally ponded morphology and the presence of dinoflagellates. Isolated channels were eroded, perhaps by outwash currents, in the vicinity of the retreating grounding line and later infilled by glaciomarine sediments. The acoustically incoherent lens-shaped zones within unit 1

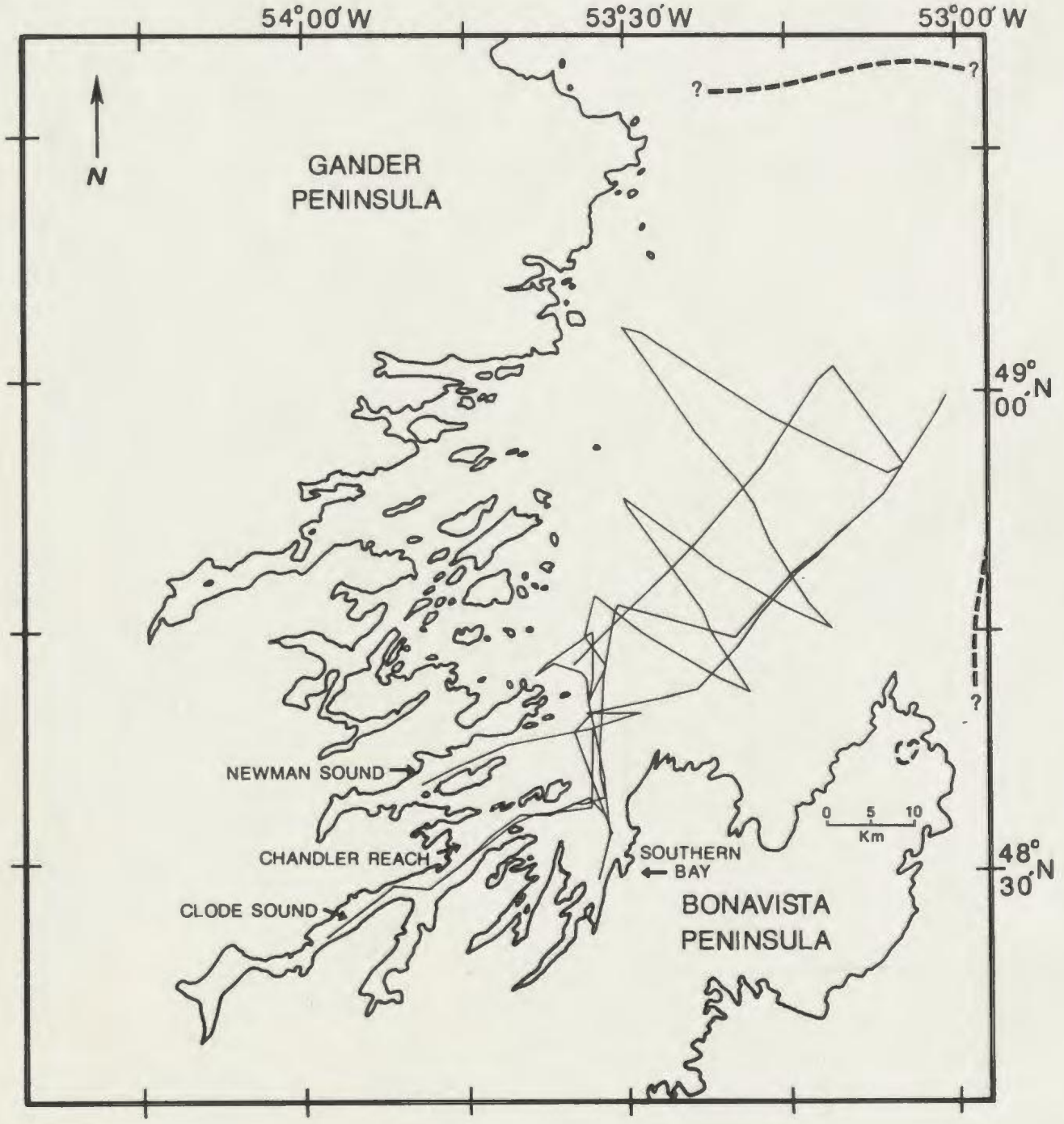

Figure 6.1. Speculative extent of Late Wisconsinan grounded ice sheet within Bonavista Bay, superimposed upon the primary seismic survey grid. Position of ice terminus (dashed line) is dependant upon the model invoked for the Late Wisconsinan maximum extent (Section 6.1), and may actually have lain much farther offshore. The eastern ice margin does not account for the possibility of an ice sheet extending from Trinity Bay. A small nunatak existed upon the NE tip of the Bonavista Peninsula (Brookes, 1989).

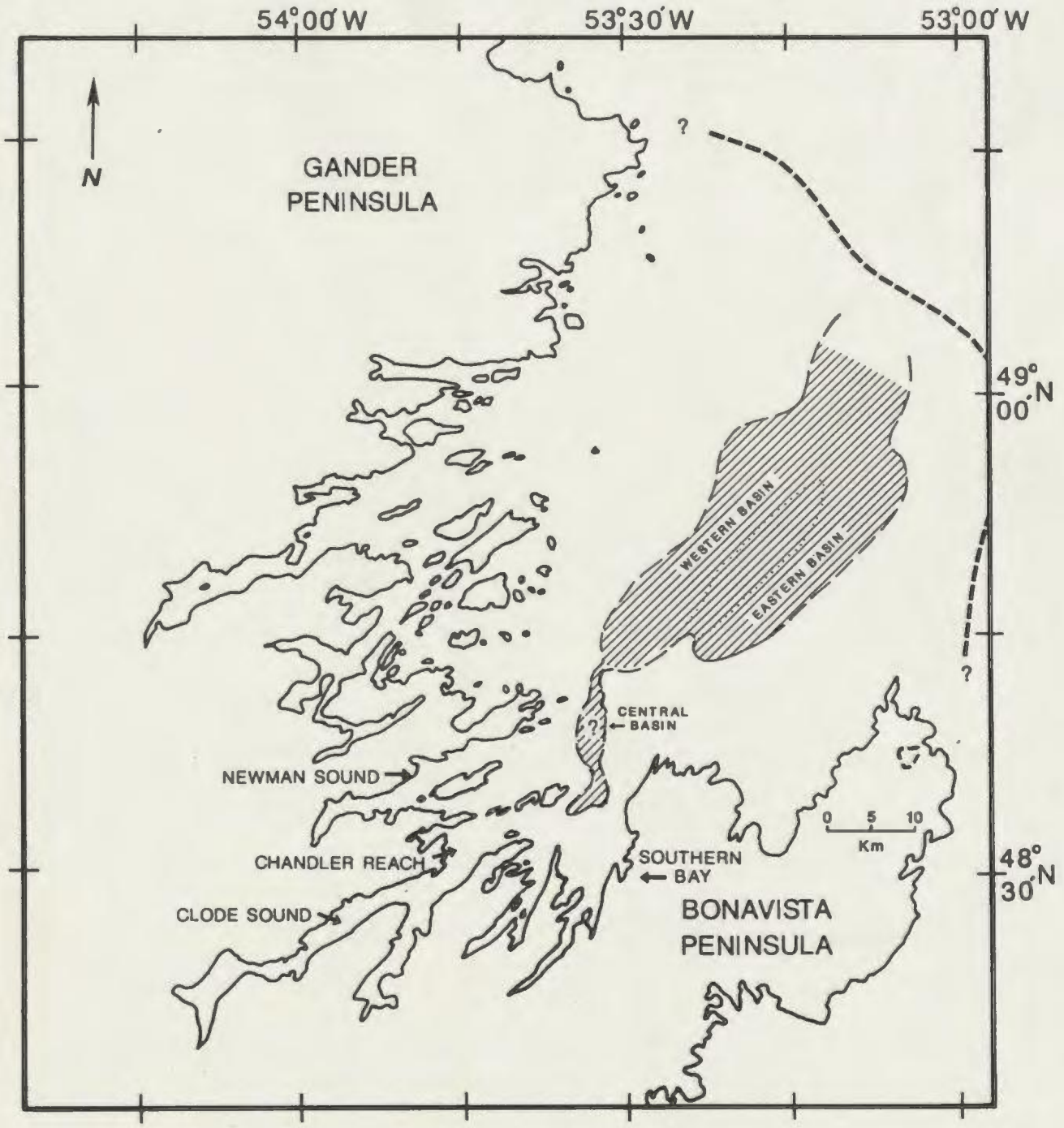

Figure 6.2. Glacial extent and the location of buoyant ice cover (hatched area) at the time of deposition of the discontinuous moraines within unit 1. The moraines are situated in the south and NW areas where the grounding line is denoted by a solid line. Thick dashed line denotes the speculative position of the glacial terminus.

may have been formed from small scale coarse debris flows (flow tills) near a southern ice margin.

The great depth to acoustic basement within the Central Basin (approximately 600 m below present sea level), and its close proximity to the outer bay, suggests that the ice sheet was probably buoyant within this basin during the later stages of deposition of unit 1 in the outer bay (Fig. 6.2). Similar to unit 1, the base of unit A may be a basal till, although the majority of this sequence was likely deposited from rain-out debris beneath floating ice. The extent of the floating ice cover within the inner bay during the deglaciation of the outer bay cannot be interpreted with certainty, due to a lack of chronological evidence.

In the outer bay, the lack of continuous moraines and prograding sequences on the basin margins implies that the grounding line did not pause for long at the basin edges. Yet, unit 1 is commonly limited to a thin veneer of basal till above 200-250 m present water depths on the margins. A broad floating ice shelf would have deposited a diamicton equivalent to the uppermost interval of unit 1 throughout the outer bay. A mechanism is therefore required to explain the often ponded morphology of the uppermost interval of unit 1. There are three possibilities: 1. Much lower relative sea levels limited deposition above a certain depth outside the basins. Lowest relative sea level on the Grand Banks was 90-110 m below present during the Late Wisconsinan

glacial maximum (Fader and King, 1981: Barrie et al., 1984; King and Fader, 1986), and may have been similarly lowered in Bonavista Bay. However, a lack of seismic evidence of resedimentation within the basins and the apparent rapidity of ice lift-off indicate that relative sea level was rising at the time when ice became buoyant within Bonavista Bay. In addition, the close proximity of Newfoundland-based ice may have resulted in isostatic crustal depression and a limited drop in relative sea level. 2. Holocene erosion by the Labrador Current removed all glacial to post-glacial sediments from the basin margins. There is, however, a lack of seismic evidence for large scale resedimentation within the basins. 3. Deposition of unit 1 outside the basins was limited by concurrent and/or post-depositional erosion from oceanic or meltwater currents. Geostrophic currents were probably concentrated on the margins by Coriolis forces, producing a counter clockwise circulation within the bay. Fine sediment would have been winnowed from glacial debris, perhaps as it settled through the water column, producing a coarse lag deposit which is not resolved by the acoustic systems used in the present study (Orheim and Elverhoi, 1981). Circulating currents beneath floating ice may also have aided in the rapid ablation of the ice shelf from the outer bay (Hughes, 1987).

Deposition of unit 1 in the deep region to the SW of the Western Basin was in the form of interfingering

diamicton and glaciomarine sediments from a proximal grounded ice margin. The presence of a similar sequence upslope to the NNE (Fig. 3.10) suggests that the margin curved around the deepest part of the basin, and was grounded on the basin margins to the east and west. It is possible that the lenticular zones of diamicton were produced by ice contact (i.e.: till tongues of King and Fader, 1986), or through debris flows from different areas of the nearby ice margin. The interpreted retreat of ice to the SW suggests that deposition of unit 1 in the SW end of the Western Basin may have persisted while the remainder of the outer bay was receiving proglacial sediments (unit 1, therefore, being diachronous). This is supported by the interpretation that the sediment source for the turbidites of unit 2 was an ice margin to the SW (Section 5.2.2). Figure 6.3 shows the interpreted ice margin position at the time when deposition of unit 1 had largely ceased within the outer bay.

Deposition of glacial sediments (unit A) within the basins of the inner bay was probably diachronous, reflecting the different basin depths and positions relative to ice retreat. Ice may have remained grounded within Newman Sound and Chandler Reach for a length of time after the deglaciation of the outer bay, and perhaps during the retreat of ice from the Central Basin. As in the Central Basin, the lowermost sediments of unit A within each basin

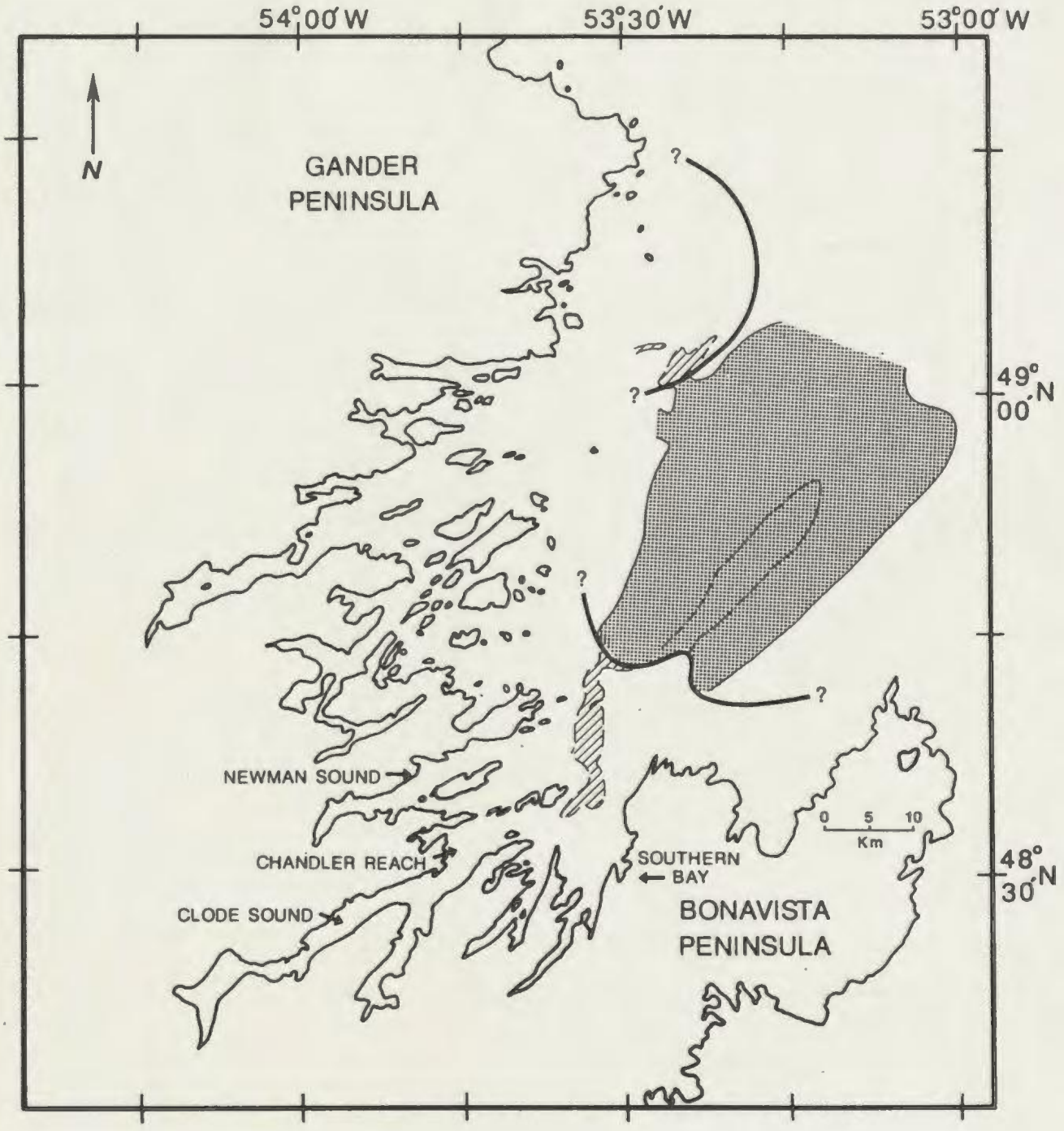

Figure 6.3. Position of ice margins at the transition between deposition of units 1 and 2 in the outer bay. Shaded areas denote zones of proglacial deposition within the Eastern and Western Basins. Ice cover is buoyant over the hatched areas.

were probably deposited as basal till. With lift-off of the ice, the majority of unit A was subsequently deposited from sub-glacial melt out. As the floating ice thinned, subaqueous deposition of unit A occurred in basins at higher elevations. The glacial and proximal glaciomarine seismic sequences within Southern Bay were deposited while the ice margin paused in its retreat from the region of the Central Basin. Within Newman Sound, currents generated by outwash eroded channels within the upper sediments of unit A which were later infilled by glaciomarine sediments.

While initial deposition of unit 2 in the outer bay may have occurred beneath floating ice, core data indicate a marked decrease in the amount of ice-rafted sediment above the transition from unit 1. This implies that in the NE of the outer bay, at least, the floating ice shelf disappeared shortly after deposition of unit 1. Ice margins, perhaps with buoyant outer shelves, persisted to the south and the west, providing sediment sources for the turbidity currents flowing to the middle of the basins. Seismic data suggest a primary sediment source was positioned to the east of the SW tip of the Western Basin. A second source may have been a lobe of ice from the Gander Peninsula or a remnant grounded ice body on a shoal region (<100 m) in the NW region of the bay (Fig. 6.3). The ice margin in the southern region of the outer bay (Fig. 6.3) may have retreated inland towards the Bonavista Peninsula while unit 2 was deposited in the

outer bay, perhaps allowing for the retreat of ice from the Central Basin during this time interval.

The hemipelagic environment which prevailed between turbidite flows hosted very limited biological activity and received high levels of terrestrial and ice-rafted sediment. The source of this terrestrial sediment was different from that of the turbidites (at least at core site 87-030-001) and may have included red clastic sediments of the Musgravetown Group which comprise most of the Bonavista Peninsula (Section 1.2). As with unit 1, the majority of sediments of unit 2 are limited to within the basins of the outer bay. By the time of deposition of unit 2, the majority of the outer bay was open to the North Atlantic (Fig. 6.3). Geostrophic currents probably entered the western side of Bonavista Bay and exited on the eastern side, concentrating their effects along the basin margins and restricting deposition of fine-grained hemipelagic sediments and perhaps the turbidites of unit 2 to within the basins.

Low abundances of pollen within unit 2 in core 87-030-001 may indicate that the surrounding coastline was not extensively vegetated and was ice covered. However, the low pollen count is probably linked to dilution by high sedimentation rates during the period when turbidity flows were active. Low dinoflagellate abundances during the same time indicate very cold, low salinity or turbid surface

waters (Scott et al., 1984). The slight increase in pollen abundances, following the end of turbiditic deposition implies that vegetation had developed somewhere in the region prior to 13,500 y BP (the transition to post-glacial deposition of unit 3, in the outer bay). Since pollen abundances remained very low within the inner bay until after 10,170 y BP (core 87-033-020; Section 4.8), the source of pollen and spores in the outer bay was probably vegetation on either of the Gander or Bonavista Peninsulas. The abundances of pollen and spores within units 2 and 1 in core 87-030-001 are generally low, probably reflecting the distance from shore of the core site (Fig. 2.1).

The deposition of proglacial sediments within the inner bay largely followed the retreat of ice cover from the Central Basin, Newman Sound and Chandler Reach. The base of unit B is probably diachronous between the different basins. Units B and 2 are also interpreted to be diachronous, since unit 2 was likely being deposited within the outer bay while the inner bay was still ice covered (at least initially). Deposition of unit B occurred initially within the Central Basin, during which time ice may have persisted within the surrounding fjords (i.e.: Newman Sound and Chandler Reach). Unit B within the Central Basin may therefore have received coarser sediment input than elsewhere within the inner bay, perhaps explaining why unit B in the Central Basin has a less acoustically transparent character than in the fjords.

By the time unit B was deposited within Newman Sound and Chandler Reach, the ice sheet had retreated inland to become entirely terrestrial (Fig. 6.4). This occurred before 12,790 y BP within Chandler Reach, as indicated from the date at the top of unit B in core 87-033-020. During the retreat of the ice margin from Chandler Reach, the terraced glacial/proglacial sediments were deposited in Clode Sound by a stillstand or minor ice re-advance. The downlapping reflections in the SW end of Chandler Reach, at the base of unit B (Fig. 3.13) probably represent prograding sediments from this ice margin within Clode Sound. However, the ice had retreated inland before most of the deposition of unit B occurred in Chandler Reach. The terraced and eroded nature of the sediments may have originated from either syn-depositional or post-depositional outwash currents, or perhaps small scale readvancement of ice into Clode Sound.

High levels of chlorite, quartz, plagioclase and K-feldspar within the clay-sized minerals of unit B in core 87-033-020 (Chandler Reach) suggest local terrestrial sources. Very low abundances of pollen and spores may partly be the result of dilution by high sediment rates, but also indicate that little vegetation had developed on the surrounding coast prior to 12,790 y BP. Low dinoflagellate abundances reflect either low surface water temperatures, salinities or high levels of suspended sediment.

Previous studies from regions to the west of the study

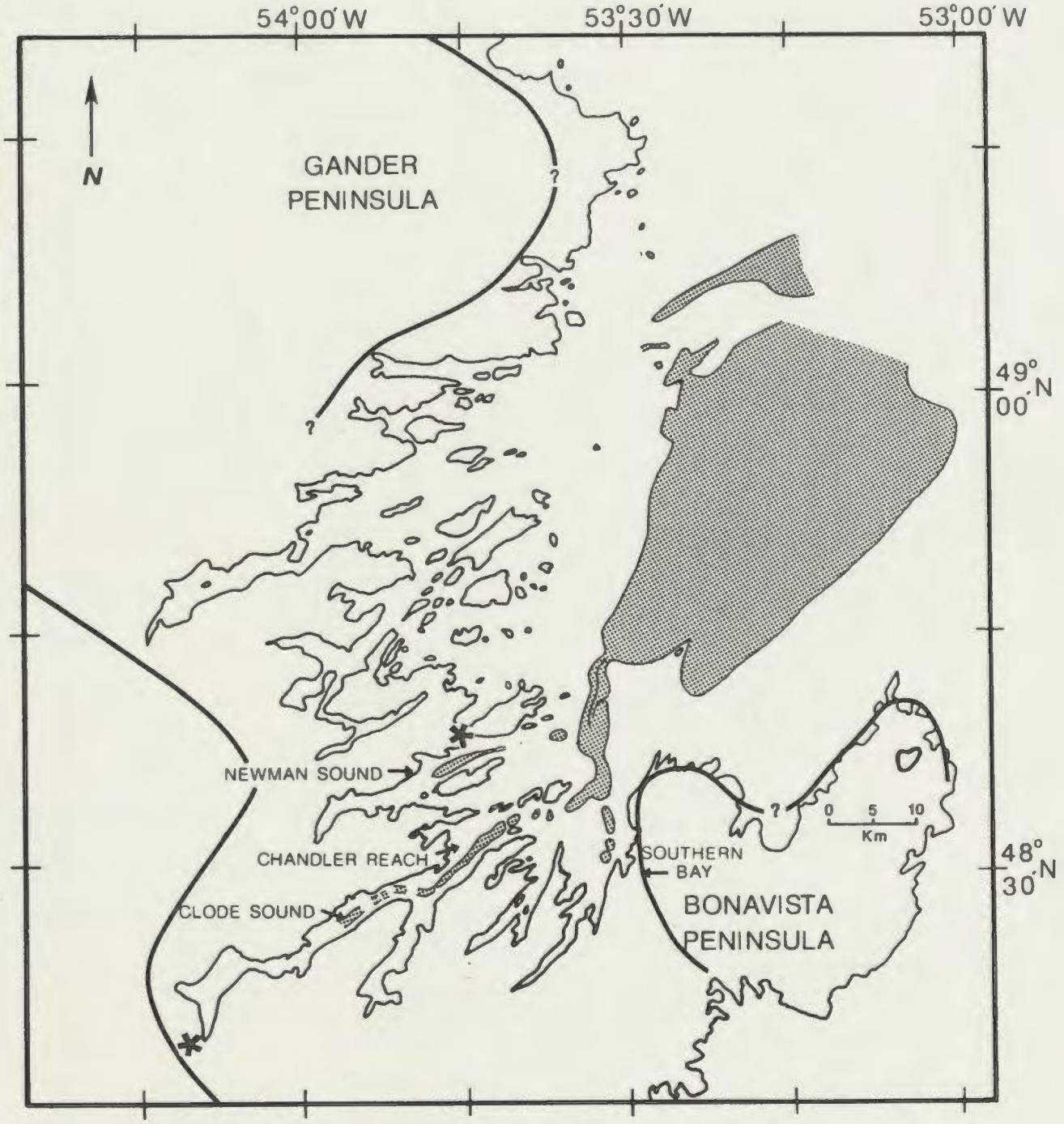

Figure 6.4. Position of ice margins following the retreat of ice from the inner bay by 12,790 y BP (minimum age of retreat). The ice margin to the SW corresponds with the approximate position of the end moraine described by Jenness (1963). The presence of ice caps on the Bonavista and Gander Peninsulas interpreted by Brookes (1989) and Grant (1974), respectively. The two stars indicate the position of delta fronts discussed within the text. The shaded areas correspond with basinal areas of deposition.

area (Section 1.4.1) have suggested that relative sea levels were higher than at present by approximately 11,000-13,000 y BP (i.e.: Dyck and Fyles, 1963; Blake, 1983, 1987). This is compatible with the retreat of the ice sheet from Bonavista Bay by 12,790 y BP as suggested by the present study. It is therefore interpreted that relative sea levels for much of the period of deposition of unit B were as high, if not higher than present day. The same is true for the subsequent period of deposition of unit C.

Outwash deltas which have been described on the shores of Newman Sound and Clode Sound (Jenness, 1963; Dyke, 1972: Section 1.3.2) probably supplied terrestrial sediment to the proglacial sediments of units B and C. Their location is indicated in figure 6.4. These features, with upper surface elevations of approximately 30 m above present sea level, were developed at the time of highest sea level stand in the region (Jenness, 1963; Dyke, 1972), and therefore during the time of proglacial deposition. Within Newman Sound, a delta front occurs on the Eastport Peninsula, on the margin of the surveyed basin (Fig 6.4). The infilled channels within the glacial sediments of unit A (Fig. 3.15) may have been eroded by early outwash currents, as ice retreated from the fjord (Fig. 6.5). The fine sediment comprising unit B probably originated as fine outwash as the delta developed. The relatively consistent thickness and acoustic character of unit B (Fig. 3.15) suggests that currents must have

Figure 6.5. A cross sectional profile of Newman Sound, showing the relationship between the development of an outwash train on the Eastport Peninsula (to the NW) and seismic units A-C.

Stage 1.) During and following the retreat of ice from Newman Sound, outwash currents erode channels within the diamicton (unit A). These are infilled by glaciomarine sediments.

Stage 2.) With relative sea level rising and development of an inland outwash train, fine sediment is input to the basin, depositing unit B. Currents (re)distribute sediments throughout the basin.

Stage 3.) Progradation of the delta front provides an influx of coarser sediment near the start of deposition of unit C. The remainder of unit C does not display downlapping reflections, perhaps reflecting a decrease in outwash volume.

NEWMAN SOUND

NW SE

1

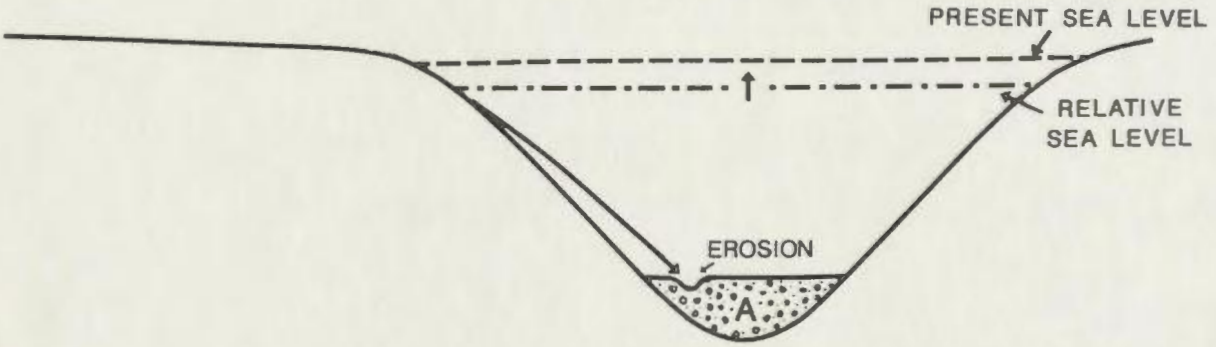

2

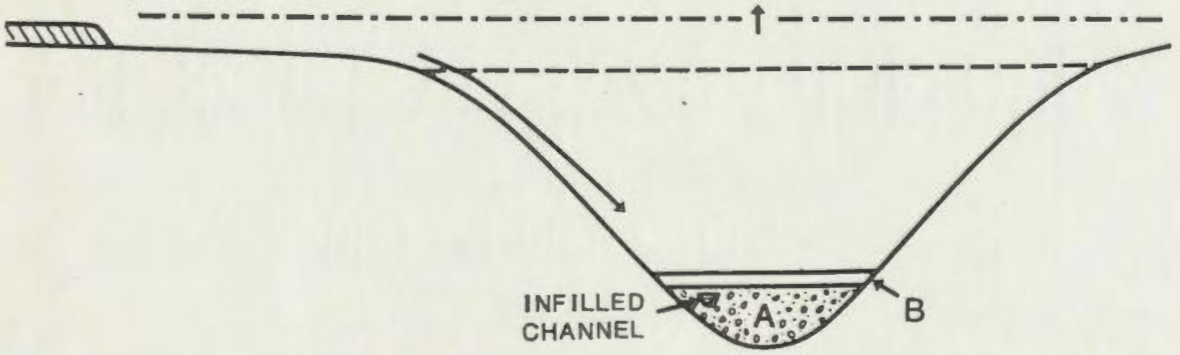

3

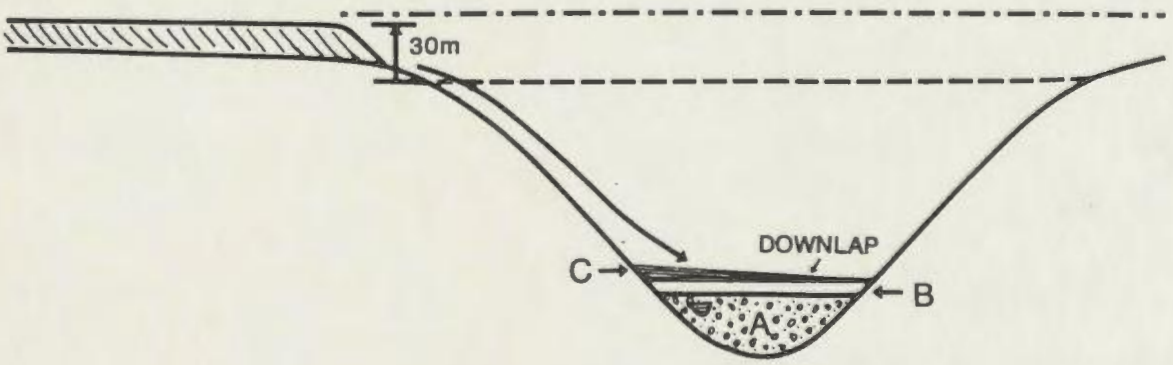

distributed sediment throughout the basin. Downlapping reflections at the contact between units B and C in Newman Sound (Fig. 3.16) suggest that the delta had prograded closer to the basin and supplied some coarser sediment into the basin by the time of transition between units B and C. Within Clode Sound, the reddish sediments which are common within the delta front probably shared a terrestrial source with the pale red mud of unit B within Chandler Reach. Similar to the origin of unit B in Newman Sound, (Fig. 6.5), fine-grained sediment was probably transported into Chandler Reach by abundant meltwater flows from this, and perhaps other outwash deposits.

Given the interpretation that sea level was high during deposition of unit B and that ice margins were inland of the coast, the question arises as to why unit B has a ponded, and not conformable morphology. It would be expected that fine-grained outwash sediment would have been transported into the fjords by near surface freshwater plumes and deposited as conformable cover (Powell, 1983). There are two possible explanations for the morphology of unit B:

i) Geostrophic currents entering the inner bay experienced Coriolis deflection towards the margins of the basins and produced a concentration of outwash flows in mid-basin. The existence of current deflection would depend on the current velocities, depositional latitude and fjord width (Syvitski, 1989). However, outwash flow should

theoretically have been deflected to the opposite side of the basin from inflowing geostrophic currents, causing preferential deposition on one side of the basin (Syvitski, 1989). Cross-sections of Newman Sound and the Central Basin suggest that this has not happened (Figs. 3.16, 3.19). Furthermore, the lack of dinoflagellates within unit B in Chandler Reach does not support any large scale influx of oceanic waters.

ii) Silt and clay may have been transported into the basins by dense meltwater plumes, flowing either along the seafloor (underflows) or within the water column (interflows). Such processes are possible in areas where the suspended sediment concentrations are very high and the salinity of the surrounding water is low (Mackiewicz et al., 1984; Syvitski, 1989). Low salinity and turbid waters would restrict the development of a benthic community (Syvitski et al., 1987). Syvitski (1989) suggested that underflows may have been common in fjords during periods of rapid ice cap retreat. However, interpreted examples of underflow sediments have been coarse-grained and deposited within 1 km of a glacial margin (Mackiewicz et al., 1984). Interflows within a low salinity environment may be a more feasible mechanism for the long distance transportation of silt and clay deposited within the deeper regions of the basins. Indeed, interflows have been proposed as controlling the deposition of fine-grained outwash muds within Queen Inlet,

Alaska (Hoskin et al., 1976).

Normal marine conditions had developed within the outer bay prior to the end of deposition of unit B within Chandler Reach (12,790 y BP). By 13,500 y BP, the influx of terrestrial sediment to the Eastern and Western Basins had slowed as the influence of glacial ice upon the outer bay diminished.

Within Chandler Reach, the transition to unit C is marked by an increase in coarse sediment and ice-rafted debris at 12,790 y BP and a transition to hemipelagic sedimentation. While the base of unit C may be diachronous between basins, ice-rafting likely began at the same time through ice dispersal. Floating ice may have originated from a local ice margin re-entering the marine environment or from regions outside Bonavista Bay. High chlorite abundances in the clay fraction, along with a sedimentation rate of 1.9 m/ka, which is 3-4 times greater than the Holocene rate in unit D, indicate a continued influence of local glacial ice. Pollen abundances remained very low throughout deposition of unit C, continuing to indicate limited vegetational development on the surrounding land. Biogenic activity, including macrofauna and dinoflagellate abundances, increased while unit C was deposited, presumably reflecting either a decrease in the amount of suspended sediment, a warming trend, or an increase in salinity. The reversal in the trend of increasing dinoflagellate

abundances at the very top of the unit may indicate a late stage terrestrial re-advance during deglaciation. There is no evidence from the present study of any large scale re-advancement of ice into the marine environment, following the deposition of unit B, suggesting that inner Bonavista Bay was under the influence of a terrestrial ice margin from 12,790 to 10,170 y BP. It is possible that a small scale readvancement of ice occurred in Clode Sound, with erosion of the terraced sediments. This, however, is uncertain.

The draping basin-fill morphology common for unit C resulted from increased deposition through suspension fallout. Terrestrial sediment was probably transported into the fjords by surface flows (overflows) (Hoskin et al., 1976), as opposed to the interflows interpreted for unit B. In Newman Sound, upper reflections of unit C were eroded (perhaps by currents associated with outwash) prior to the onset of Holocene sedimentation.

Post-glacial normal marine sedimentation developed diachronously within Bonavista Bay. In the outer bay, the influence of glacial ice had ceased by 13,500 y BP. Deposition of normal marine sediments was probably limited by current activity to the Eastern and Western Basins, as were the sediments of units 1 and 2. Development of a post-glacial, normal marine hemipelagic environment occurred later in the inner bay, at 10,170 y BP within Chandler Reach, reflecting the continued presence of glacial ice near

the coast. The increase in the abundances of pollen and spores within units D and 3 reflects development of vegetation within the entire region after the final ice retreat. The gradual increase in dinoflagellate abundances which occurs within post-glacial sediments throughout the bay probably reflects decreased suspended sediment content and increasing salinity and temperature of waters following deglaciation.

Post-glacial sediments on the basin margins of the outer bay probably experienced syn-depositional erosion and winnowing from a continuation of the current activity which affected units 1 and 2. However, the surface erosion of reflections within post-glacial unit 3 indicates that post-depositional erosion has removed sediment from the basin margins and occasionally within the basins (i.e.: Fig. 3.10). The underlying unit 2 has also experienced post-depositional erosion in areas where unit 3 is absent. Within the inner bay, post-glacial sediments (unit D) have also been limited by erosion to the center of the basins. This post-depositional erosion has entirely removed unit D in places and truncated underlying reflections of unit C (Fig. 3.18). The apparent increase in levels of erosion within the post-glacial depositional environment of Bonavista Bay may reflect increased current flow rates during the Holocene. Geostrophic current activity may have intensified during the early Holocene as the Labrador

Current received increasing input of bottom waters from Baffin Bay (Aksu, 1983). Within the last 3000 years, the inner NE Newfoundland shelf has experienced increasing current activity as the core of the Labrador Current has moved into shallower waters (Fillon, 1976). Erosion of Holocene sediments has been noted in previous studies to the NE of the study area, on the continental shelf, (Miller et al., 1985; Miller, 1987; Macpherson, 1988) and slope, (Carter et al., 1979). Erosion within the study area by the Labrador Current has probably been intensified on the basin margins by the same Coriolis effects which have been invoked to explain the distribution patterns of units 1 and 2 in the outer bay. Concentration and redirection of flow within the deep, narrow region to the SW of the Western Basin could have produced the erosion of unit 3 and most of unit 2 from within the deepest part of the outer bay (Fig. 3.10).

6.2.2. Terrestrial Correlation

The interpretations of previous workers in the region (Section 1.4.1) are consistent with results of the present study. The rapid retreat of an ice sheet from Bonavista Bay agrees with Jenness' (1963) interpretation that late Pleistocene ice had rapidly retreated from an offshore position to the inland end moraine which divides the inner and outer drift zones (Fig. 1.3). As the only terrestrial indicator of an ice front position, the end moraine

represents the most likely position for the ice margin during the period of deposition of unit C (12,790 to 10,170 y BP), at least in the region of the inner bay. The ice margin probably retreated further inland than the end moraine at some point during the time of deposition of unit B, but re-advanced at or near 12,790 y BP. The re-advance and continued influence of glacial ice within the region until about 10,170 y BP is compatible with a cooling trend observed by Macpherson and Anderson (1985) to have followed an earlier period of deglaciation within the Notre Dame Bay area, to the west of the study area (Section 1.4.1).

The low pollen abundances within proglacial sediments of the inner bay suggest that the region of the outer drift zone, beyond the end moraine, was not significantly vegetated until after approximately 10,170 y BP. This may reflect the continued influence of separate, possibly remnant ice caps on the Gander Peninsula (Grant, 1974; Butler et al., 1984) and Bonavista Peninsula (Brookes, 1989). The presence of pollen and spores within unit 2 of the outer bay does indicate that vegetation had developed somewhere within the region prior to 13,500 y BP, and therefore that the neighbouring peninsulas were probably not completely ice covered. The model presented does require separate ice masses on the Gander and Bonavista Peninsulas to act as sediment sources for the proglacial sediments of unit 2 in the outer bay. Ice probably persisted on these

flanking headlands while retreat began and progressed within the inner bay.

6.3 Implications for Existing Models

The model presented is a reconstruction of the deglacial history of Bonavista Bay. On the basis of data from the study area it is not possible to define the maximum Late Wisconsinan glacial extent on the Northeast Newfoundland Shelf. While the presence of grounded ice in the bay during the last glaciation allows models 1 and 2 (Section 6.1) to be discarded, the glacial distribution of either model 3 or 4 may have prevailed. However, a preferred model is indicated by the interpreted sequence of events during the deglaciation.

In the maximalist model 3, the ice sheet extending onto the shelf would be relatively thick, given that it would be the outer margin of a single, Newfoundland-based ice cap. Such an ice sheet would be expected to ablate gradually, at least during initial deglaciation. Although frozen or dry-based ice conditions may have initially prevailed, the ice sheet would likely have become wet-based over time (as proposed by King and Fader (1986) for the Scotian Shelf). Wet-based ice within Bonavista Bay during a gradual retreat further offshore would likely have produced more basal till deposition than did occur (Carey and Ahmad, 1961). The veneer of till within Bonavista Bay is very thin when

compared with deposits of up to 80 m thickness from areas such as St. Georges Bay on the west coast of Newfoundland (Shaw and Forbes, 1990). The presence of a thick melt out sequence (unit A) in the inner bay indicates that the ice sheet did contain substantial entrained debris. Alternately, if the ice sheet maintained dry-base conditions and deposited very little sediment until lift-off, then a large mass of ice landward of the grounding line would have made the rapid ice retreat in Bonavista Bay unlikely (Carey and Ahmad, 1961). Therefore, a straightforward retreat of the ice sheet proposed in model 3 is not compatible with the deglaciation of the study area.

Model 4, whereby the Newfoundland Ice Cap was drawn down and channelized in Bonavista Bay, would likely have seen a lesser ice thickness at glacial maximum than model 3. As sea level rose, early in the deglaciation, the ice sheet would probably have become rapidly buoyant at its outer margin. The retreat of the ice sheet from Bonavista Bay may then have progressed rapidly. The timing of deglaciation of the bay would have depended on the offshore extent of the ice at glacial maximum. If the ice did not extend much beyond the mouth of the bay, then lift-off may have occurred early in the deglaciation. If so, it might be expected that the buoyancy line would have re-advanced, and either till tongues or moraines would have been developed (King and Fader, 1986). Alternately, if the channelized ice extended

onto the outer shelf at glacial maximum, it might be expected that a thicker basal till would have developed in Bonavista Bay as the ice retreat occurred offshore. However, King et al. (1987) have interpreted occurrences on the Norwegian and Scotian Shelves where subglacial erosion has continued upglacier from a depositional terminus.

Theories on the dynamics of collapsing ice sheets may provide a solution to some of the problems with the deglaciation of models 3 and 4 (i.e.: Hughes, 1987). It is possible that during the Late Wisconsinan deglaciation Bonavista Bay (along with other bays) acted as an outlet through which part of the Newfoundland Ice Cap collapsed. The effect of rising sea levels, early in deglaciation, may have been to reduce the basal friction of a grounded ice sheet within the bay, allowing ice from the inland ice cap to collapse through developing ice streams into the ocean (Hughes, 1987). Ablation by calving at the end of the streams would have been rapid (Ruddiman and McIntyre, 1981; Denton and Hughes, 1981a; Denton and Hughes, 1983). Previously deposited Quaternary sediments would have been eroded by flow within the grounded portion of the stream (Hughes, 1987) and the sediment sequence observed by the present study would have been deposited during and subsequent to the late stages of deglaciation. The extent of grounded stream flow beyond Bonavista Bay would have depended on the volume and dynamics of flow. At the end of

the surge, the diminished elevation of terrestrial ice and rising sea levels would have seen a rapid retreat of the grounding line. Rapid ablation by calving at the seaward margin of the ice shelf may have been aided by oceanic currents (Hughes, 1987).

This scenario is not unlike that outlined by model 4, except that the channelized flow occurred after, rather than prior to, the Late Wisconsinan glacial maximum. Surging ice streams could either have been a re-activation of flow in model 4 or a late stage event in the deglaciation of the ice sheet of model 3. The ice surge model does serve to compress the deglaciation of the bay into the late stages of the Late Wisconsinan, at a time when retreat would be rapid and re-advances minimal. Once the ice had retreated into the inner bay, the reduced thickness of the terrestrial ice cap would have allowed the fjords to empty of ice rapidly. The remaining ice cap might then have stabilized or re-advanced to the position of the end moraine, reflecting the climatic reversal which followed the rapid deglaciation (Macpherson and Anderson, 1985).

CHAPTER 7

CONCLUSIONS

7.1 Summary

High-resolution seismic reflection data from the open, outer region of Bonavista Bay display three seismic units overlying acoustic basement. These units occur primarily within two broad, shallow basins. The surveyed inner region of Bonavista Bay contains narrow, deep basins which commonly host four seismic units above acoustic basement. Correlation of lithofacies within piston cores with six of the seven seismic units allows the identification of glacial, proglacial and post-glacial sequences throughout Bonavista Bay.

Bonavista Bay was host to a grounded Late Wisconsinan ice sheet which extended beyond the limits of the survey grid. The last major erosional advance may have been during the Late Wisconsinan glacial maximum or as part of a deglacial surge, driven by a collapsing ice cap to the SW. Deglaciation of the bay was rapid and occurred at a time of rising sea level. A thin basal till (unit 1) was deposited initially within the outer bay beneath grounded ice. With lift-off, an ice shelf was rapidly formed over the basins of the outer bay. Retreat of the grounding line paused only briefly on the basin margins, where discontinuous moraines were deposited, prior to development of an ice shelf

throughout much of the outer bay. The ice sheet had also become buoyant within the northeasternmost basin of the inner bay by this stage (Central Basin). Diamictons (units 1 and A) were deposited within the basins by rain-out of debris beneath the floating ice. Deposition on the basin margins was limited by oceanic or meltwater currents, which may also have aided in the rapid ablation of the ice shelf. Ice margins persisted near the SW and western regions of the outer bay and provided sediment for proglacial turbidity currents within the basins, along with continuous terrestrial and ice-rafted sediment (unit 2). Geostrophic currents largely limited deposition to within the basins.

While unit 2 was being deposited within the outer bay, the basins of the inner bay were gradually being deglaciated. Fine-grained outwash sediment (unit B), transported by interflows, was rapidly deposited in the basins as the ice margin retreated to a terrestrial position. This retreat was complete by at least 12,790 y BP, at which time sea level was probably higher than present day. The region of the inner bay remained under the influence of one or more ice margins until 10,170 y BP, with basinal deposition of a hemipelagic, ice-rafted sequence (unit C). The position of the ice margin during this time corresponds with an end moraine mapped by Jenness (1963). Ice caps also persisted on the Gander and Bonavista Peninsulas. Normal marine conditions were established

within the outer bay by 13,500 y BP, while the inner bay was receiving proglacial sedimentation. With final ice retreat, normal marine conditions were established throughout Bonavista Bay by 10,170 y BP. Holocene erosion by the Labrador Current has strongly affected both Holocene and perhaps Wisconsinan sediments.

7.2 Suggested Further Research

Additional research within and beyond the study area would serve to verify the interpretations of the present study and assist in developing a more regional model. The following suggestions for further work are presented:

1. A seismic survey from Bonavista Bay to beyond the shelf edge would provide an indication of the Late Wisconsinan maximum glacial extent. Also, one or more long E-W traverses beyond the bay might define the lateral extent of ice and indicate whether Bonavista Bay contained channelized ice flows. Seismic surveys within the shallower western region of the bay would provide indications of Late Quaternary events outside the survey area of the present study.

2. A date from near the top of glacial sediments would be invaluable in determining the timing of deglaciation within the region, assuming that a suitable volume of carbonate sample for dating could be collected from an additional core. A TOM date would be less desirable, given

the presence of old carbon in some of the surrounding Palaeozoic metasediments.

3. Additional coring, with the use of the Long Core Facility where possible, would serve to groundtruth some of the interpretations of seismic units made in Chapter 5. There are a number of recommended sites: i) within the innermost basins of Southern Bay, ii) within Clode Sound, on the sediment terraces, iii) within the outer basins, away from the basin margins, and iv) in the deep region in the SW of the Western Basin. At the latter site, erosion of post-glacial and proglacial sediments (Fig. 3.10) would permit the collection of a series of cores in mid-basin from progressively increasing depths within the sedimentary sequence.

4. Current meter data from Bonavista Bay would determine the present distribution and velocities of flow of the Labrador Current, therefore supporting or disproving the idea of Coriolis deflection and concentration of eroding currents upon the basin margins.

5. Micropalaeontological and/or more detailed palynological studies would serve to better define palaeo-environmental changes interpreted from the cores.

REFERENCES

Aksu, A.E., 1983. Holocene and Pleistocene dissolution cycles in deep-sea cores of Baffin Bay and Davis Strait: palaeoceanographic implications. Marine Geology, 53: 331-348.

Andrews, J.T., 1987. The Late Wisconsinan glaciation and deglaciation of the Laurentide Ice Sheet. In: North America and adjacent oceans during the last deglaciation. W.F. Ruddiman and H.E. Wright, Jr. (Editors). Geological Society of America, The Geology of North America, v. K-3, Boulder, Colorado, pp. 13-37.

Andrews, J.T. and Jennings, A.E., 1986. Influence of sediment source and type on the magnetic susceptibility of fiord and shelf deposits, Baffin Island and Baffin Bay, N.W.T. Canadian Journal of Earth Sciences, 24: 1386-1401.

Barrie, C.Q. and Piper, D.J.W., 1982. Late Quaternary marine geology of Makkovik Bay, Labrador. Geological Survey of Canada, Paper 81-17. 37 p.

Barrie, J.V., Lewis, C.F.M., Fader, G.B. and King, L.H., 1984. Seabed processes on the northeastern Grand Banks of Newfoundland; modern reworking of relict sediments. Marine Geology, 57: 209-227.

Bell, K. and Blekinsop, J., 1975. The geochronology of eastern Newfoundland. Nature, 254: 410-411.

Bell, K., Blekinsop, J., Berger, A.R. and Jayasinge, N.R., 1979. The Newport Granite: its age, geological setting and implications for the geology of northeastern Newfoundland. Canadian Journal of Earth Sciences, 16: 264-269.

Bell, T., Rogerson, R.J., Klassen, R.A. and Dyer, A., 1987. Acoustic survey and glacial history of Adams Lake, outer Nachvak Fjord, northern Labrador. In: Current research, part A. Geological Survey of Canada, Paper 87-1A, pp. 101-110.

Biscaye, P.E., 1965. Mineralogy and sedimentation of Recent deep sea clay in the Atlantic Ocean and adjacent seas and oceans. Geological Society of America Bulletin, 76: 803-832.

Blackwood, R.F., 1976. The relationship between the Gander and Avalon Zones in the Bonavista Bay region, Newfoundland. Unpublished M.Sc. thesis, Memorial University of Newfoundland, St. John's, Newfoundland. 156 p.

Blackwood, R.F., 1977. Geology of the east half of the Gambo (2D/16) map area and the northwest portion of the St. Brendan's (2C/13) map area, Newfoundland. Newfoundland Department of Mines and Energy, Mineral Development Division, Report 77-5. 20 p.

Blackwood, R.F., 1978. Northeastern Gander Zone, Newfoundland. In: Report on activities, Newfoundland Department of Mines and Energy, Mineral Development Division, Report 78-1, pp. 72-79.

Blackwood, R.F. and Kennedy, M.J., 1975. The Dover Fault: western boundary of the Avalon Zone in northeastern Newfoundland. Canadian Journal of Earth Sciences, 12: 320-325.

Blake, W. Jr., 1983. Geological Survey of Canada radiocarbon dates XXIII. Geological Survey of Canada, Paper 83-7. 34 p.

Blake, W. Jr., 1987. Geological Survey of Canada radiocarbon dates XXVI. Geological Survey of Canada, Paper 86-7. 60 p.

Blekinsop, J., Cucman, P.F. and Bell, K., 1976. Age relationships along the Hermitage Bay-Dover Fault system, Newfoundland. Nature, 262: 377-378.

Brookes, I.A., 1984. Glaciation of Bonavista Peninsula, northeast Newfoundland: relative chronology and contrasts in style. In: American Quaternary Association, 8th biennial meeting, Program and abstracts. University of Colorado, Boulder, Colorado, pg. 16.

Brookes, I.A., 1989. Glaciation of Bonavista Peninsula, northeast Newfoundland. The Canadian Geographer, 33: 2-18.

Butler, A.J., Miller, H.G. and Vanderveer, D.G., 1984. Geoscience studies in the Weir's Pond area northeast of Gander, Newfoundland. In: Current research, Newfoundland Department of Mines and Energy, Report 84-1, pp. 271-278.

Carey, S.W. and Ahmad, N., 1961. Glacial-marine sedimentation. In: Proceedings of the 1st International Symposium on Arctic Geology, 2, pp. 865-894.

Carlson, P.R., Powell, R.D. and Rearic, D.M., 1989. Turbidity-current channels in Queen Inlet, Glacier Bay, Alaska. Canadian Journal of Earth Sciences, 26: 807-820.

Carter, L., Schafer, C.T. and Rashid, M.A., 1979. Observations on depositional environments and benthos of the continental slope and rise, east of Newfoundland. Canadian Journal of Earth Sciences, 16: 831-846.

Carver, R.E., 1971. Procedures in sedimentary petrology. Wiley-Interscience, New York, NY. 653 p.

Christie, A.M., 1950. Geology of Bonavista Map-Area, Newfoundland. Geological Survey of Canada, Paper 50-7. 39 p.

CLIMAP Project Members, 1976. The surface of the ice-age Earth. Science, 191: 1131-1137.

Colman-Sadd, S.P., Hayes, J.P. and Knight, I., 1990. Geology of the island of Newfoundland. Geological Survey Branch, Newfoundland Department of Mines and Energy, Map 90-01.

Combaz, A., 1967. Un microbios du Trémadocian dans un sondage d'Hassi-Messaoud. Actes de la Société Linnéene de Bordeaux, Sér. B, 104: 1-26.

Dal Bello, A.E., 1977. Stratigraphic position and petrochemistry of the Love Cove Group, Glovertown-Traytown map area, Bonavista Bay, Newfoundland, Canada. Unpublished M.Sc. thesis, Memorial University of Newfoundland, St. John's, Newfoundland. 159 p.

Dale, C.T., 1979. A study of high resolution seismology and sedimentology on the offshore Late Quaternary sediments northeast of Newfoundland. Unpublished M.Sc. thesis, Dalhousie University, Halifax, Nova Scotia. 181 p.

Dale, C.T. and Haworth, R.T., 1979. High resolution reflection seismology studies on Late Quaternary sediments of the northeast Newfoundland continental shelf. In: Current research, part B. Geological Survey of Canada, Paper 79-1B, pp. 357-364.

Dallmeyer, R.D., Blackwood, R.F. and Odom, A.L., 1981. Age and origin of the Dover Fault: tectonic boundary between the Gander and Avalon Zones of the northeastern Newfoundland Appalachians. Canadian Journal of Earth Sciences, 18: 1431-1442.

Dallmeyer, R.D., Hussey, E.M., O'Brien, S.J. and O'Driscoll, C., 1983. Chronology of tectonothermal activity in the western Avalon Zone of the Newfoundland Appalachians. Canadian Journal of Earth Sciences, 20: 355 363.

Dec, T., Knight, I. and O'Brien, S.J., 1989. Sedimentological studies in the Eastport Basin: notes on the petrography of the late PreCambrian Connecting Point Group and provenance implications. In: Current research, Newfoundland Department of Mines, Geological Survey of Newfoundland, Report 89-1, pp. 63-79.

Denton, G.H. and Hughes, T.J.,(Editors) 1981a. The last great ice sheets. John Wiley and Sons, New York, NY, 484 p.

Denton, G.H. and Hughes, T.J., 1981b. The Arctic Ice Sheet, an outrageous hypothesis. In: The last great ice sheets. G.H. Denton and T.J. Hughes (Editors). John Wiley and Sons Inc., New York, N.Y., pp. 437-467.

Denton, G.H. and Hughes, T.J., 1983. Milankovitch theory of ice ages: hypothesis of ice sheet linkage between regional insolation and global climate. Quaternary Research, 20: 125-144.

Dredge, L.A. and Thorleifson, L.H., 1987. The Middle Wisconsinan history of the Laurentide Ice Sheet. Géographie physique et Quaternaire, 41: 215-235.

Duenff, J., 1954. Microorganismes planctoniques (Hystrichospheres) dans le Dévonien du Massif amoricain. Compte Rendu, Sommaire des Séances de la Société Géologique de France, Paris, 11: 239-242.

Dyck, W. and Fyles, J.G. 1963. Geological Survey of Canada radiocarbon dates II Geological Survey of Canada Paper 63-21. 31 p.

Dyke, A.S., 1972. A geomorphological map and description of an emerged Pleistocene delta, Eastport Peninsula, Newfoundland. Maritime Sediments, 8: 68-72.

Dyke, A.S. and Prest, V.K., 1987. Late Wisconsinan and Holocene history of the Laurentide Ice Sheet. Géographie Physique et Quaternaire, 41: 237-264.

Fader, G.B. and King, L.H., 1981. A reconnaissance study of the surficial geology of the Grand Banks of Newfoundland. In: Current research, part A. Geological Survey of Canada, Paper 81-1A, pp. 45-81.

Fillon, R.H., 1976. Hamilton Bank, Labrador Shelf: postglacial sediment dynamics and paleo-oceanography. Marine Geology, 20: 7-25.

Flint, R.F., 1940. Late Quaternary changes of level in western and southern Newfoundland. Bulletin of the Geological Society of America, 51: 1757-1780.

Flint, R.F., 1971. Glacial and Quaternary geology. John Wiley, New York, NY. 892 p.

Folk, R.L., 1974. Petrology of sedimentary rocks. Hemphill, Austin, Texas. 183 p.

Gipp, M.R., 1989. Late Wisconsinan deglaciation of Emerald Basin, Scotian Shelf. Unpublished M.Sc. thesis, Memorial University of Newfoundland, St. John's, Newfoundland. 219 p.

Gipp, M.R. and Piper, D.J.W., 1989. Chronology of Late Wisconsinan glaciation, Emerald Basin, Scotian Shelf. Canadian Journal of Earth Sciences, 26: 333-335.

Grant, D.R., 1974. Prospecting in Newfoundland and the theory of multiple shrinking ice caps. In: Current research, part A. Geological Survey of Canada, Paper 74-1A, pp. 215-216.

Grant, D.R., 1977. Glacial style and ice limits, the Quaternary stratigraphic record, and changes of land and ocean level in the Atlantic provinces, Canada. Géographie physique et Quaternaire, 31: 247-260.

Grant, D.R., 1980. Quaternary sealevel change in Atlantic Canada as an indicator of crustal delevelling. In: Earth rheology, isostacy and eustacy. N.A. Morner (Editor). John Wiley and Sons Inc., New York, pp. 201-214.

Grant, D.R. and King, L.H., 1984. A stratigraphic framework for the Quaternary history of the Atlantic provinces, Canada. In: Quaternary stratigraphy of Canada- A Canadian contribution to IGCP Project 24. R.J. Fulton (Editor). Geological Survey of Canada, Paper 84-10, pp. 173-191.

Hanmer, S., 1981. Tectonic significance of the northeastern Gander Zone, Newfoundland: an Acadian ductile shear zone. Canadian Journal of Earth Sciences, 18: 120-135.

Harland, R., 1983. Distribution maps of Recent dinoflagellate cysts in bottom sediments from the North Atlantic Ocean and adjacent seas. Palaeontology, 26: 321-387.

Haworth, R.T., Williams, H. and Keen, C.E., 1985. North American Continent-Oceans Transect Program; Transect D-1: North Appalachian mountains across Newfoundland to south Labrador Sea. Decade of North American Geology (DNAG) report accompanied by two maps. Geological Society of America. 9 p.

Hayes, A.O., 1948. Geology of the area between Bonavista and Trinity Bays, eastern Newfoundland. In: Geological Survey of Newfoundland, Bulletin 32, pp. 1-37.

Hofmann, H.J., Hill, J. and King, A.F., 1979. Late Precambrian microfossils, southeastern Newfoundland. In: Current research, part B. Geological Survey of Canada, Paper 79-1B, pp. 83-98.

Hoskin, C.M. and Burrell, D.C., 1972. Sediment transport and accumulation in a fjord basin, Glacier Bay, Alaska. Journal of Geology, 80: 539-551.

Hoskin, C.M., Burrell, D.C. and Freigag, G.R., 1976. Suspended sediment dynamics in Queen Inlet, Glacier Bay, Alaska. Marine Science Communications, 2: 95-108.

Hughes, T.J., Borns, H.W. Jr., Fastook, J.L., Kite, J.S., Hyland, M.R. and Lowell, T.V., 1985. Models of glacial reconstruction and deglaciation applied to Maritime Canada and New England. In: Late Pleistocene history of northeastern New England and adjacent Quebec. H.J.W. Borns, P. LaSalle and W.B. Thompson (Editors). Geological Society of America, Special Paper 197, Boulder Colorado, pp. 139-150.

Hughes, T.J., Denton, G.H. and Grosswald, M.G., 1977. Was there a late-Würm Arctic ice sheet? Nature, 266: 596-602.

Hughes, T.J., 1987. Ice dynamics and deglaciation models when ice sheets collapsed. In: North America and adjacent oceans during the last deglaciation. W.F. Ruddiman and H.E. Wright, Jr. (Editors). Geological Society of America, The Geology of North America, v. K-3, Boulder, Colorado, pp. 183-220.

Hussey, E.M., 1979. The stratigraphy, structure and petrochemistry of the Clode Sound map area, northwestern Avalon Zone, Newfoundland. Unpublished M.Sc. thesis, Memorial University of Newfoundland, St. John's, Newfoundland. 312 p.

Hutchins, R.W., McKeown, D.L. and King, L.H., 1976. A deep tow high resolution seismic system for continental shelf mapping. Geoscience Canada, 3: 95-100.

Ives, J.D., 1978. The maximum extent of the Laurentide Ice Sheet along the east coast of North America during the last glaciation. Arctic, 31: 24-54.

Jackson, M.L., Tyler, S.A., Willis, A.L., Bourbeau, G.A. and Pennington, R.P., 1948. Weathering sequence of clay size minerals in soil and sediments. Journal of Physical and Colloid Chemistry, 52: 1237-1260.

Jenness, S.E., 1957. Gander Lake (East Half), Newfoundland. Geological Survey of Canada, Map 3-1957 (With marginal notes).

Jenness, S.E., 1958a. Geology of the Newman Sound map-area, Northeastern Newfoundland. Geological Survey of Newfoundland, Report 12. 53 p.

Jenness, S.E., 1958b. Geology of the Gander River Ultrabasic Belt, Newfoundland. Geological Survey of Newfoundland, Report 11. 58 p.

Jenness, S.E., 1960. Late Pleistocene glaciation of eastern Newfoundland. Geological Survey of America Bulletin, 71: 161-180.

Jenness, S.E., 1963. Terra Nova and Bonavista map-areas, Newfoundland. Geological Survey of Canada, Memoir 327. 184 p.

Jukes, J.B., 1843. General report on the Geological Survey of Newfoundland during the years 1839-1840. In: Excursions in and around Newfoundland during the years 1839-1840, Volume 2. John Murray, London, pp. 195-354.

Kennedy, M.J., 1976. Southeastern margin of the northeastern Appalachians; late Precambrian orogeny on a continental margin. Geological Society of America Bulletin, 87: 1317-1325.

Kennedy, M.J. and McGonigal, M.H., 1972. The Gander Lake and Davidsville Groups of northeastern Newfoundland: new data and geotectonic implications. Canadian Journal of Earth Sciences, 9: 452-459.

King, L.H. and Fader, G.B.J., 1986. Wisconsinan glaciation of the Atlantic continental shelf of southeast Canada. Geological Survey of Canada, Bulletin 363. 72 p.

King, L.H. and Fader, G.B.J., 1988. Late Wisconsinan ice on the Scotian Shelf. Geological Survey of Canada, Open File No. 1972. 15 p.

King, L.H., Rokoengen, K., Fader, G.B.J. and Gunleiksrud, T., 1991. Till-tongue stratigraphy. Geological Society of America Bulletin, 103: 637-659.

King, L.H., Rokoengen, K. and Gunleiksrud, T., 1987. Quaternary seismostratigraphy of the Mid Norwegian Shelf, 65°-67°30'N. - A till tongue stratigraphy. Continental Shelf and Petroleum Technology Research Institute A/S, Publication 114, Trondheim, Norway. 58 p.

Kirby, F.T., Ricketts, R.J. and Vanderveer, D.G., 1988. Preliminary surficial geology maps of the Bonavista Bay region; 2C/5,6,11,12,13, 2D/8. Newfoundland Department of Mines and Energy, Mineral Development Division. Open File 1693.

Knight, I. and O'Brien, S.J., 1988. Stratigraphy and sedimentology of the Connecting Point Group and related rocks, Bonavista Bay, Newfoundland: an example of a late Precambrian Avalonian basin. In: Current research, Newfoundland Department of Mines, Mineral Development Division, Report 88-1, pp. 207-228.

Leeder, M.R., 1982. Sedimentology: process and product. Allen and Unwin, London, U.K. 344 p.

Lewis, C.F.M. and Parrott, D.R., 1987. Iceberg scouring rate studies, Grand Banks of Newfoundland. In: Current research, part A, Geological Survey of Canada, Paper 87-1A, pp. 825-833.

Lundqvist, J., 1965. Glacial geology in northeastern Newfoundland. Geologiska Foreningensi, 87: 285-306.

Mackiewicz, N.E., Powell, R.D., Carlson, P.R. and Molnia, B.F., 1984. Interlaminated ice-proximal glacimarine sediments in Muir Inlet, Alaska. Marine Geology, 57: 113-147.

Macpherson, J.B., 1982. Postglacial vegetational history of the eastern Avalon Peninsula, Newfoundland, and Holocene climatic change along the eastern Canadian seaboard. Géographie physique et Quaternaire, 36: 175-196.

Macpherson, J.B., 1988. The late Pleistocene-Holocene pollen record from the northeast Newfoundland shelf: comparison with the terrestrial record. Report submitted to Atlantic Geoscience Centre, Dartmouth, Nova Scotia. 10 p.

Macpherson, J.B. and Anderson, T.W., 1985. Further evidence of late glacial climatic fluctuations from Newfoundland: pollen evidence from a north coast site. In: Current research, part B. Geological Survey of Canada, Paper 85-1B, pp. 383-390.

Mayewski, P.A., Denton, G.H. and Hughes, T.J., 1981. Late Wisconsin ice sheets in North America. In: The last great ice sheets. G.H. Denton and T.J. Hughes (Editors). John Wiley and Sons Inc., New York, pp. 67-238.

McCartney, W.D., 1958. Geology of the Sunnyside map area, Newfoundland. Geological Survey of Canada, Paper 58-8. 21 p.

McCartney, W.D., 1967. Whitbourne map area, Newfoundland. Geological Survey of Canada, Memoir 341. 135 p.

McGonigal, M.H., 1973. The Gander and Davidsville Groups: major tectonostratigraphic units in the Gander Lake area, Newfoundland. Unpublished M.Sc. thesis, Memorial University of Newfoundland, St. John's, Newfoundland. 121 p.

McLaren, S.A., 1988. Quaternary seismic stratigraphy and sedimentation of the Sable Island Sand Body, Sable Island Bank, outer Scotian Shelf. Unpublished M.Sc. thesis, Dalhousie University, Halifax, Nova Scotia. 95 p.

Miller, A.A.L., Scott, D.B. and Smith, D., 1985. Post glacial paleo-oceanography, northeast Newfoundland shelf. Technical Report No. 4, Centre for Marine Geology, Dalhousie University, Dartmouth, Nova Scotia and Geological Survey of Canada Open File 1194. 39 p.

Miller, A.A.L., 1987. Post glacial paleo-oceanography, northeast Newfoundland shelf: part II. Technical Report No. 4, Part II. Centre for Marine Geology, Dalhousie University, Dartmouth, Nova Scotia. 43 p.

Mudie, P.J. and Guilbault, J.P., 1982. Ecostratigraphic and paleomagnetic studies of Late Quaternary sediments on the northeast Newfoundland shelf. In: Current research, part B. Geological Survey of Canada, Paper 82-1B, pp. 107-116.

O'Brien, S.J., 1987. Geology of the Eastport (west half) map area, Bonavista Bay, Newfoundland. In: Current research, Newfoundland Department of Mines and Energy, Mineral Development Division, Report 87-1, pp. 257-270.

O'Brien, S.J. and Knight, I., 1988. The Avalonian geology of southwest Bonavista Bay: portions of the St. Brendan's (2C/13) and Eastport (2C/12) map areas. In: Current research, Newfoundland Department of Mines and Energy, Mineral Development Division, Report 88-1, pp. 193-205.

Orheim, O. and Elverhoi, A., 1981. Model for submarine glacial deposition. Annals of Glaciology, 2: 123-128.

Parsons, M.G., 1987. The Middle Cambrian, Upper Cambrian, and Lower Tremadoc acritarchs of Random Island, Trinity Bay, southeastern Newfoundland. Unpublished M.Sc. thesis, Memorial University of Newfoundland, St. John's, Newfoundland. 546 p.

Piper, D.J.W., 1974. Manual of sedimentological techniques. Unpublished research guide, Department of Geology and Oceanography, Dalhousie University, Halifax, Nova Scotia. 92 p.

Piper, D.J.W., 1978. Turbidite muds and silts on deepsea fans and abyssal plains. In: Sedimentation in submarine canyons, fans and trenches. D.J. Stanley and G. Kelling (Editors). Dowden, Hutchinson and Ross, Stroudsburg, Pennsylvania, pp. 163-175.

Piper, D.J.W. and Slatt, R.M., 1977. Late Quaternary clay-mineral distribution on the eastern continental margin of Canada. Geological Society of America Bulletin, 88: 267-272.

Powell, R.D., 1983. Glacial-marine sedimentation processes and lithofacies of temperate tidewater glaciers, Glacier Bay, Alaska. In: Glacial-marine sedimentation. B.F. Molnia (Editor). Plenum Press, New York, pp. 185-232.

Powell, R.D., 1984. Glacimarine processes and inductive lithofacies modelling of ice shelf and tidewater glacier sediments based on Quaternary examples. Marine Geology, 57: 1-52.

Quinlan, G. and Beaumont, C., 1981. A comparison of observed and theoretical postglacial relative sea level in Atlantic Canada. Canadian Journal of Earth Sciences, 18: 1146-1163.

Quinlan, G. and Beaumont, C., 1982. The deglaciation of Atlantic Canada as reconstructed from the postglacial relative sea-level record. Canadian Journal of Earth Sciences, 19: 2232-2246.

Reusch, D.N. and O'Driscoll, C.F., 1987. Geological and metallogenic investigations in the western half of the Love Cove Group (NTS 2D/1,2,8), Avalon Zone, Newfoundland. Current research, Newfoundland Department of Mines and Energy, Mineral Development Division, Report 87-1, pp. 93-101.

Rogerson, R.J., 1982. The glaciation of Newfoundland and Labrador. In: Prospecting in areas of glaciated terrain-1982. P. Davenport (Editor). Canadian Institute of Mining and Metallurgy, pp. 37-55.

Ruddiman, W.F. and McIntyre, A., 1981. The mode and mechanism of the last deglaciation: oceanic evidence. Quaternary Research, 16: 125-134.

Scott, D.B., Mudie, P., Vilks, G. and Younger, D.C., 1984. Latest Pleistocene-Holocene paleoceanographic trends on the continental margin of eastern Canada: foraminiferal, dinoflagellate and pollen evidence. Marine Micropaleontology, 9: 181-218.

Seramur, K.C. and Powell, R.D., 1987. Temperate glacimarine lithofacies interpreted from seismic facies. In: Proceedings of the 12th International Congress of INQUA, Ottawa, Canada. p. 262.

Shackleton, N.J. and Opdyke, N.D., 1973. Oxygen isotope and palaeomagnetic stratigraphy of equatorial Pacific core V28-238: oxygen isotope temperatures and ice volumes on a 10^5 year and 10^6 year scale. Quaternary Research, 3: 39-55.

Shaw, J. and Forbes, D.L., 1990. Late Quaternary sedimentation in St. George's Bay, southwest Newfoundland: acoustic stratigraphy and seabed deposits. Canadian Journal of Earth Sciences, 27: 964-983.

Shepard, F.P., 1954. Nomenclature based on sand-silt-clay ratios. Journal of Sedimentary Petrology, 24: 151-158.

Strong, D.F., 1979. Proterozoic tectonics of northwestern Gondwanaland; new evidence from eastern Newfoundland. Tectonophysics, 54: 81-101.

Syvitski, J.P.M., 1989. On the deposition of sediment within glacier-influenced fjords: oceanographic controls. Marine Geology, 85: 301-329.

Syvitski, J.P.M., Burrell, D.C. and Skei, J.M.,(Editors) 1987. Fjords: processes and products. Springer, New York. 397 p.

Timofeev, B.V., 1957. O novoi gruyppe iskopaemykh spor (On a new group of fossil spores). Ezhegodnik Vsessyuznae Paleontologiecheskoe Obshchestvo (Annual of the All-Union Paleontological Society), 16: 280-284.

Tucker, C.M., 1974. A series of raised Pleistocene deltas, Halls Bay, Newfoundland. Maritime Sediments, 10: 1-7.

Vail, P.R., Todd, R.G. and Sangree, J.B., 1977. Seismic stratigraphy and global changes of sea level, part 5: Chronostratigraphic significance of seismic reflections. In: Seismic stratigraphy - Applications to hydrocarbon exploration. C.E Payton (Editor). American Association of Petroleum Geologists, Memoir 26, pp. 99-116.

Vanderveer, D.G., 1988. Surficial geology maps of the Gander Peninsula region. Newfoundland Department of Mines and Energy, Mineral Development Division. Maps 88-12/14/19/20. Open Files 1575 and 1682.

Vanguestaine, M., 1973. New acritarchs from the upper Cambrian of Belgium. In: Mikrofossilii drevneyskikh otlozheniy, TRUDY III, Mezhdunarodnoy Palinoligicheskoy Konfereentsii, Novosibirsk, 1971, Akademiya Nauk, S.S.S.R., Siberskoe Otdeleie, Institut Geologii i Geofizikii. Izdatelstvo "Nauka", Moskva. (Microfossils of the oldest deposits, Proceedings of the 3rd International Palynological Conference, Novosibirsk, 1971, Academy of Sciences of the U.S.S.R., Siberian Branch, Institute of Geology and Geophysics. Publishing House "Nauka", Moscow), pp. 28-30.

Vincent, J.S. and Prest, V.K., 1987. The Early Wisconsinan history of the Laurentide Ice Sheet. Géographie physique et Quaternaire, 41: 199-213.

Visher, G.S., 1969. Grain size distributions and depositional processes. Journal of Sedimentary Petrology, 39: 1074-1106.

Von Huene, R., Larson, E. and Crough, J., 1973. Preliminary studies of ice-rafted erratics as indicators of glacial advances in the Gulf of Alaska. In: Initial reports of the Deep Sea Drilling Project, 18. L.D. Kulm, R. Von Huene (Editors). United States Government Printing Office, Washington, D.C., pp. 835-842.

Williams, H., 1976. Tectonostratigraphic subdivision of the Appalachian Orogen. In: Abstracts with Programs, 8, no. 2. Geological Society of America, Northeast Section Annual Meeting, pg. 200.

Williams, H., Kennedy, M.J. and Neale, E.R.W., 1972. The Appalachian Structural Province. In: Variations in tectonic styles in Canada. R.A. Price and R..W. Douglas (Editors). Geological Association of Canada, Special Paper 11, pp. 181-216.

Williams, H. and Hatcher, R.D. Jr., 1982. Suspect terranes and accretionary history of the Appalachian orogen. Geology, 10: 530-536.

Younce, G.B., 1970. Structural geology and stratigraphy of the Bonavista Bay region, Newfoundland. Unpublished Ph.D thesis, Cornell University, Ithaca, New York. 188 p.